EPA-650/4-73-003

November 1973

Environmental Protection Technology Series

DETERMINATION OF CORONAL OZONE PRODUCTION BY HIGH VOLTAGE POWER TRANSMISSION LINES

Office of Research and Development
U.S. Environmental Protection Agency
Washington, D.C. 20460

EPA-650/4-73-003

DETERMINATION OF CORONAL OZONE PRODUCTION BY HIGH VOLTAGE POWER TRANSMISSION LINES

by

Frank C. Whitmore and Robert L. Durfee

VERSAR Incorporated
6621 Electronic Drive
Springfield, Virginia 22151

Contract No. 68-02-0553
Program Element No. 1H1326
Formerly 110501

EPA Project Officer: Elbert C. Tabor

Quality Assurance and Environmental Monitoring Laboratory
National Environmental Research Center
Research Triangle Park, North Carolina 27711

Prepared for

OFFICE OF RESEARCH AND DEVELOPMENT
U. S. ENVIRONMENTAL PROTECTION AGENCY
Washington, D. C. 20460

November 1973

This report has been reviewed by the Environmental Protection Agency and approved for publication. Approval does not signify that the contents necessarily reflect the views and policies of the Agency, nor does mention of trade names or commercial products constitute endorsement or recommendation for use.

ABSTRACT

A sub-scale simulation of a high-voltage transmission line was constructed and operated in a chamber roughly 1.5 meters long by 0.5 meter in diameter to determine ozone production characteristics. Effects of voltage and corona power, conductor size and surface condition, air temperature, relative humidity, and air flow rate (wind velocity) on ozone yield were determined. Of these, corona power (voltage), relative humidity, and air flow rate exhibited significant effects on ozone yield. Averaged yield values ranged from about 3 gm/kw-hr at high humidity (75-80 per cent) to about 7 gm/kw-hr at low humidity (25-30 per cent).

ACKNOWLEDGMENTS

The authors wish to express their gratitude to Mr. Elbert C. Tabor, the EPA Project Officer for this program, for his patience and consideration throughout. We must also express our thanks to Professor M. M. Newman of the Lightning and Transients Research Institute, Minneapolis, Minnesota, for his guidance and advice in the electrical aspects of the program.

It then remained to select an appropriate altitude, below which all of the ozone so produced would be contained. This height of our cylindrical container was chosen to be one kilometer, based on the typical height of an inversion layer being below this altitude and other considerations.

Thus, we assume that:

(1) The ozone produced is at a constant (average) rate based on the mean values from our work described herein (and assuming that the average relative humidity of Sites (2) and (3) is 25-30 per cent, that of Site (1) 50 per cent, and a linear relationship between ozone yield and relative humidity on either side of the selected mean);

(2) The ozone so produced is maintained in a constant cylindrical volume contained within the circular areas about the sites as described above and a height of one kilometer; and

(3) The ozone concentration throughout the volume is constant (alternatively, an average concentration may be considered).

The steady-state (or limiting) ozone concentrations calculated on the basis of these and the other assumptions as described previously, are as follows (air density = 1.2×10^3 gm/cu m; ozone density = 2.14×10^3 gm/cu m):

Site (1) - Amos, W. Va. (B = 5.5 gm/kw-hr; V = 2.06×10^{13} cu m)

O_3 Half-Life (hr)	C_∞ (ppb by volume)
1	1.2×10^{-3}
10	1.2×10^{-2}
100	1.2×10^{-1}

Site (2) - Four Corners, N. Mex. (B = 8 gm/kw-hr; V = 2.06×10^{13} cu m)

O_3 Half-Life (hr)	C_∞ (ppb by volume)
1	4.9×10^{-4}
10	4.9×10^{-3}
100	4.9×10^{-2}

Site (3) - Los Angeles, Calif. (B = 8.0 gm/kw-hr; V = 1.02×10^{12} cu m)

O_3 Half-Life (hr)	C_∞ (ppb by volume)
1	6.8×10^{-3}
10	6.8×10^{-2}
100	6.8×10^{-1}

The linear dependence of the steady-state concentration of ozone lifetime shows clearly that the lifetime is the single most important factor considered here in determining the relative contribution of transmission lines to local ozone levels. In reality, any wind condition other than calm will dramatically reduce the local contribution which can be attributed to transmission lines.

Lifetime measurements of ozone in smoggy air[9] in a glass container indicate a half-life under these conditions of about one hour. Other work with cleaner air in a metal enclosure[10] has resulted in reported half-lives of ozone of up to 8.2 hours. It is very difficult to relate these values to free air above the three selected sites, but it appears reasonable to assign a half-life of a few hours for Site (3), so that the corresponding C_∞ would be on the order of 10^{-2} ppb. Thus, coronal ozone production would not appear to be a sizeable contribution to the ambient ozone level in the area of Site (3).

The ozone half-life for Sites (1) and (2) may be of the order of five hours (possibly ten hours in the Four Corners area), and from the analysis the contribution from transmission lines on the order of 10^{-2} ppb for Site (1) and 5 x 10^{-3} ppb for Site (2). Both would have to be considered insignificant contributions. One could conclude from the above analysis that, even under atmospheric conditions of relative calm, transmission lines appear to contribute only minimally to local ozone levels. However, until applicable values of ozone lifetimes in free air are available, the actual contribution remains only a rough estimate.

In 1969 it was estimated that over 300,000 miles (540,000 km) of high-voltage (69 kV-765 kV) transmission lines were operating in the contiguous 48 states of the United States[11], and an estimate of 250,000 miles (450,000 km) in 1966 was made by Rose[12]. A reasonable estimate at present appears to be 350,000 miles (630,000 km). A reasonable projection for 1990 appears to be 500,000 miles (900,000 km)[11], unless significant new construction of underground lines is begun soon.

At an overall average of 4 kw/mile (2.22 kw/km) of corona loss on all of these lines, and an average ozone yield of 5 gm/kw-hr, the total yearly productions over the country in 1973 and 1990 are estimated to be:

1973 - 6.1 x 10^7 kg/yr (6.0 x 10^4 tons/yr)
1990 - 8.8 x 10^7 kg/yr (8.7 x 10^4 tons/yr)

These amounts of ozone spread over the entire area of the country would not appear to be significant. However, in actual fact, transmission lines tend to be concentrated about urban areas as discussed previously. Although this would tend to magnify the effects of the ozone so produced, the quantities involved do not appear to be significant to local air quality if any degree of mixing occurs.

7.0 CONCLUSIONS AND RECOMMENDATIONS

The following conclusions and recommendations are based on the results obtained from the program, and from analysis and interpretation of the results.

7.1 Conclusions

(1) The experimental method used and the results observed and consistent with previous efforts in the field and represent simulation of an operating transmission line in terms of environmental conditions in the region where ozone is produced (coronal sheath about the conductor);

(2) Ozone yield (in gm/kw-hr) was not found to be affected significantly by conductor geometry, surface condition, or air temperature;

(3) Ozone yield exhibited a complex dependence on longitudinal air flow rate (wind velocity);

(4) Ozone yield exhibited a relatively strong dependence on relative humidity, increasing as humidity was decreased. Yields were more constant at higher humidity and ranged from 5 to 8 gm/kw-hr at relative humidities above about 40 per cent;

(5) Ozone yields were low at values of corona power dissipation (which, in turn, was a complex function of applied voltage) near the ozone production threshold, and reached an apparently constant value at higher values of corona power dissipation;

(6) At least two ozone decomposition processes were observed in the experiment, one with a time constant (e-fold decrement) on the order of ten seconds and the other with a time constant on the order of ten minutes. Both processes appeared to be affected by relative humidity; and

(7) Ozone from transmission lines appear to contribute only minimally to local ozone levels in areas where concentrations of transmission and distribution lines exist. However, this result is based on extremely rough estimates of ozone lifetimes in free air.

7.2 Recommendations

(1) The decomposition processes involved in ozone destruction should be defined, particularly those processes which could limit the accuracy of ozone production studies in enclosed volumes and those which could affect persistence in free air; and

(2) Since corona losses are greatly increased by precipitation, and since neither ozone yields nor decomposition processes occurring during precipitation appear to be well-defined at present, it is recommended that possible effects of precipitation on ozone production by transmission lines be studied in more detail.

8.0 BIBLIOGRAPHY

1. (a) W. P. Baker, J. Elec. Eng. Ed. 2, 103-113, 1964 - Pergamon Press, Great Britain.

   (b) E. Rawlinson, et al; IRE, Control & Science, 113, 705, 1966.

2. W. R. Smythe, "Static and Dynamic Electricity", McGraw-Hill, 1939, pp 119-120. (units in CGS).

3. EHV Transmission Line Reference Book, Edison Electric Institute, 1968, pp 124-127.

4. Federal Register, 36, 8195 ff (April 30, 1971).

5. A. H. Foley & F. Olsen; AIEE - Project EHV, pp 340-346, June 1960.

6. H. N. Scherer, et al, IEEE Transactions T72550-2, presented at the IEEE PES Summer Meeting, San Francisco, Calif; July 9-14, 1972.

7. "Principal Electric Facilities in the United States", published by the Federal Power Commission, 1972.

8. EHV Transmission Life Reference Book. Edison Electric Institute, 1968, pp 127-170.

9. (a) Haagen-Smit, A.J., and M. M. Fox, Ind. Eng. Chem, 48, pp 1484-7 (1956).

   (b) Haagen-Smit, A. J., and L. G. Wayne, "Atmospheric Reactions and Scavenging", in "Air Pollution" (A. C. Stern, ed.), Vol. 1,2 ed., pp. 168-71. Academic Press, New York, N.Y. (1968).

10. (a) R. Sabersky, et al; Environmental Sci & Tech; 7, 347 (1973).

    (b) F. Mueller, et al; Environmental Sci & Tech, 7, 342 (1973).

BIBLIOGRAPHIC DATA SHEET

1. Report No. EPA-650/4-73-003

2.

3. Recipient's Accession No.

4. Title and Subtitle
Determination of Coronal Ozone Production by High Voltage Power Transmission Lines

5. Report Date Issued November 1973

6.

7. Author(s)
Frank C. Whitmore and Robert L. Durfee

8. Performing Organization Rept. No.

9. Performing Organization Name and Address
Versar, Incorporated
6621 Electronic Drive
Springfield, Virginia 22151

10. Project/Task/Work Unit No.
Program Element 1H1326

11. Contract/Grant No.
68-02-0553

12. Sponsoring Organization Name and Address
Environmental Protection Agency
National Environmental Research Center, RTP
Quality Assurance and Environmental Monitoring Laboratory
Research Triangle Park, North Carolina 27711

13. Type of Report & Period Covered
Final Report

14.

15. Supplementary Notes
Formerly Program Element 110501

16. Abstracts
A sub-scale simulation of a high-voltage transmission line was constructed and operated in a chamber roughly 1.5 meters long by 0.5 meter in diameter to determine ozone production characteristics. Effects of voltage and corona power, conductor size and surface condition, air temperature, relative humidity, and air flow rate (wind velocity) on ozone yield were determined. Of these, corona power (voltage), relative humidity, and air flow rate exhibited significant effects on ozone yield. Averaged yield values ranged from about 3 gm/kw-hr at high humidity (75-80 per cent) to about 7 gm/kw-hr at low humidity (25-30 per cent).

17. Key Words and Document Analysis. 17a. Descriptors
Air pollution
Ozone
Power Transmission lines
Electric corona
Sources
Measurement

17b. Identifiers/Open-Ended Terms
Ozone concentrations
Transmission line simulation

17c. COSATI Field/Group 13B

18. Availability Statement
Unlimited

19. Security Class (This Report)
UNCLASSIFIED

20. Security Class (This Page)
UNCLASSIFIED

21. No. of Pages
129

22. Price

ABSTRACT

A sub-scale simulation of a high-voltage transmission line was constructed and operated in a chamber roughly 1.5 meters long by 0.5 meter in diameter to determine ozone production characteristics. Effects of voltage and corona power, conductor size and surface condition, air temperature, relative humidity, and air flow rate (wind velocity) on ozone yield were determined. Of these, corona power (voltage), relative humidity, and air flow rate exhibited significant effects on ozone yield. Averaged yield values ranged from about 3 gm/kw-hr at high humidity (75-80 per cent) to about 7 gm/kw-hr at low humidity (25-30 per cent). Application of these results to three areas of high concentration of transmission lines showed that, under minimal wind conditions, such transmission line concentrations can produce sizeable local ozone levels.

ACKNOWLEDGMENTS

The authors wish to express their gratitude to Mr. Elbert C. Tabor, the EPA Project Officer for this program, for his patience and consideration throughout. We must also express our thanks to Professor M. M. Newman of the Lightning and Transients Research Institute, Minneapolis, Minnesota, for his guidance and advice in the electrical aspects of the program.

TABLE OF CONTENTS

TABLE OF CONTENTS (Continued)

LIST OF TABLES

LIST OF FIGURES

LIST OF FIGURES (Continued)

Page

LIST OF FIGURES (Continued)

Page

GLOSSARY OF SYMBOLS USED

Symbols Used in Section 2.0

The work described in this report was strongly interdisciplinary, involving physics, electrical engineering, chemistry, and chemical engineering inputs among others. The symbols used in the analytical equations were primarily those typical of the various disciplines, even though this practice resulted in the use of the same symbol for several quantities in a few instances. This list of terms should aid in the understanding of the work.

a	=	radius of conducting shell surrounding test line
b	=	radius of test line
C	=	general symbol for capacitance
C_o	=	standard (reference) capacitor used in electrical measurements in test section
C_3, C_4	=	capacitance of variable elements in Schering bridge
e	=	constant = 2.7183
E_R	=	voltage (ac) drop across R_1 (Figure 6) as measured by test meter
$\bar{E}_R$	=	average of E_R values (Figure 6)
F	=	frequency in hertz
h	=	height of conducting sphere from ground plane (equation 3 ff)
i_m	=	meter current (Figures 5 and 6)
i_{series}	=	current flow through C_o calibration circuit in Figure 5
k_o	=	permittivity of free space
n	=	summing index for summuation (equation 3 ff)
R_1, R_2	=	resistive elements used in calibration (Figures 5 and 6)
R_3, R_4	=	variable resistive element in Schering bridge
r	=	effective series resistance of test cell
R_m	=	meter internal series resistance (Figure 6)
R_{par}	=	effective resistance of meter in shunt with R_2 (Figures 5 and 6)

GLOSSARY OF SYMBOLS (Continued)

R_t	=	total series resistance in Figures 5 and 6
V	=	symbol for applied voltage in a general sense
V_1	=	voltage drop across R_1 in Figure 5
V_c	=	critical voltage for corona onset (Figure 12)
V_o	=	applied high voltage in Figure 6 for AC meter calibration
X	=	capacitive reactance of test cell
Z_x	=	test sample impedance
Z_o	=	standard/comparison impedance in Schering bridge
Z_3, Z_4	=	variable impedances in Schering bridge
α	=	$\cosh^{-1}\left({}^{h}/_{a}\right)$ [equation 3 ff]
ε	=	dielectric constant of air
π	=	constant = 3.1416
ω	=	angular frequency as $2\pi f$ where f is the powder frequency

Symbols Used in Sections 4.0 and 6.0

a	=	constant = $\left(\frac{V\lambda}{BP}\right)$ in equation (14)
b	=	constant = $\left(\frac{1}{BP}\right)$ in equation (14)
B	=	ozone yield (gm/kw-hr)
C	=	concentration of ozone
C_e	=	equilibrium concentration of ozone at $\left(\frac{dc}{dt}\right) = o$
C_o	=	original ozone concentration ($t = o$)
C_∞	=	final ozone concentration ($t = \infty$)
C_{ozone}	=	ozone concentration as determined by monitor
e	=	constant = 2.7183
M	=	mass
P	=	corona power (watts)
Q	=	air flow rate (m^3/sec)
RH	=	relative humidity (per cent)
t	=	elapsed time
V	=	volume (m^3)
α	=	ozone production rate (gm/min)
λ	=	time constant
ρ_{O_3}	=	density of ozone at test conditions (gm/m^3)

1.0 INTRODUCTION

In recent years it has become obvious that ozone has great significance as an air pollutant due to its ability to cause human discomfort, plant damage and significant chemical damage to plastics and rubber. Perhaps the most important aspect of ozone is its role as a chemical intermediary or as an end product in the formation of photochemical smog.

Major sources of ozone in the biosphere appear to include transport *via* vertical mixing from the ozone-rich stratosphere and photolysis of products from combustion and photosynthesis processes. Other apparently minor sources include production by natural electrical processes (natural corona and lightning) and electrical machinery. None of these sources has been well-characterized as to their importance to air quality, or even with respect to the mechanisms involved in ozone formation within the biosphere or transport from the stratosphere.

The program reported herein has been carried out in an attempt to evaluate the magnitude of the contribution to the ozone level within the biosphere arising from the corona associated with high voltage transmission lines. In order to allow the widest possible range of atmospheric and electrical variables, the study has been conducted in a sub-scale simulation chamber which is described in detail below.

The program had as its major objectives the experimental determination of ozone yields from high-voltage electrical transmission lines, and the subsequent use of this information to determine the possible significance of the ozone so formed on air quality in the vicinity of one or more transmission lines. The report includes a detailed description of the apparatus and experimental methods used to determine ozone yields from corona loss about metal conductors used in power transmission, analysis and interpretation of the data obtained, and an analysis of the significance of ozone production from operating lines at selected sites of varying climatic conditions and transmission line concentration. All of the experimental data obtained during the program are presented in tabular form as Appendix A.

2.0 ELECTRICAL AND PHYSICAL CHARACTERISTICS OF THE EXPERIMENTAL APPARATUS

2.1 General Considerations

The requirements for this experiment were such that it was essential to provide good electrical insulation of all portions of the high voltage system from the specific portion under test so that minimal interferences existed in terms of ozone production from non-related corona discharges. In addition, it was desirable that accurate measurement and some control of such parameters as relative humidity, air velocity and air temperature be available. In view of these specific requirements the system was designed as is shown schematically in Figure 1 and in the photographs of Figures 2 and 3. The predominant feature of this system was the high voltage assembly, terminated on top by a 25 cm diameter polished aluminum sphere and terminating horizontally in the plastic cylindrical structure shown in more detail in Figure 2. The six-inch diameter copper bus-bar was terminated in a corona ring whose center was pierced to allow the test specimen to be attached to the interior support clamp. The other end of the test specimen was secured in a clamp affixed to the 18 cm diameter polished aluminum termination sphere. The entire high voltage termination and test wire was contained in an acrylic plastic chamber 1.22 meters long and terminated at each end by acrylic plastic domes 0.76 meters in diameter. The ground (return) electrodes consisted of two copper plates 0.91 by 0.30 meters cemented to the inside wall of the acrylic cylinder equidistant from the end terminations. The electrodes were so spaced that the separation of electrode to test speciment was 0.23 meters. The sealed plastic envelope surrounding the test specimen thus served to provide electrical as well as environmental protection for the test system.

2.2 Electrical System

The power supply chosen for this work had the capability of delivering

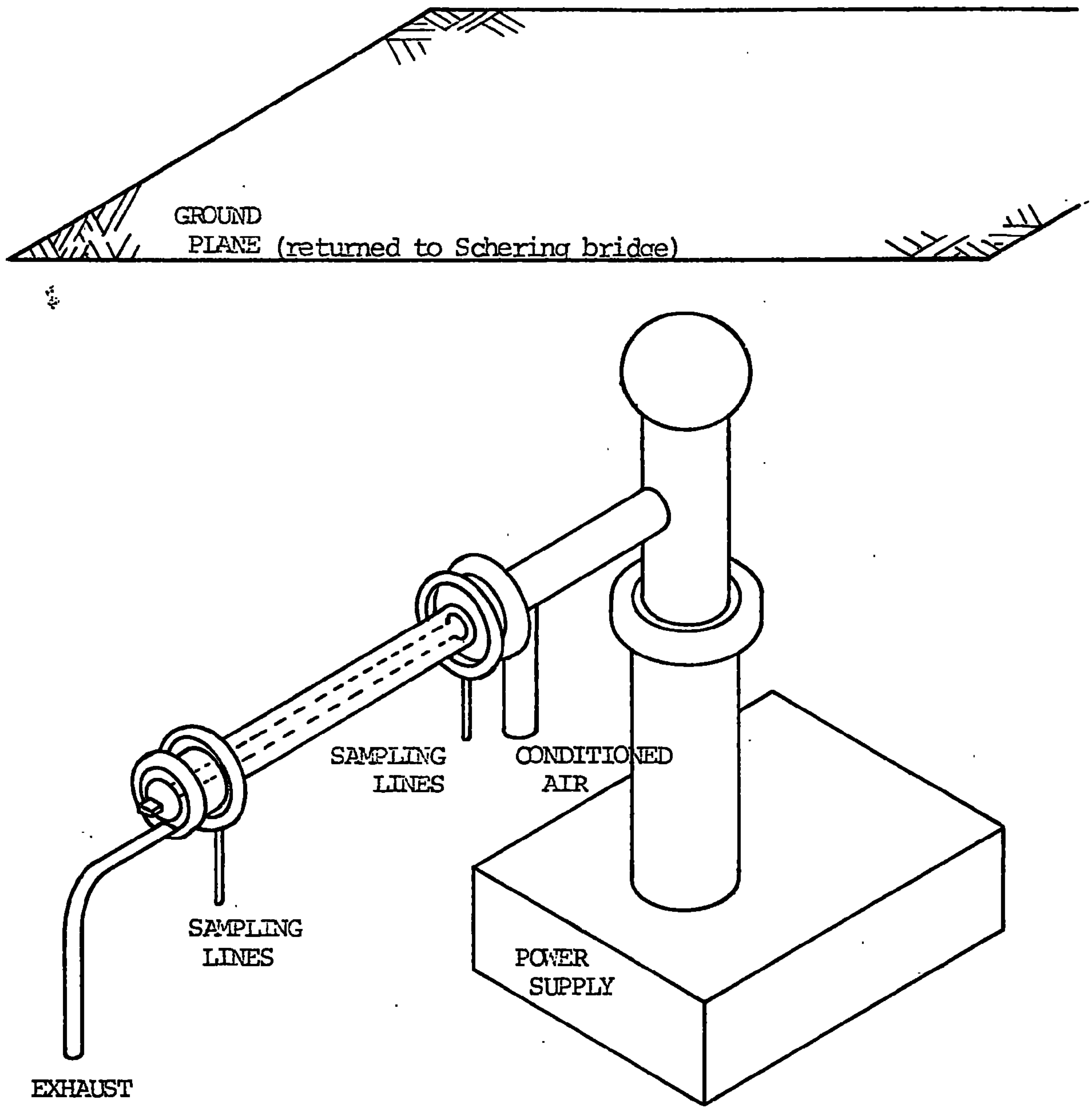

Figure 1. Ozone Production from High Voltage Transmission Line Test Facility.

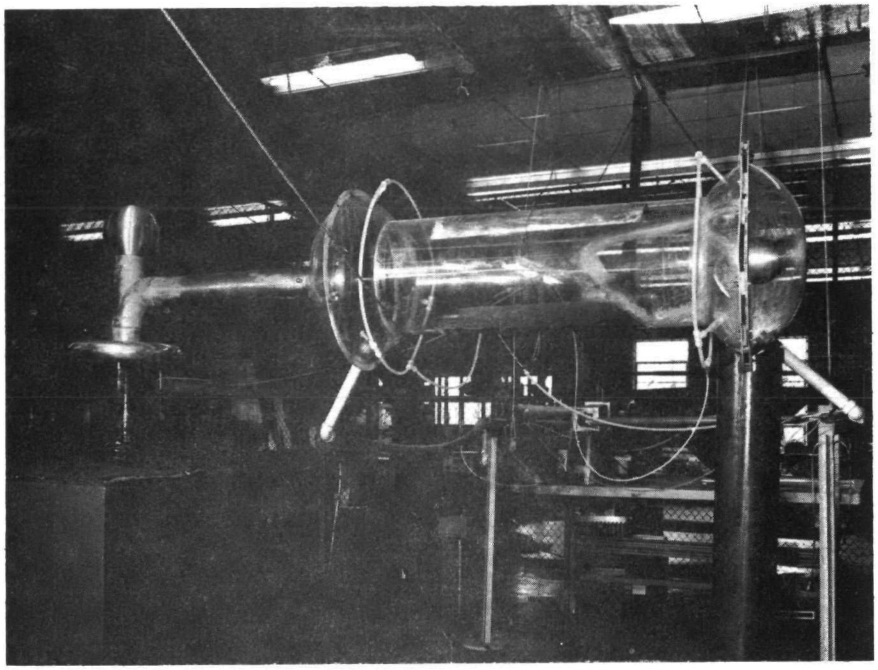

Figure 2. Overall View of Test Chamber and Air Flow System.

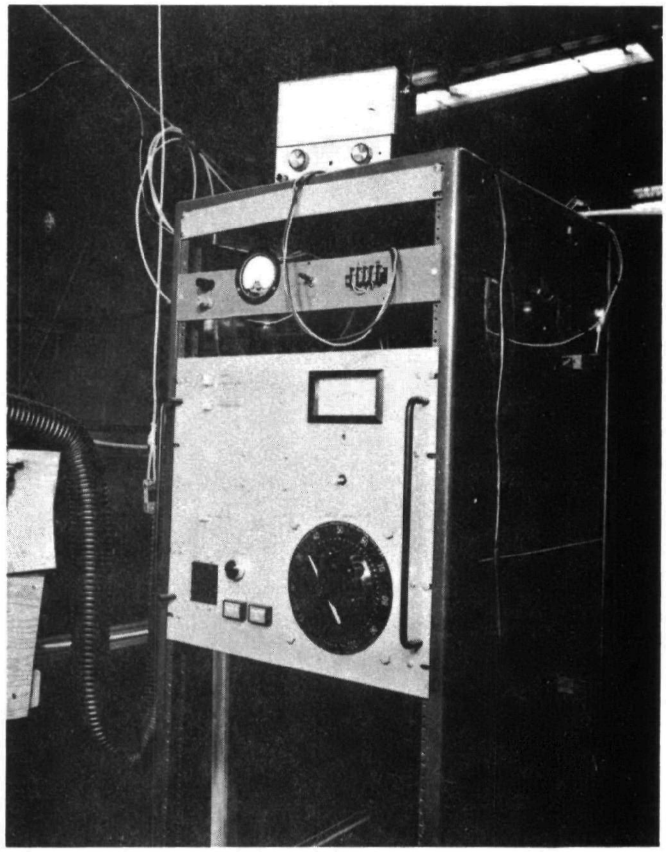

Figure 3. Power Supply Unit and Control Console.

some 10 milliamps at a maximum RMS voltage of 150,000 volts (60 Hertz AC). The supply terminated in the large porcelain insulator shown in Figure 2 to which was added the passive electrical network.

The electrical portion of the experimental program required the accurate measurement of all corona losses associated with the test specimen, in order to determine losses as a function of the electrical, physical and environmental variables of the experiment. The most practical method for accomplishing this measurement was through the use of a Schering bridge [(1)] which is particularly adapted to the measurement of relatively small capacitances in unbalanced high voltage currents. Schematically, the Schering bridges takes the form as shown in Figure 4, wherein Z_x is the unknown impedance, Z_o is a standard impedance, usually a high quality capacitor, and Z_3, Z_4 are the adjustable components of the bridge.

Whereas Z_o is often an off-the-shelf, very high quality capacitor with voltage rating sufficient for the highest test voltage to be used, in this program the alternate approach of sphere-to-plane capacitor was used for Z_o (nominally designed for 50 picofarads, 200K volts). As shown in Figures 1 and 2, the high voltage assembly was terminated vertically in a polished 25 cm aluminum sphere located approximately 1 meter below a large (4 meter x 6 meter) ground plane. This capacitance served as the Z_o component of the Schering bridge. The rest of the high voltage assembly was carefully shielded and polished so as to minimize the leakage resistances and corona spots, and to fix (if not to minimize) stray corona losses.

2.2.1 Standard Capacitor

The most direct method of measurement of Z_o is to place a precision resistance stack in series with Z_o, apply high voltage to the series circuit and measure the (ac) current as a function of applied voltage. The actual arrangement was as shown schematically in Figure 5.

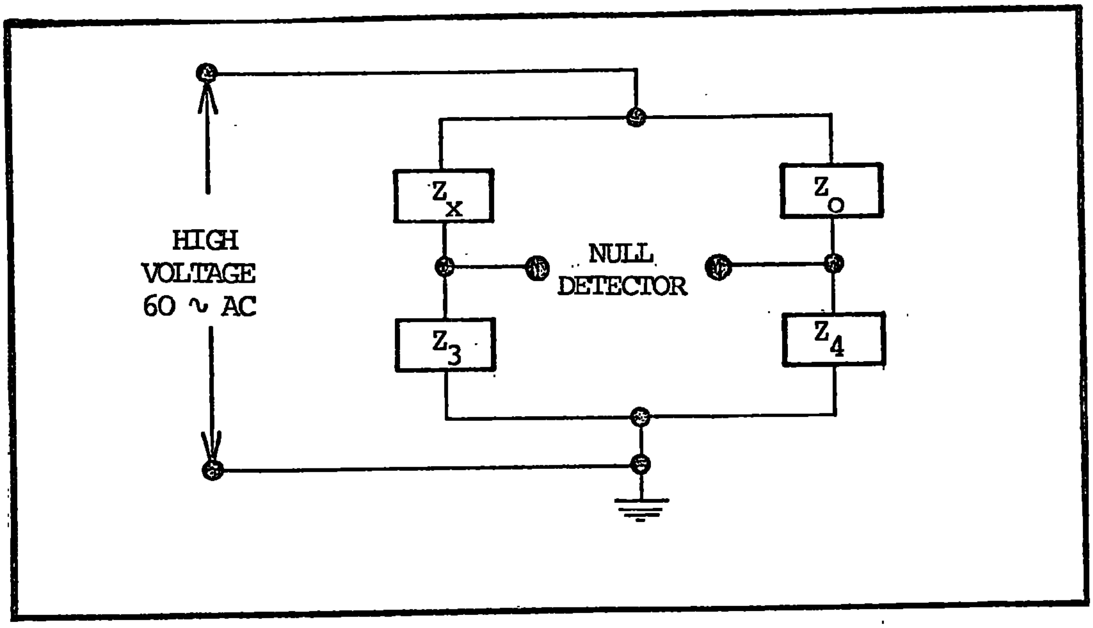

Figure 4. Schematic of Schering Bridge Circuit

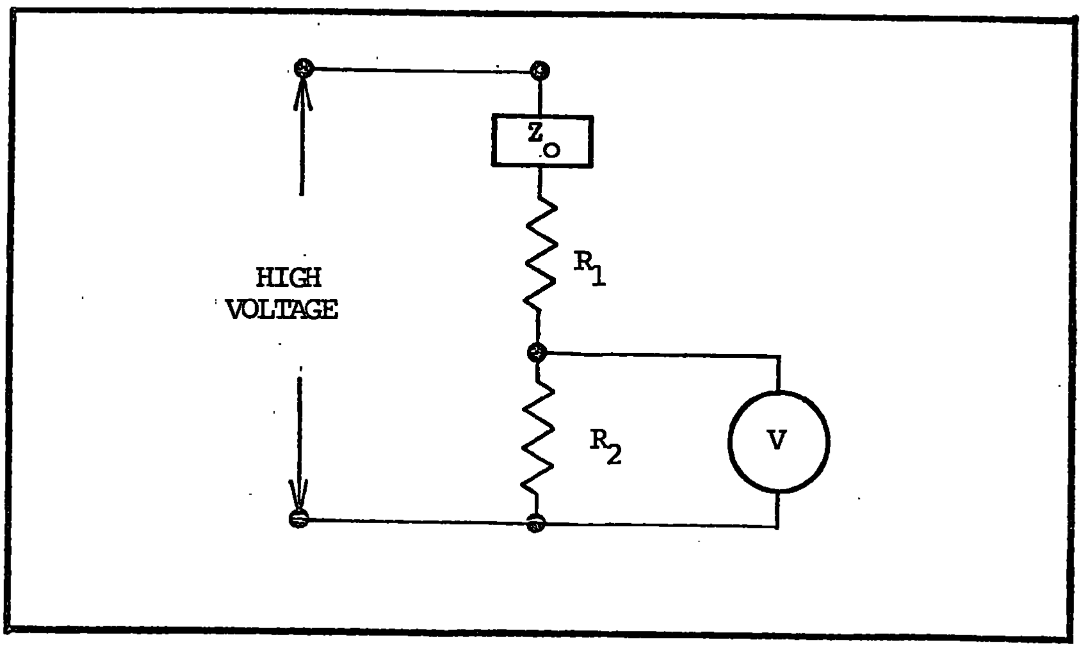

Figure 5. Schematic of Circuit for Measurement of Z_o.

From Figure 5, it can be shown that

$$C_o = \frac{V_2}{\omega} \left\{ \frac{1}{V^2 R_1^{\,2} - V_1^{\,2} R^2} \right\}^{1/2} \qquad (1.)$$

where V is the applied voltage, V_2 is the drop across R_2 and $\omega = 2\pi f$. The above equation assumes that the resistance shunted across R_2 is sufficiently large as to not seriously affect the current through the series R-C circuit, a condition which may not be correct. In the experiment described herein, the meter exhibited a 10^4 ohm per volt characteristic, which for the 50 volt scale would introduce 5×10^5 ohms in shunt with R_2 which must be taken into consideration. The actual value of C_o was then computed by converting the observed meter reading into an equivalent series current through the meter, computation of the corresponding current through R_2, computation of the total series current-through the capacitor C_o and then the computation of C_o. This experiment was repeated several times under different ambient conditions of relative humidity, atmospheric pressure and air temperature, with the result that (to the precision of this measurement) none of these parameters affected the final result for C_o. A typical set of data is shown in Table 1. The equation used to compute C_o is given by:

$$C = \frac{i_{series}}{\omega V} \quad \text{where } \left(\frac{1}{\omega C}\right)^2 >> R^2 \ . \qquad (2.)$$

From the data in Table 1 the average value of C_o may be taken as 5.61×10^{-12} farads, with a probable error of $\pm\ 0.03 \times 10^{-12}$ farads.

2.2.2 Meter Calibration for Measurement of Standard Capacitor

To be assured of the validity of the ac measurements, the 10^4 ohm/volt ac voltmeter was calibrated using the circuit shown in Figure 6, where R_1 and R_2 were standard decade resistance boxes. The results of this measurement are

Table 1. Experimental Data for Measurement of C_o.

V (KV)	Measured Values of E_R (volts)						$\bar{E}_R$ (volts)	i_m (amps)	i_{series} (amps)	C_o (farads x 10^{12})
10	5.8	5.2	5.2	5.1	5.1	5.2	5.25	1.04×10^{-5}	2.02×10^{-5}	5.38
15	8.3	8.2	8.1	7.9	7.9	7.8	8.03	1.66×10^{-5}	2.33×10^{-5}	5.67
20	11.3	10.9	11.2	10.8	10.5	10.8	10.91	2.18×10^{-5}	4.23×10^{-5}	5.64
25	14.2	13.8	13.8	13.3	13.3	13.3	13.61	2.72×10^{-5}	5.28×10^{-5}	5.60
30	16.0	16.2	16.5	16.4	16.4	16.2	16.33	3.27×10^{-5}	6.35×10^{-5}	5.57
35	19.9	19.1	19.1	19.2	18.9	18.9	19.17	3.83×10^{-5}	7.42×10^{-5}	5.63
40	21.9	21.1	22.1	21.9	21.9	21.8	21.77	4.35×10^{-5}	8.44×10^{-5}	5.60
45	24.2	24.3	24.3	24.7	24.8		24.46	4.89×10^{-5}	9.45×10^{-5}	5.58
50	26.9	26.9	26.9	27.0	27.0		26.94	5.39×10^{-5}	10.45×10^{-5}	5.56

Air Temp (82°F) 27.8°C

Relative Humidity 64%

Barometric Pressure: 758 mmHg

$C_o = (5.61 \pm .03) \times 10^{-12}$ farads

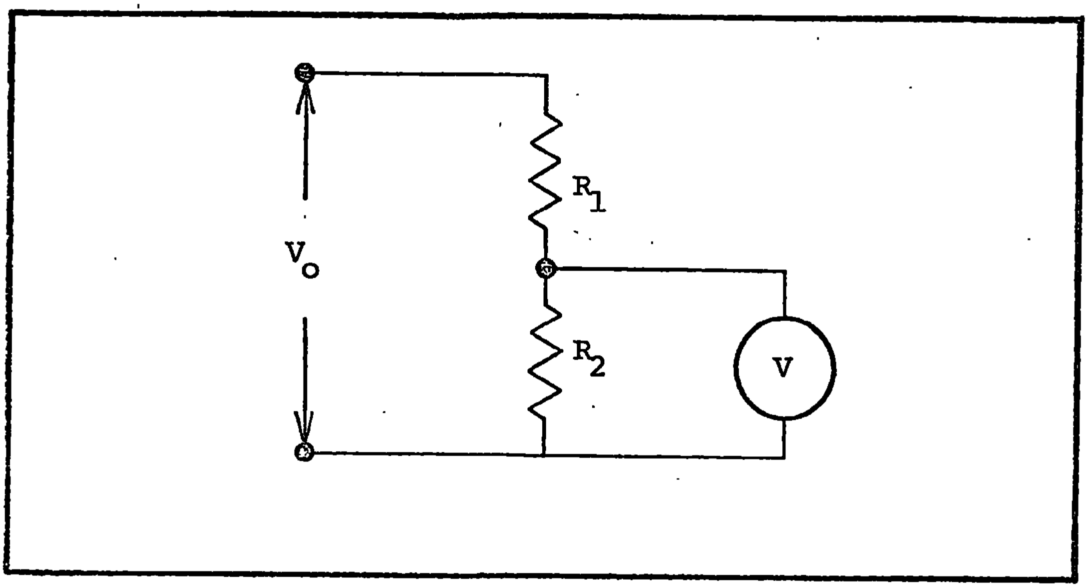

Figure 6. Schematic Circuit for Meter Calibration

shown in Table 2. The important fact to note on Table 2 is that the values of R_2 were similar to those experienced in the measurements associated with the determination of the standard capacitance. Certainly, the experimental data indicate that the meter readings were of sufficient accuracy to be utilized for this experiment.

In order to place the experimental value of C_o into proper perspective, the capacitance of a conducting spherical shell of radius (a) removed from an infinite conducting plane by a distance (h) has a capacitance given by[2] (converted to MKS rather than ESU units as given in the cited reference):

$$C_o = 1.1 \times 10^{-12} \, a \sinh \alpha \sum_{n=1}^{\infty} \operatorname{cosech}(n\alpha) \, , \qquad (3.)$$

where h = a cosh α. In the actual physical layout, a = 12.7 cm and h = 1.14 meters, so that cosh α = 9.0 and α = 2.89. In this circumstances, sinh α ~ cosh α. Now (cosech nα) = (sinh nα)$^{-1}$, and since cosh α ~ sinh α, then cosech nα ~ $\frac{e^{-n\alpha}}{2}$ and sinh ~ $\frac{e^{\alpha}}{2}$. Hence,

$$C_o \sim 1.1 \times 10^{-12} \, a \left(\frac{e^{\alpha}}{2}\right) \sum_{n=1}^{\infty} \frac{e^{-n\alpha}}{2} \sim \frac{1.1 \times 10^{-12} a}{4} \qquad (4.)$$

$$C_o \sim 3.5 \times 10^{-12} \text{ farads.}$$

The approximations used clearly were justified numerically and also in terms of the basic physics of the problem in that the overhead screen used is not actually infinite. The experimental capacitance was somewhat larger than the theoretical value since the former value also included whatever stray capacitances existed in shunt with C_o and thus could not be differentiated experimentally. Incidentally, for an isolated sphere of radius (a), the capacitance is given by:

$$C = 4\pi k_o a \, , \qquad (5.)$$

Table 2. Voltmeter Calibration Data

V_o (volts)	R_1 (ohms)	R_2 (ohms)	R_M (ohms)	R_{PAR} (ohms)	R_T (ohms)	Current (amps x 10^4)	Voltage Calculated (volts)	Voltage Measured (volts)
118	130K	100K	500K	83.4K	213.4K	5.52	46.0	46.0
"	160K	"	"	"	243.4K	4.85	40.4	40.3
"	200K	"	"	"	283.4K	4.16	34.7	34.6
"	300K	"	"	"	383.4K	3.08	25.7	25.7
"	400K	"	"	"	483.4K	2.44	20.4	20.3
"	"	200K	"	143 K	543 K	2.17	31.0	31.0
"	700K	"	"	"	843 K	1.40	20.1	20.0
"	"	150K	"	115 K	815 K	1.445	16.7	16.8
"	"	100K	"	83.4K	783.4K	1.505	12.2	12.3
"	"	50K	"	45.5K	745.5K	1.57	7.18	7.00

which for the given geometry represents a capacitance of the order of 12×10^{-12} farads. Thus, the actual theoretical value should lie between the extremes of 12×10^{-12} farads as upper bound and 3.5×10^{-12} farads as a lower bound.

2.2.3 Electrical Bridge Measurements

The actual realization of the bridge shown schematically in Figure 4 consists of Z_o the standard air capacitance discussed above, Z_x the test specimen and chamber assembly, with Z_3 and Z_4 consisting of parallel decade resistance boxes and decade capacitance boxes. Since the null detector in Figure 4 must be such as to apply a minimal shunting effect across the terminals of the bridge and must also have a large dynamic range, a dual channel differential amplifier-input unit was used with an oscilloscope. Balance was accomplished by adjusting the components of Z_3 and Z_4 for minimum signal on the scope, but, because of the rectifying character of the system, it was found that a second requirement for balance lay in the removal of as much of the 60~ component as possible, as shown by the purest third harmonic signal on the scope.

The existence of rectification within the test section is, of course, associated with the irreversible losses from the formation of the corona. This effect is quite graphically shown in Figure 7 which is a plot of the dc ground return current from the test section plotted against the square root of the applied voltage (data included in Table 3). The characteristic square law plot is shown in Figure 7.

The analysis of the bridge circuit of Figure 4 shows that, for the current through the null detector to be zero, it is necessary that:

$$Z_oZ_3 - Z_xZ_4 = 0$$

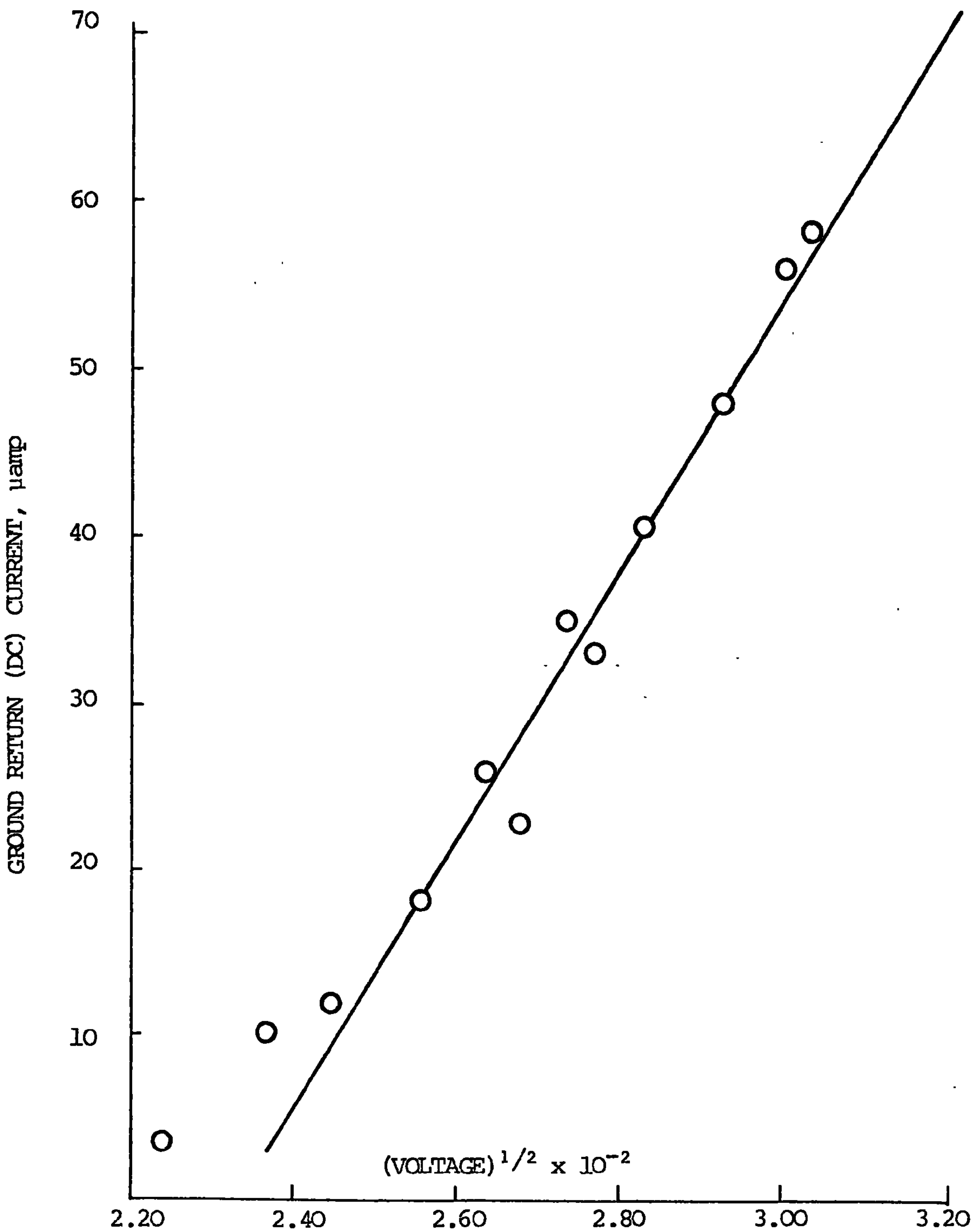

Figure 7. Square Law Characteristic of 0.635 cm Diameter Test Specimen.

VERSAR INC.

Table 3. DC Characteristics of 0.635 cm Diameter Test Conductor

Applied Voltage (kilovolts)	DC Current (μamps)	$V^{1/2} \times 10^{-2}$	DC Power (watts)
50	3.5	2.24	0.175
56	10	2.37	0.560
60	12	2.45	0.720
66	18	2.56	1.188
70	26	2.64	1.82
72	23	2.68	1.66
75	35	2.74	2.63
76	33	2.77	2.51
80	41	2.83	3.28
86	48	2.93	4.13
90	56	3.00	5.04
92	58	3.03	5.49

where Z_X is the impedance of the test section consisting of series capacitance X and loss resistance r, Z_o is the standard capacitance, and Z_3, Z_4 are parallel combinations consisting of R_3, C_3 and R_4, C_4 respectively. Clearly, equation (6.) represents two conditions (since most of the impedances are complex) on the seven components of the bridge circuit, three of the components being fixed - *i.e.*, X, r and C_o. The result of these considerations suggests that balance will affix only two of the remaining components.

In terms of the assigned meaning of the various components, the balance equation (5.) becomes, in general:

$$X = C_o \frac{R_4}{R_3} \left\{ \frac{1 + \omega^2 R_3{}^2 C_3{}^2}{1 + (\omega R_3 C_3)(\omega R_4 C_4)} \right\} \qquad (7.)$$

and

$$rX = R_4 C_4 - R_3 C_3 \left\{ \frac{1 + \omega^2 R_4{}^2 C_4{}^2}{1 + (\omega C_3 R_3)(\omega C_4 R_4)} \right\} \qquad (8.)$$

where $\omega = 2\pi f$ has the usual meaning. It is generally assumed (since two of the four variable components can be selected to have arbitrary but appropriate values) that

$$\omega^2 R_4{}^2 C_4{}^2 \ll 1, \text{ and } \omega^2 R_3{}^2 C_3{}^2 \ll 1,$$

whereupon the detailed balance equations (6.) and (7.) assume their usual and simpler form:

$$X = C_o \frac{R_4}{R_3} \qquad (7'.)$$

and

$$rX = R_4 C_4 - R_3 C_3 \qquad (8'.)$$

In practice, it was found to be more practical to utilize the general form of the balance equations for this program rather than to attempt in each case to effect balance so that the simplified equations could be used.

In carrying out the actual bridge measurements it was deemed appropriate to interchange the R-C components making up Z_3 and Z_4 at random in order to reduce the possibility of systematic errors due to an incorrect calibration of these components which otherwise have been assumed to be correct as labeled.

The data on the salient electrical features of the system are presented in Appendix A in Tables A-1 and A-2. A summary of values for r, X and Corona Power is presented in Figures 8 through 11 which are taken from Tables A-1 and A-2. The data for a wire of 0.635 cm diameter demonstrates unusual behavior in that both the X/C_o ratio and corona power show markedly different behavior above and below a critical relative humidity of 70%. Similar behavior is shown in Figure 10 for the X/C_o ratio for a 1.04 cm diameter wire. Figure 11, which shows the Corona Power for the 1.04 cm diameter wire, indicates a general independence of power dissipated on relative humidity. In no case was there an indication that air temperature or relative air velocity had an appreciable effect on the electrical characteristics of the test system.

In a further attempt to understand the electrical characteristics, we have plotted the corona power in watts versus $(V-V_c)^2$ for two wire diameters in Figure 12. For the 0.635 cm wire V_c = 35 kV, and for the 1.04 cm wire V_c = 43.5 kV. Using the relations from EHV Transmission Line Reference Book [(3)], we find that the critical field for corona is approximately 26 kV/cm for the 0.635 wire and approximately 22.5 kV/cm for the 1.04 cm wire. These values suggest that the larger wire was rather badly surface roughened and serves to explain the lack of effect of further surface treatment of this wire (by NaOH etching).

As an additional check on the accuracy of the electrical measurements we note that the capacitance per unit length of a pair of concentric cylinders

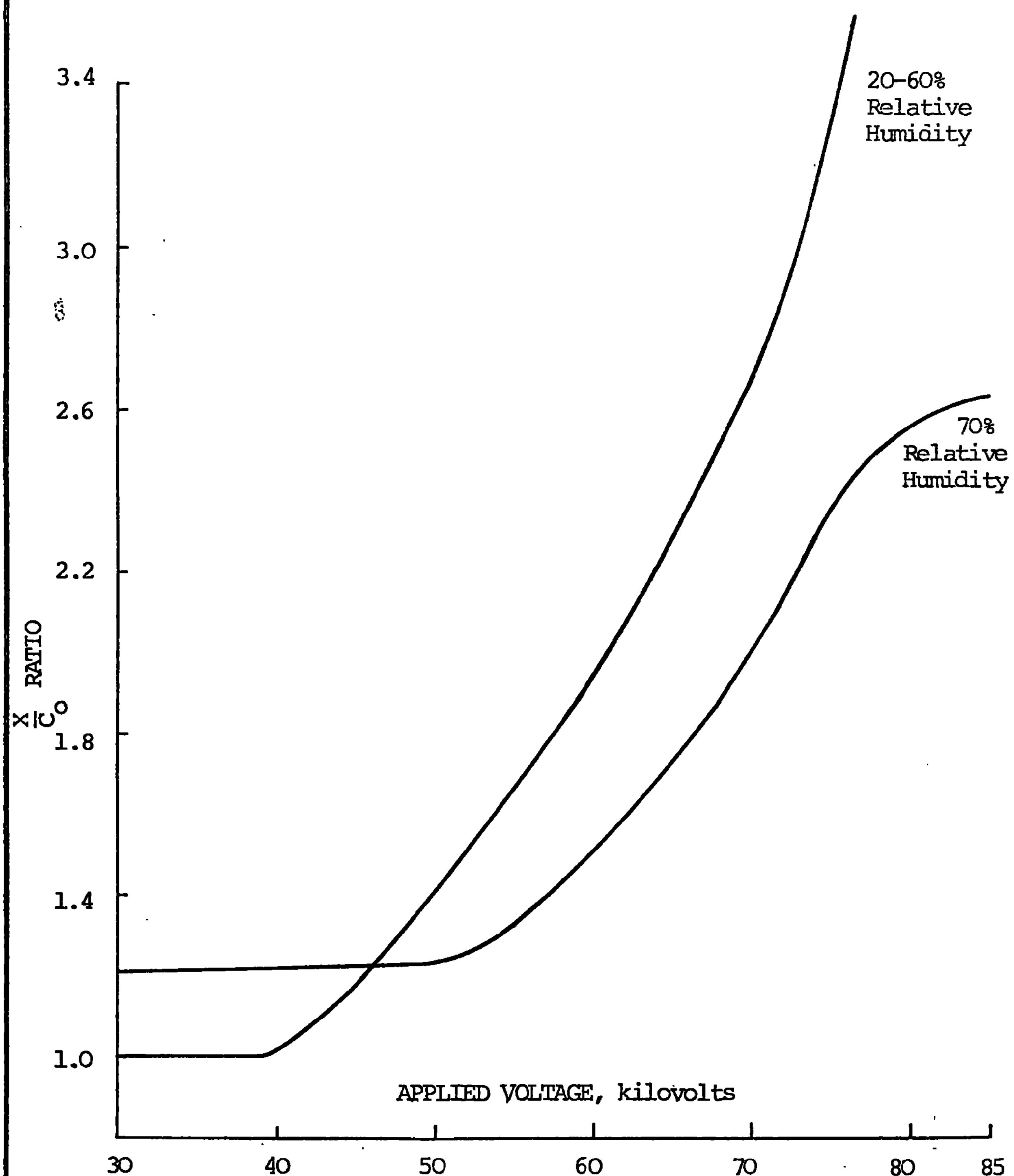

Figure 8. Plot of $\frac{X}{C_o}$ Ratio Versus Voltage for 0.635 cm Diameter Sample.

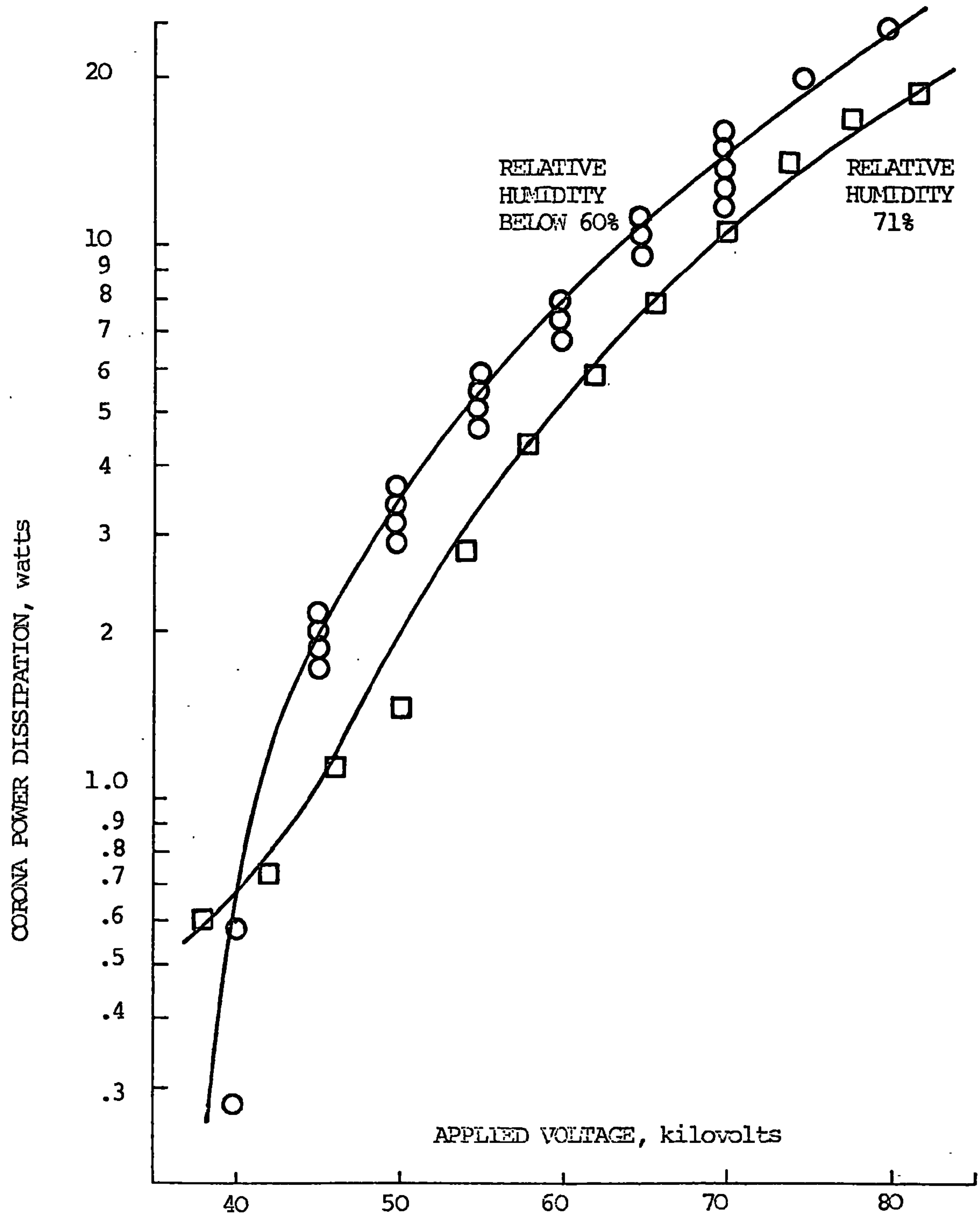

Figure 9. Corona Power Dissipation for 0.635 cm Diameter Sample.

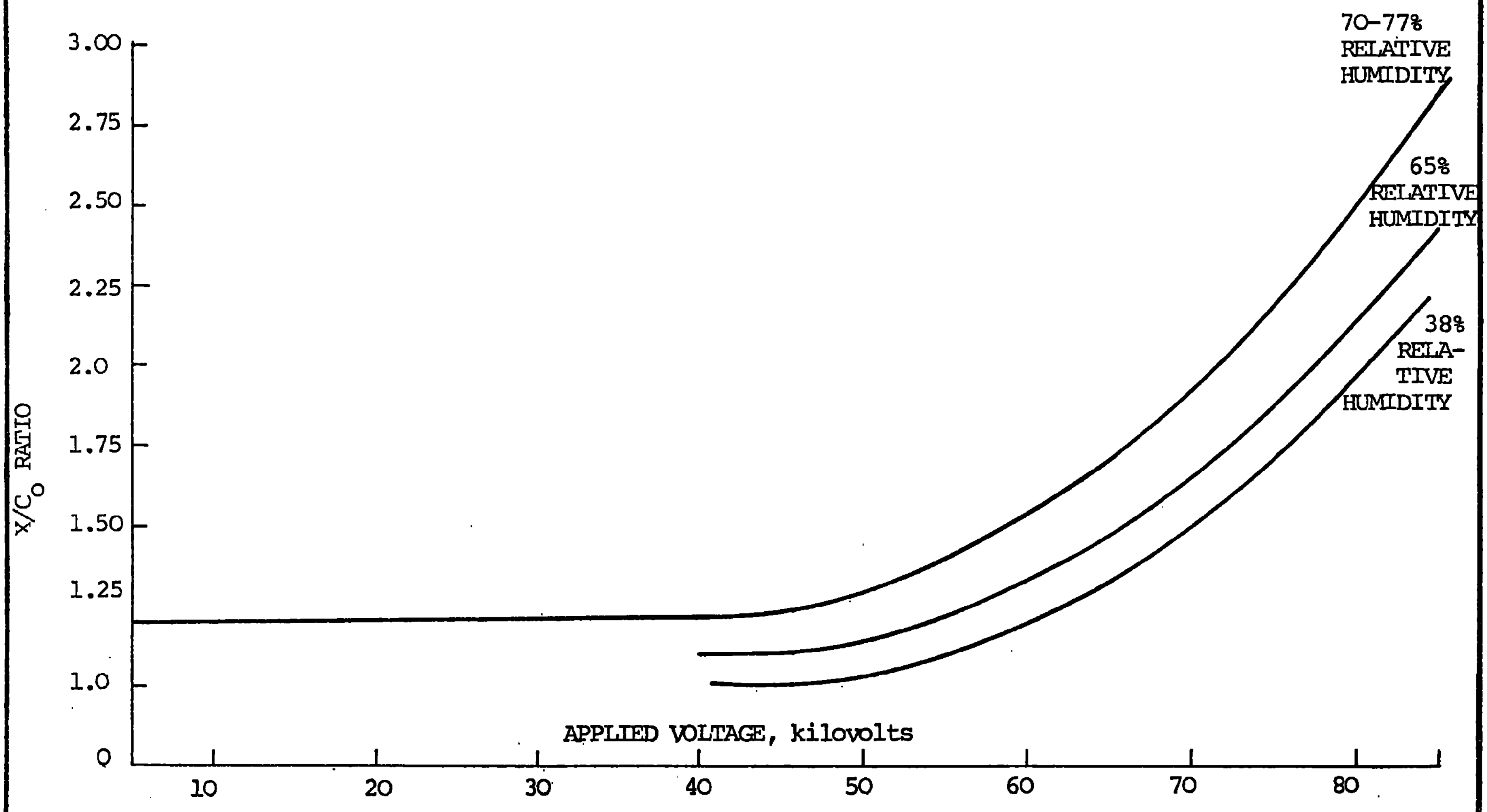

Figure 10. Plot of X/C_o Ratio Versus Voltage for 1.04 cm Diameter Sample.

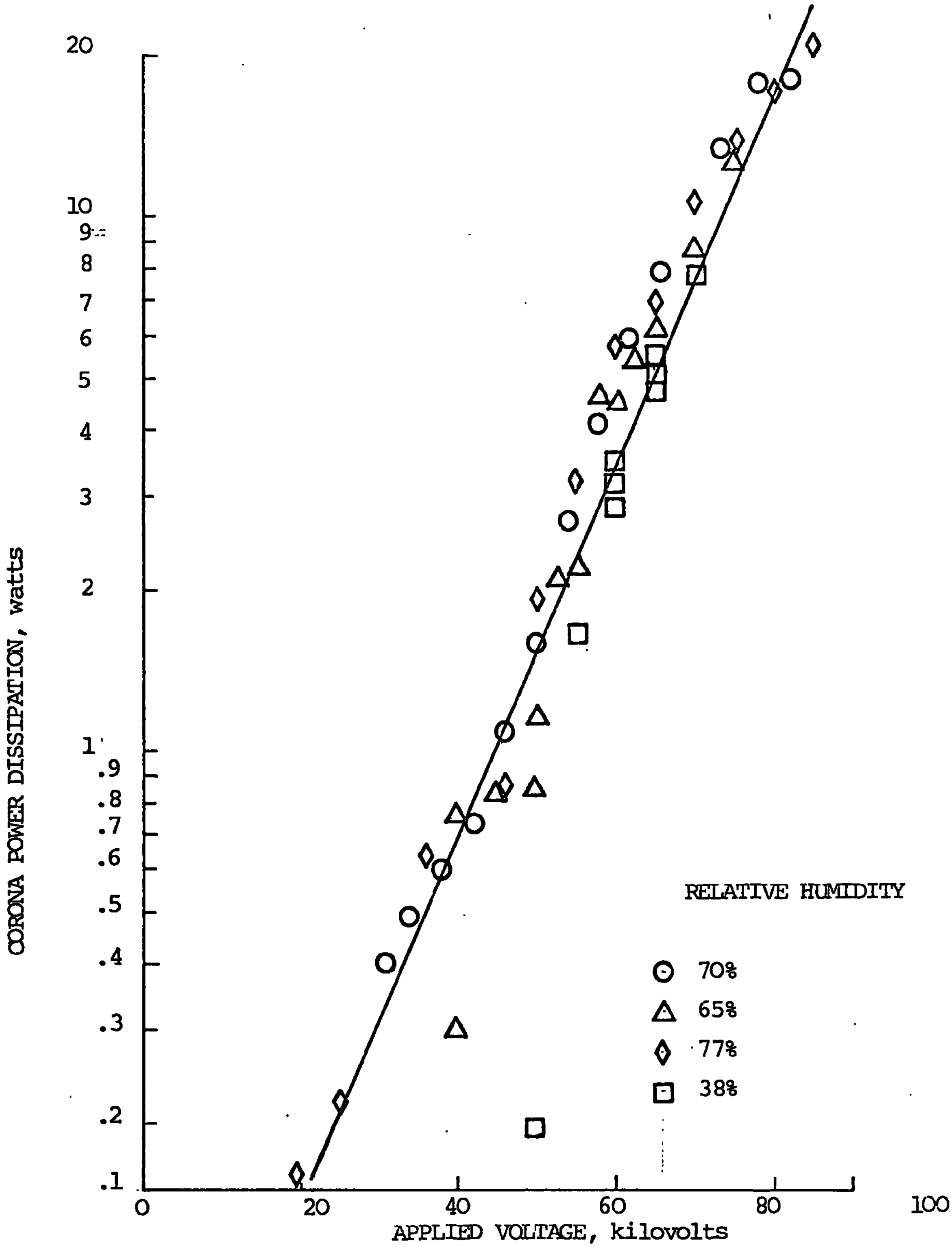

Figure 11. Corona Power Dissipation for 1.04 cm Diameter Sample.

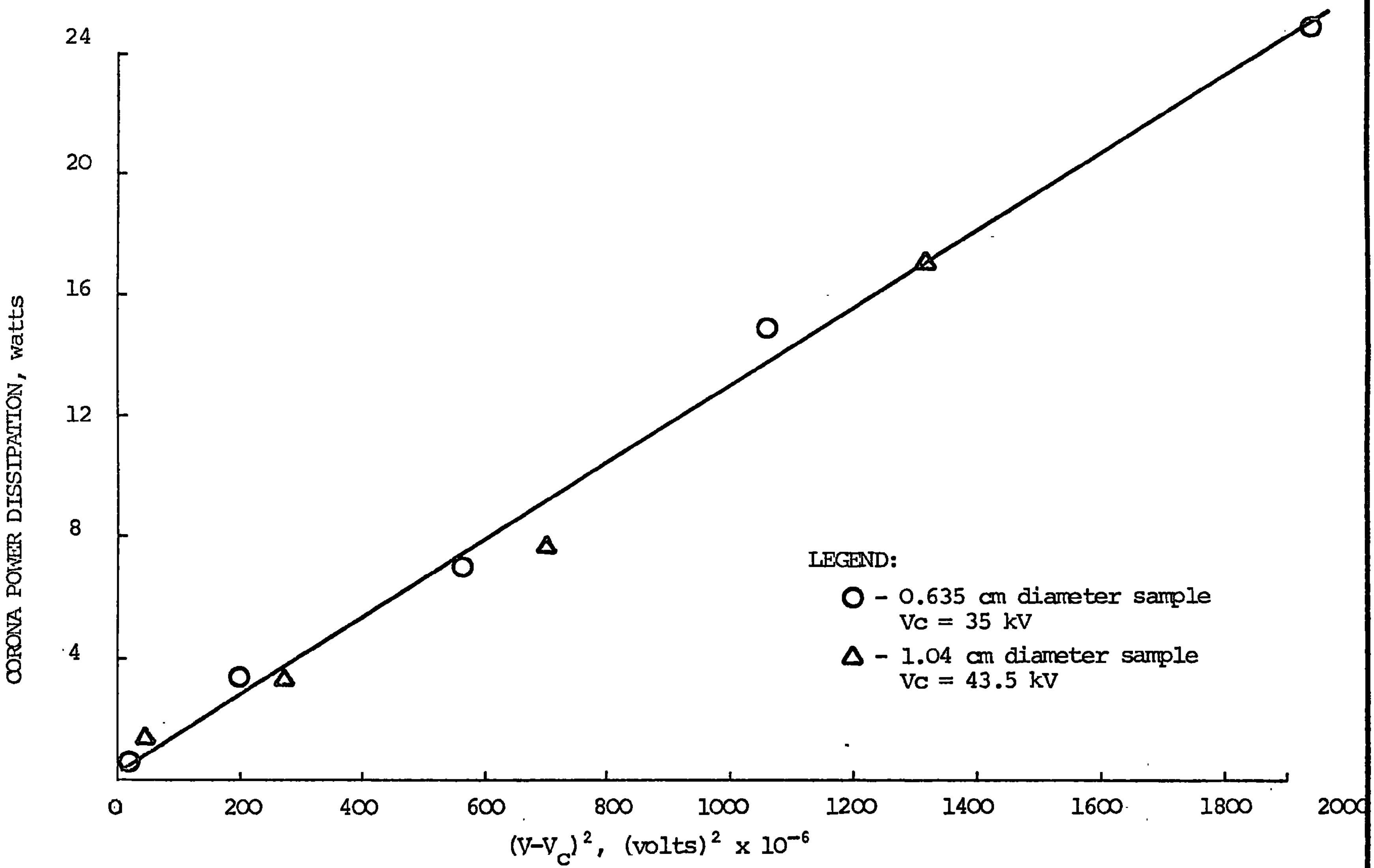

Figure 12.: Plot of Corona Power Dissipation versus $(V-V_c)^2$ for Two Conductor Sizes.

of radii a and b respectively, when b > a, is given as

$$C = 2\pi\varepsilon \, [\log_e (\frac{b}{a})]^{-1} \text{ farads,} \tag{9.}$$

which for the 0.635 cm wire yields a capacitance of

$$C \sim 15 \times 10^{-12} \text{ farads.}$$

Referring to Figure 8, the X/C ratio at the limit of zero voltage approaches unity, whereby $X = C = 5.61 \times 10^{-12}$ farads. Recalling, from Figure 2 that the cylinders were not continuous, we realize that the effective capacitance should be somewhat less than that for a pair of concentric cylinders.

2.3 Test Sample Selection and Attachment in Test Chamber

The two test samples had the following characteristics:

(a) 0.635 cm diameter - nominal gage size 2, seven aluminum strands each of nominal gage 0.023 cm.

(b) 1.04 cm diameter - nominal gage size 2/0, seven aluminum strands each of nominal gage 0.033 cm.

The test specimen, cut to a length of 1.52 meters was clamped into a four jaw chuck mounted behind the corona ring which terminated the rigid high voltage assembly and thence passed through a small hole in the center of the corona ring. The other end of the test specimen was fastened into a polished brass holder rigidly fastened to the 15 cm termination sphere. The chuck assembly was provided with an adjustment screw, accessible through the side of the horizontal high voltage connector, which was provided in order to put the specimen under sufficient tension to insure its being concentric within the test chamber.

3.0 GAS HANDLING SYSTEM AND OZONE CONCENTRATION ANALYSIS

3.1 General Description

A schematic of the gas handling system is shown in Figure 13, and the photograph in Figure 14 indicates the physical layout and approximate dimensions of the system. The basic high velocity pump for the system was a dual industrial vacuum cleaner exhausting into the outside air through an activated charcoal filter to remove the ozone formed. Flow regulation was accomplished by use of the shunting valve shown in Figure 13. Air temperature within the air flow system was determined by a mercury-in-glass thermometer placed in a baffled box so as to insure full exposure. Similarly, relative humidity was determined with an in-line humidity meter. Flow velocity in both input line (nominal 10 cm diameter) and exhaust line (nominal 3.8 cm diameter) was determined by pitot tubes in conjunction with stationary manometers calibrated against a standard wet test meter. All tubing in the air flow system was PVC pipe cemented and taped to prevent leaks.

The ozone sampling system is shown schematically in Figure 15 and photographically in Figure 16. Flow in the sampling lines was maintained at 2.1 liters/min by use of a pressure/vacuum pump monitored by flowmeters. Flowmeters were used to monitor the sampling flow into the manifold and to monitor the replacement air during ozone lifetime measurements. All small diameter tubing used in the sampling system was Teflon with Teflon or stainless steel fittings. The sampling manifold was provided to allow simultaneous sampling by a chemiluminescent ozone meter and by bubble tubes for standardization. Ozone measurements were made under standard conditions using the ozone meter at the proper internal (900 cc/min) sampling rate.

3.2 Air Leaks in System

In order to test the system for leaks which would serve to dilute

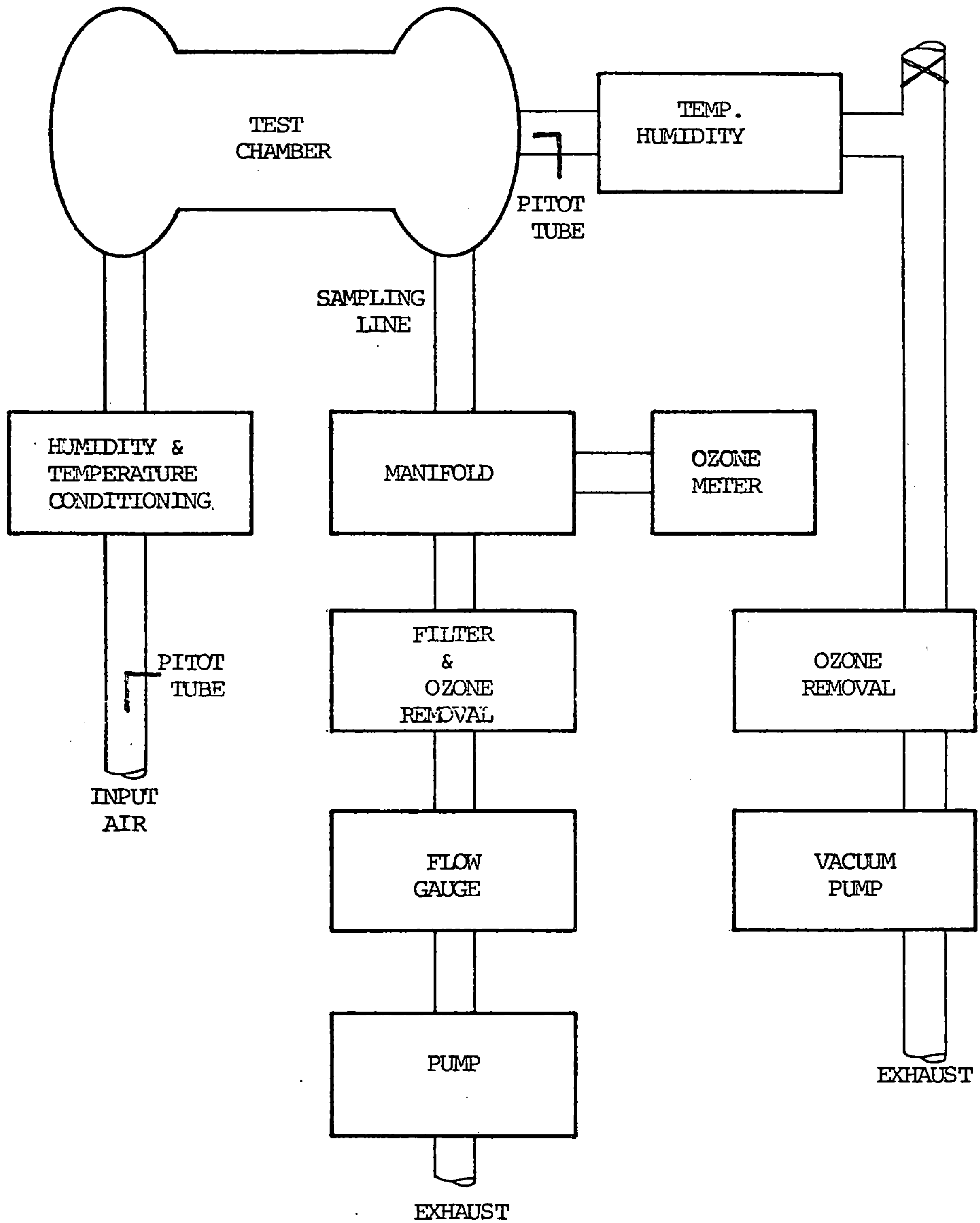

Figure 13. Schematic Diagram of Air Flow and Sampling Systems.

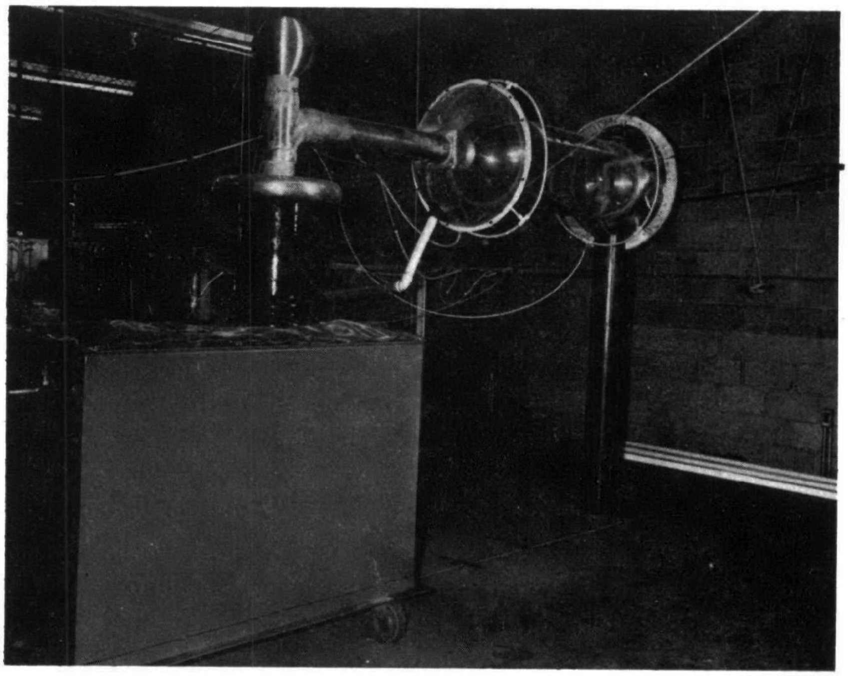

Figure 14. Overall View of Test Chamber and Air and Ozone Sampling Systems.

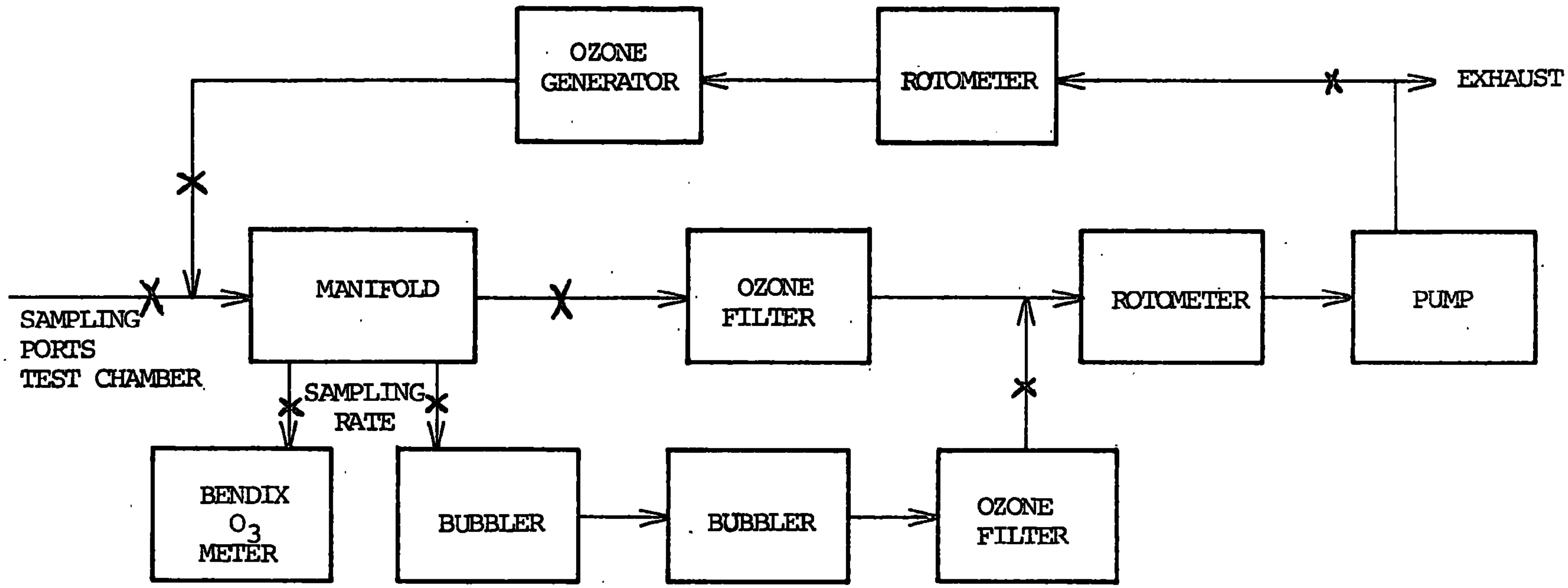

Figure 15. Schematic Diagram of Ozone Sampling and Calibration System.

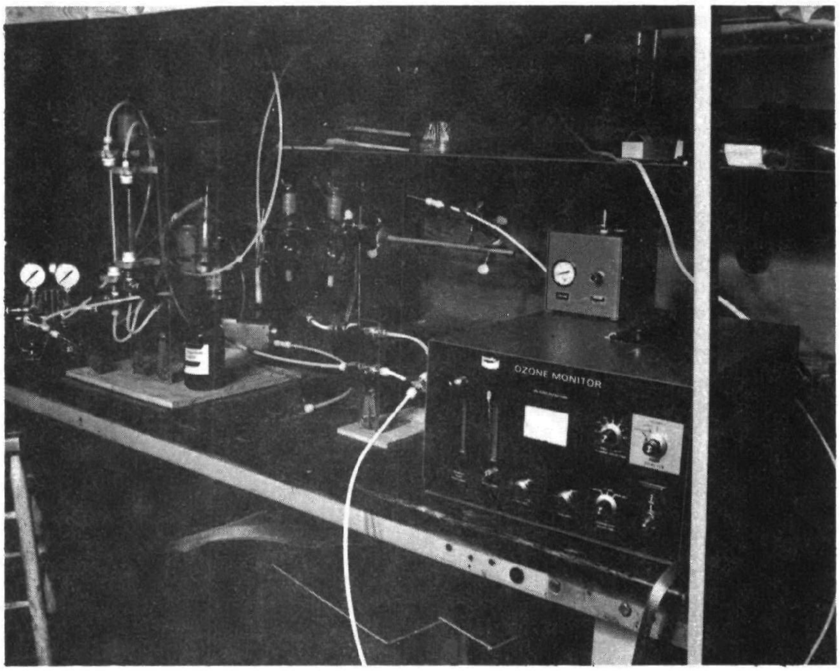

Figure 16. Ozone Monitoring and Calibration System.

the ozone-laden efflux air, the input line (76.5 cm^2 cross section) was fitted with a pitot tube and inclined manometer system. By adjusting the efflux flow from 0.5 in. (1.27 cm) of water head to a maximum of 1.62 in. (4.12 cm) of water head (velocity range from 14.3 m/sec to 26.8 m/sec) and simultaneously determining the velocity within the input tube, it was possible to estimate the losses (negative losses) by comparing the throughput within the two lines. The data are presented in Table 4. Clearly, when proper account is taken of the velocity differences corrected for by the typical 0.9 pre-factor, there is substantial agreement between the two flows, indicating no significant air leakage into the system.

3.3 Ozone Meter Calibration

The chemiluminescent ozone meter was calibrated initially and the calibration checked weekly by use of the procedure outlined in the Federal Register 36, 8195 ff (April 30, 1971)[4]. The solutions utilized for calibration were an absorbing reagent (KH_2PO_4, Na_2HPO_4 and KI), As_2O_3 standard solution, a standard iodide solution and a starch indicator solution made up as indicated in the above reference; all reagents used were analytical reagent grade or better. Using the procedure outlined in Section 8 of the cited reference [4], the spectrophotometer calibration curve was constructed, as shown in Figure 17.

Note on Figure 17 that the calibration (and, of course, all subsequent determinations) were made at 454nm, which was the wavelength providing the greatest sensitivity on our instrument. This is a deviation from Reference 4, but not an important one.

In the calibration of the ozone meter, the flow system shown schematically in Figure 15 was used. The ozone generator shown in Figure 16 was constructed along the lines of that suggested by Figure D2 in the Federal Register[4]. In the calibration procedure, 10 ml of the absorging reagent was pipetted into each all-glass impingers which were immediately closed and connected to the flow system through the sampling manifold. The ethylene (CP grade) and the flow rate to the ozone meter were adjusted and the calibration run allowed to continue for 10 minutes, after which the exposed solutions

Table 4. System Air Influx Compared to Air Efflux

INFLUX LINE (76.5 cm^2 diameter)			EFFLUX LINE (13 cm^2 diameter)			
Head ($cm\ H_2O$)	Velocity (m/sec)	Flow (m^3/sec)	Head ($cm\ H_2O$)	Velocity (m/sec)	Flow (m^3/sec)	Flow Corrected* (m^3/sec
.033	2.28	1.75×10^{-2}	1.27	14.4	1.87×10^{-2}	1.78×10^{-2}
.048	2.79	2.14×10^{-2}	1.78	17.5	2.28×10^{-2}	2.16×10^{-2}
.056	2.07	2.29×10^{-2}	2.28	19.3	2.51×10^{-2}	2.26×10^{-2}
.061	3.15	2.41×10^{-2}	2.54	20.3	2.64×10^{-2}	2.38×10^{-2}
.0685	3.35	2.56×10^{-2}	2.79	21.3	2.77×10^{-2}	2.50×10^{-2}
.076	3.50	2.68×10^{-2}	3.06	22.3	2.90×10^{-2}	2.61×10^{-2}
.081	3.60	2.66×10^{-2}	3.30	23.2	3.02×10^{-2}	2.72×10^{-2}
.086	3.73	2.86×10^{-2}	3.56	24.0	3.12×10^{-2}	2.82×10^{-2}
.088	3.81	2.92×10^{-2}	4.11	25.9	3.37×10^{-2}	3.04×10^{-2}

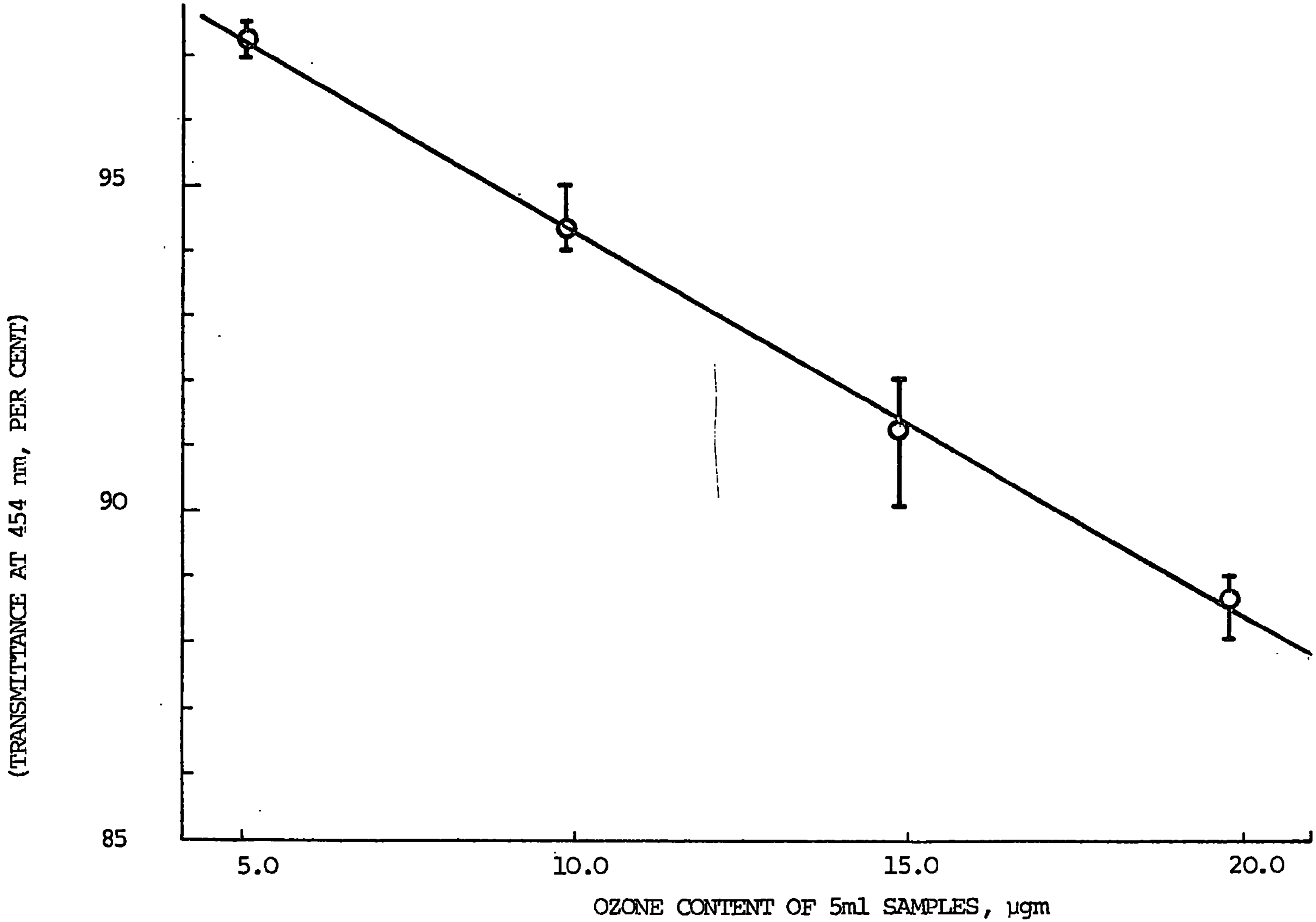

Figure 17. Spectrophotometric Calibration for Ozone Concentration Measurements

were measured on the photometer and the concentration of ozone determined from the calibration (Figure 17). Provisions were made to allow concentration ranges of 100 to 1000 $\mu g/m^3$ of ozone for the test calibration. In the weekly calibration setup the flow rate through the ozone generator was adjusted to produce 700 $\mu gm/m^3$ (0.35 ppm) of ozone for a spot check of the instrument.

3.4 Lifetime Measurements

To determine the lifetime of ozone in the test chamber under varying conditions of relative humidity and air temperature, the following procedure was utilized. Ozone, at a concentration of the order of 1 ppm, was introduced into the flow system upstream from the test chamber. After allowing a sufficient time for mixing, as evidenced by a steady concentration indicated at the sampling site, the line pumps were shut off to reduce the flow through the test chamber to zero. The sampling pump was then connected to the imput prots on the test fixture and adjusted to introduce 2.1 liter/min of ozone-free air. This input, coupled with the extraction rate of 2.1 liter/min by the sampling system, resulted in the establishment of reproducible and steady flow conditions within the test section. Ozone concentration measurements were then taken at thirty (30) second intervals for a total elapsed time of thirty (30) minutes.

Typical data are shown in semi-log plots in Figure 18 through 20. A summary of life-time data as a function of relative humidity is shown in Figure 21.

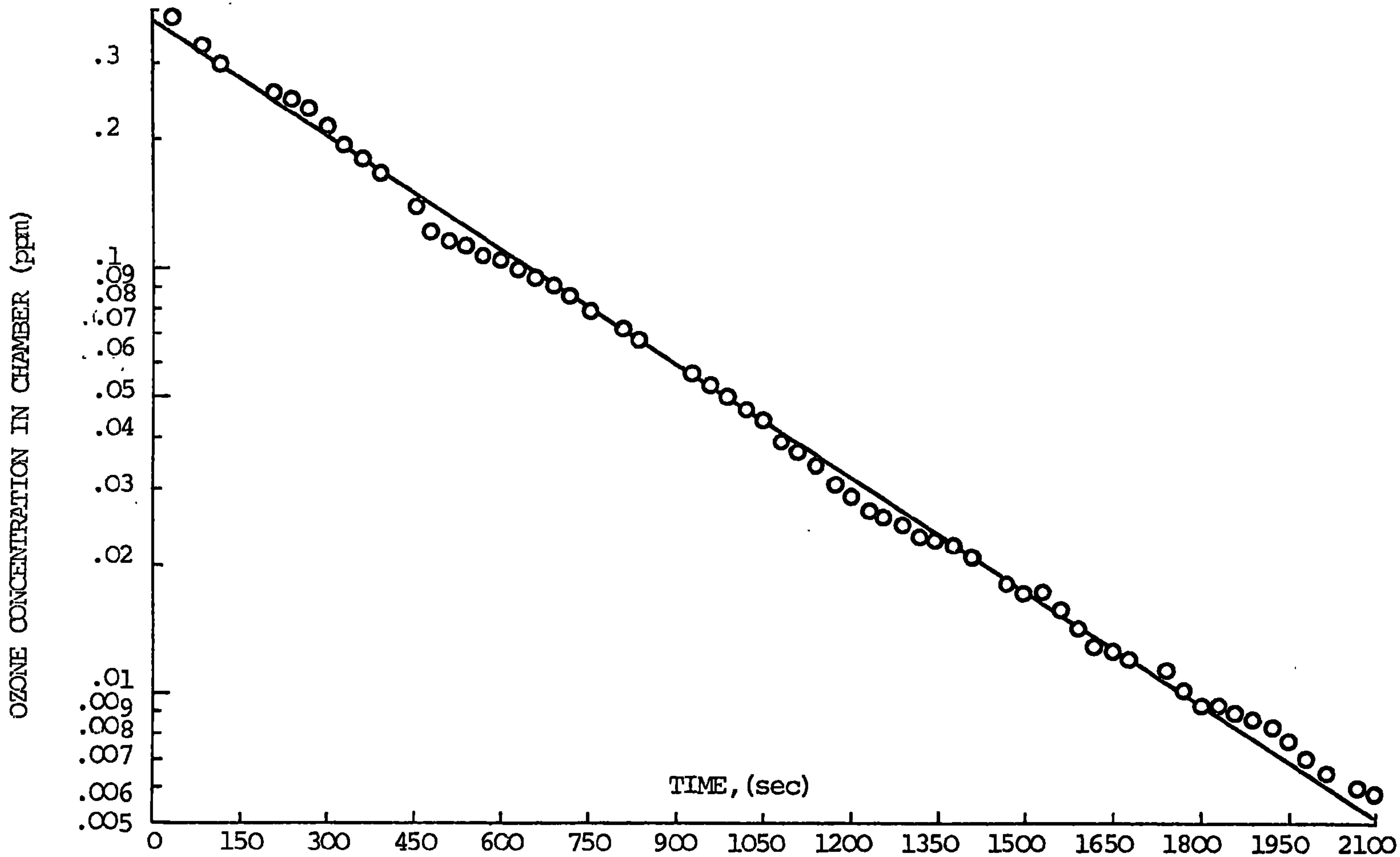

Figure 18. Ozone Concentration versus Time for 40% R.H., 296°K, 1.04 cm Diameter Sample

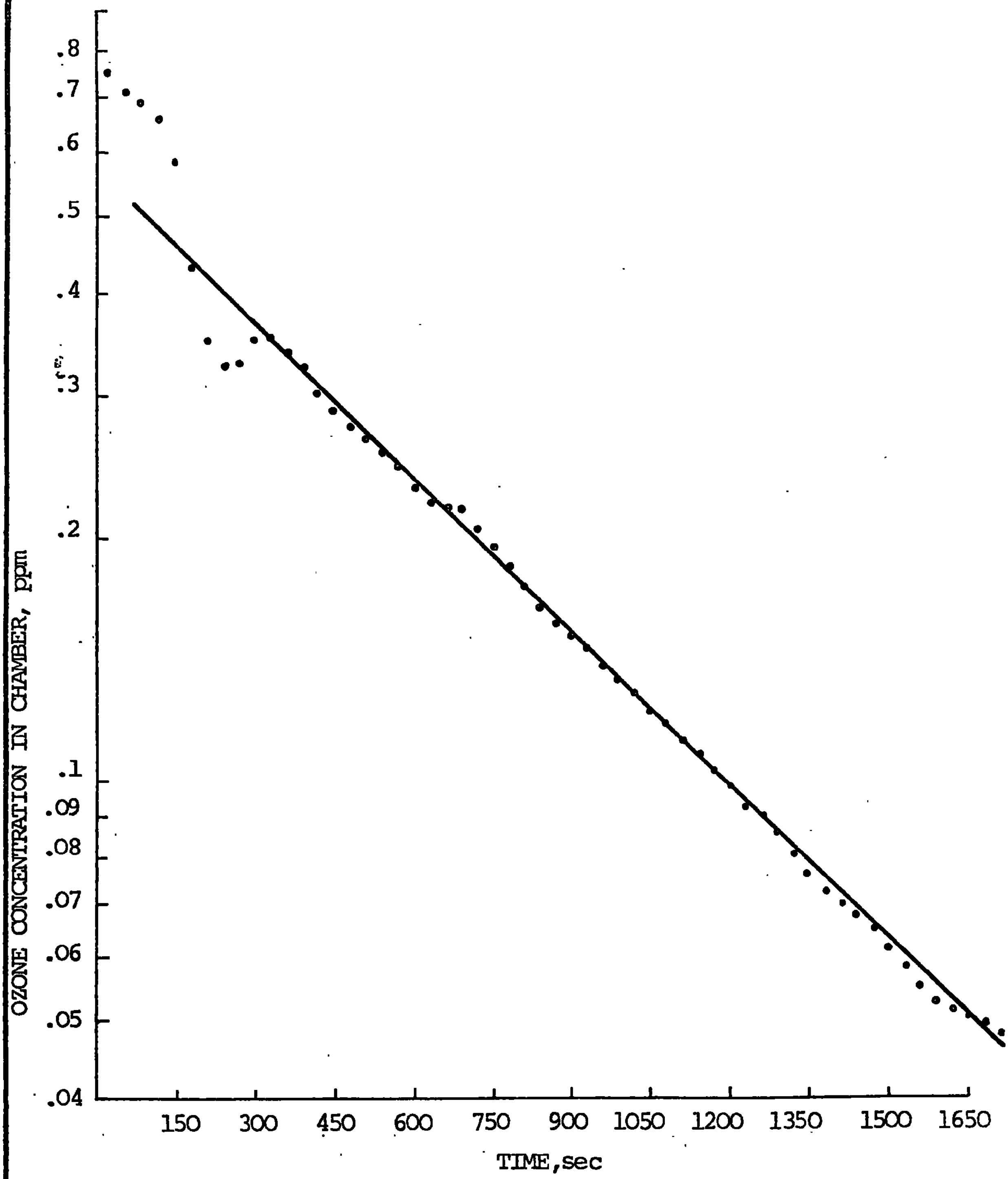

Figure 19. Ozone Concentration versus Time for 51% RH, 294°K, and 1.04 cm Sample Diameter.

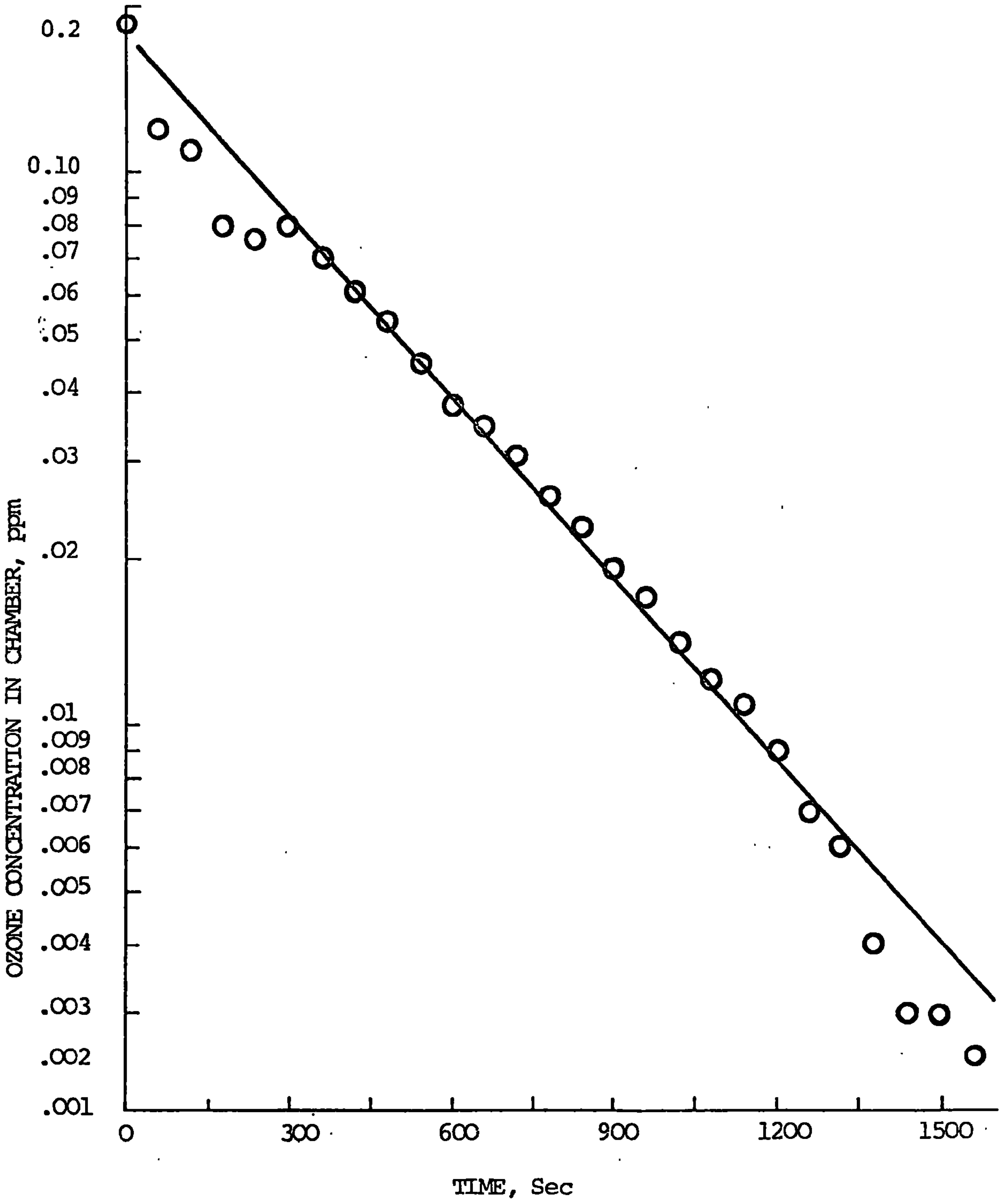

Figure 20. Ozone Concentration versus Time for 68% RH, 297°K, and 1.04 cm Sample Diameter.

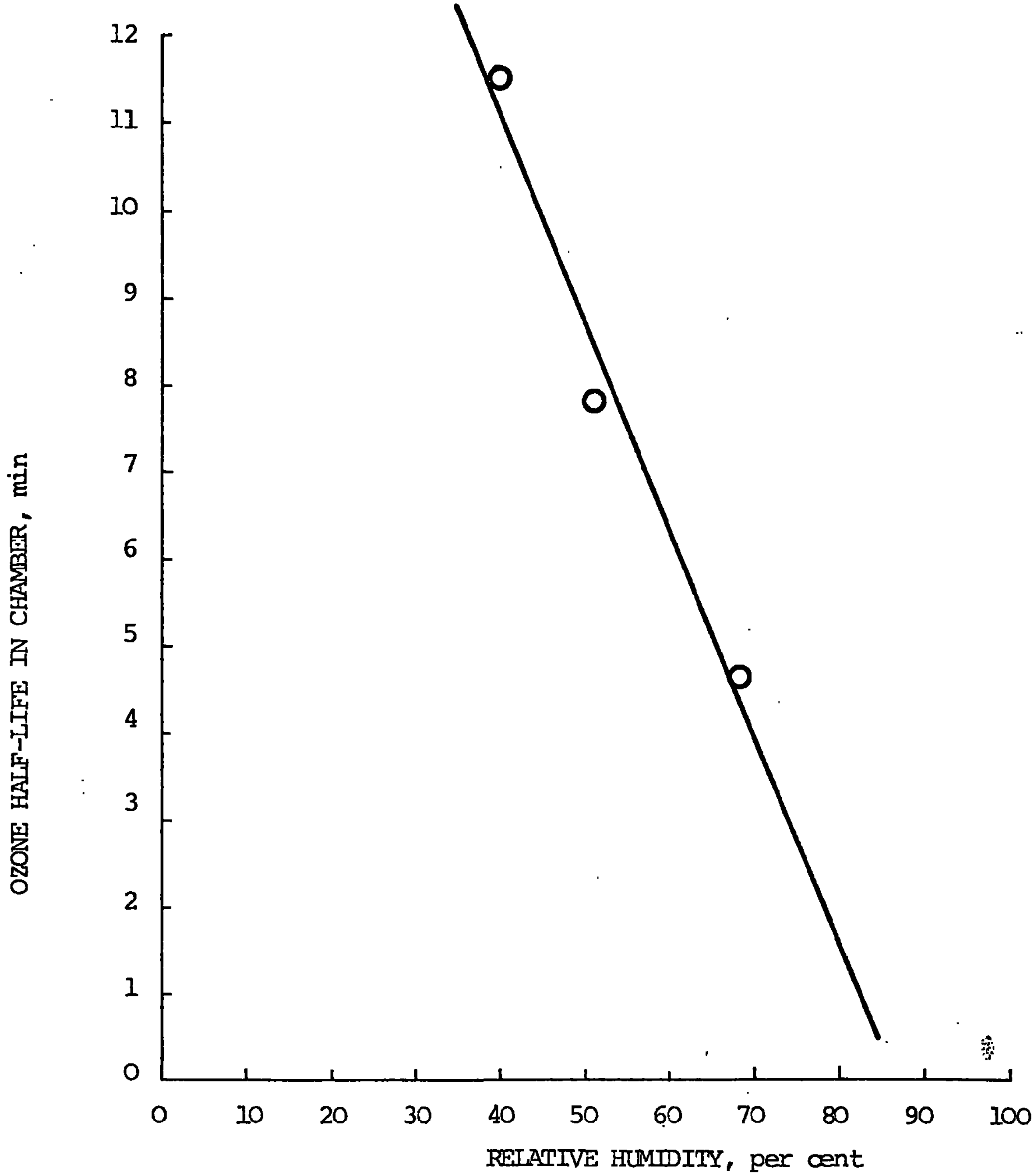

Figure 21. Effect of Relative Humidity on Ozone Half-Life in the Test Chamber.

4.0 EXPERIMENTAL RESULTS

4.1 General

Using the equipment and methods described in previous sections of the report, data collection required the following basic measurements for each test point:

- Barometric pressure
- Chamber pressure
- Chamber temperature
- Chamber relative humidity
- Background ozone level in chamber and test line
- Zero level and calibration of ozone meter
- Air flow velocity lead on input and efflux lines
- Applied high voltage
- Bridge balance conditions
- Ozone measurements in ppm
- Sampling volume flow in sampling manifold and in ozone meter
- Ethylene pressure and flow rate to ozone meter.

To compute the ozone production in grams per minute from the basic concentration measurements, advantage was taken of the calibration of the ozone meter which reads parts per million by volume. Then the rate of ozone production was determined as follows:

$$\alpha \text{ (gm/min ozone)} = Q \text{ (m}^3\text{/sec)} \times \rho_{O_3} \text{(gm/m}^3\text{)} \times C_{ozone} \text{(ppm)}, \qquad (10.)$$

where the ozone density was computed from the reference density of 2.14 gm/liter at 760 mm Hg and 273°K, using the perfect gas law. The chamber temperature was assumed to be that in the exhaust line from the test chamber.

VERSAR INC.

The corona power for each voltage was obtained from the bridge measurements as reported above. The yield for ozone production was then calculated from the relationship:

$$B = \frac{6 \times 10^4 \alpha}{P}$$

where B is expressed in gm/kw-hr, α in grams O_3/min, P in watts and the numerical factor serves to correct the units.

The results of a number of such measurements of B are included in Appendix A as Table A-3 for the 0.635 cm. diameter aluminum specimen and Table A-4 for the 1.04 cm. diameter aluminum specimen.

4.2 Ozone Production as a Function of Applied Voltage and Current (Corona Power)

Clearly, the rate of ozone formation, α, can be expected to increase from zero at some onset voltage at which corona-like processes begin, and to increase with voltage up to sparkover. The ozone yield, B, should be determined by the conditions in the plasma and should depend to a lesser extent on the applied voltage than α. The data presented herein are somewhat limited in terms of voltage applied in that the physical conditions of the samples and chamber were such that full breakdown (sparkover) with the accompanying noisy discharge occurred at 86 to 92 kV, depending somewhat on the atmospheric conditions and immediate previous history of the test chamber.

The test chamber was designed to operate at voltages up to 200 kV (peak-to-peak ac), and the observed breakdown limitation was probably a result of surface imperfections on the samples. This effect will be discussed further in Section 5.0.

A typical plot of ozone yield versus applied voltage for the 1.04 cm.

sample is presented in Figure 22. The internal consistency and reproducibility of the data are very good, as shown by the bars enclosing maximum and minimum values at the stated conditions. A more meaningful plot of the same yield data as a function of corona power dissipation is presented in Figure 23. Figure 23 shows that, as the power dissipation increased, ozone yield increased until a steady value of about 5.5 gm/kw-hr was attained. Although the same trend is present on Figure 22, the attainment of a steady value of ozone yield is masked as compared to Figure 23 because of the non-linear relationship between corona power dissipation and voltage.

The attainment of a constant ozone yield at higher values of voltage and corona power dissipation is more clearly shown on Figures 24 and 25, respectively, for the 0.635 cm. diameter sample. At the lower air flow rate the "constant" yield attained was about 5.2 gm/kw-hr, which is consistent with the value for the larger wire. Similar plots can be obtained from other data in Tables A-3 and A-4 in Appendix A.

4.3 Effects of Air Flow Velocity

Assume an equation of continuity which equates the change in mass of ozone in the test chamber as being equal to the rate of production less the losses due to recombination or decomposition (by whatever process) and less the loss due to the efflux of air from the chamber, *viz.*:

$$\frac{dM}{dt} = BP - (\lambda M + QC) \qquad (12.)$$

where
- B = ozone yield (gm/kw-hr)
- P = Corona Power (kw-hr/sec)
- λ = decay constant (sec^{-1})
- Q = flow rate (m^3/sec)
- C = ozone concentration (V/V) gm/m^3
- V = volume of test chamber (m^3)

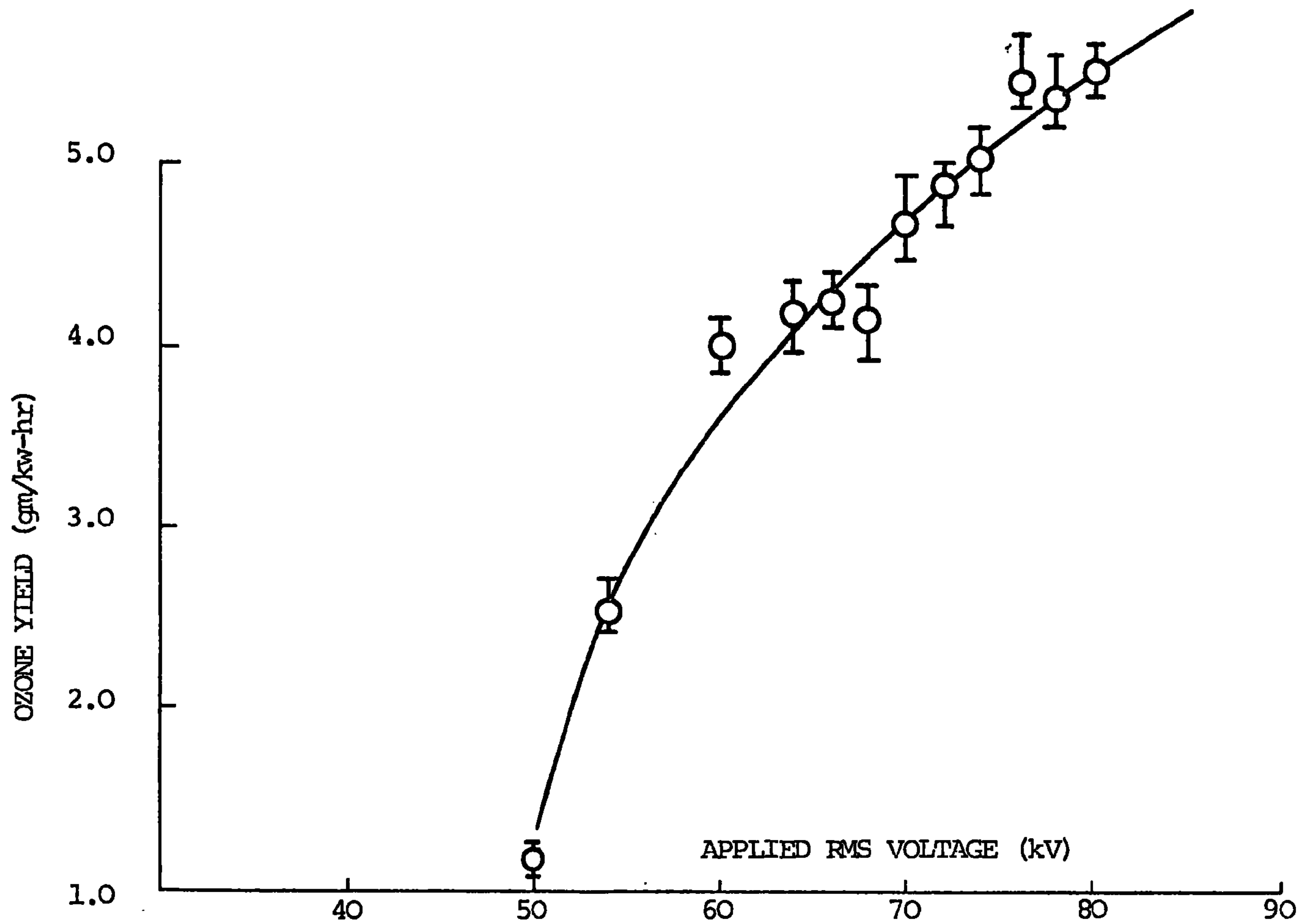

Figure 22. Plot of Ozone Yield versus Applied Voltage for 1.04 cm Diameter Sample (Temp. = 299.5°K, Relative Humidity = 65°)

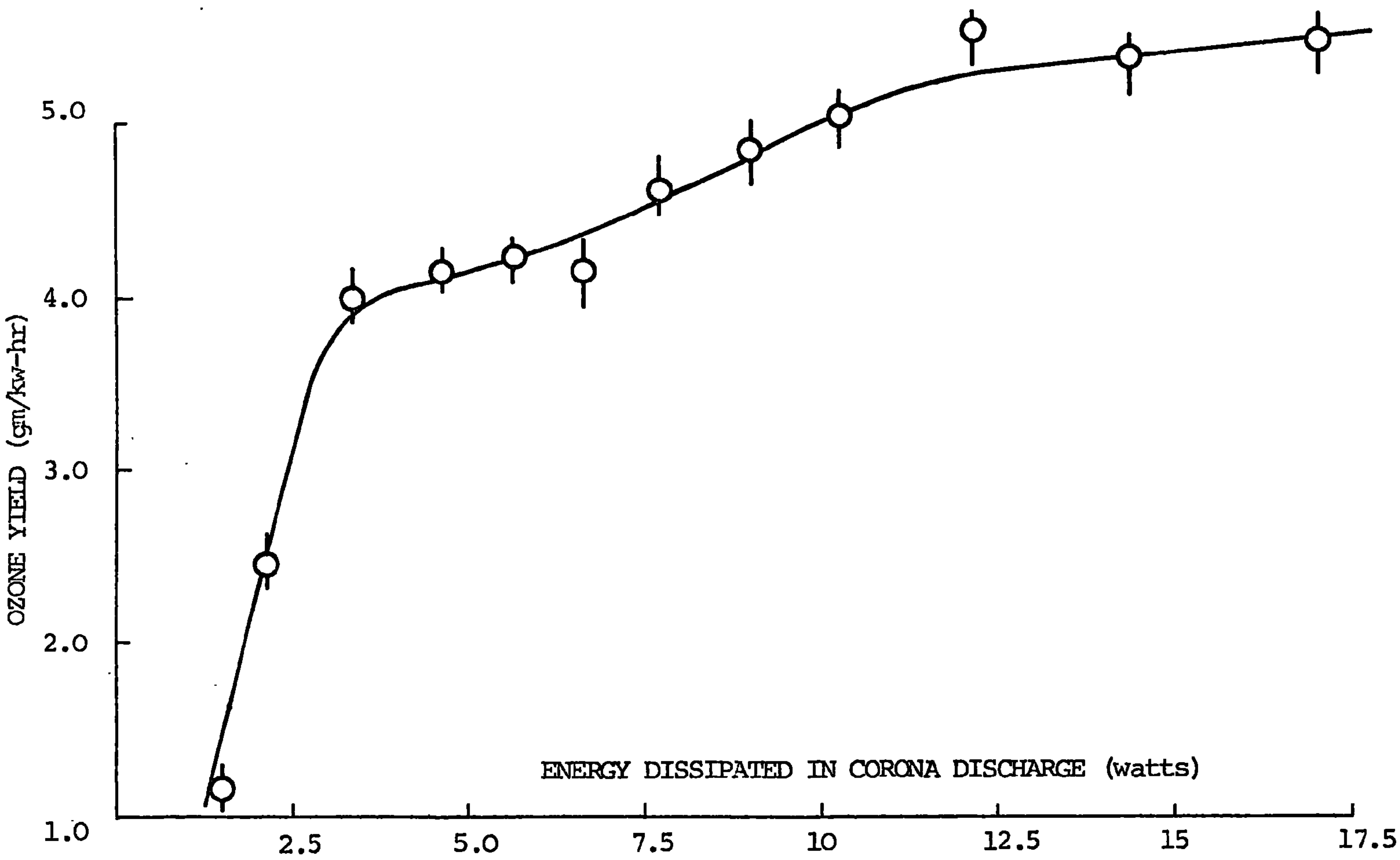

Figure 23. Plot of Ozone Yield for 1.04 cm Diameter Sample versus Corona Power Dissipation (Conditions on Figure 22)

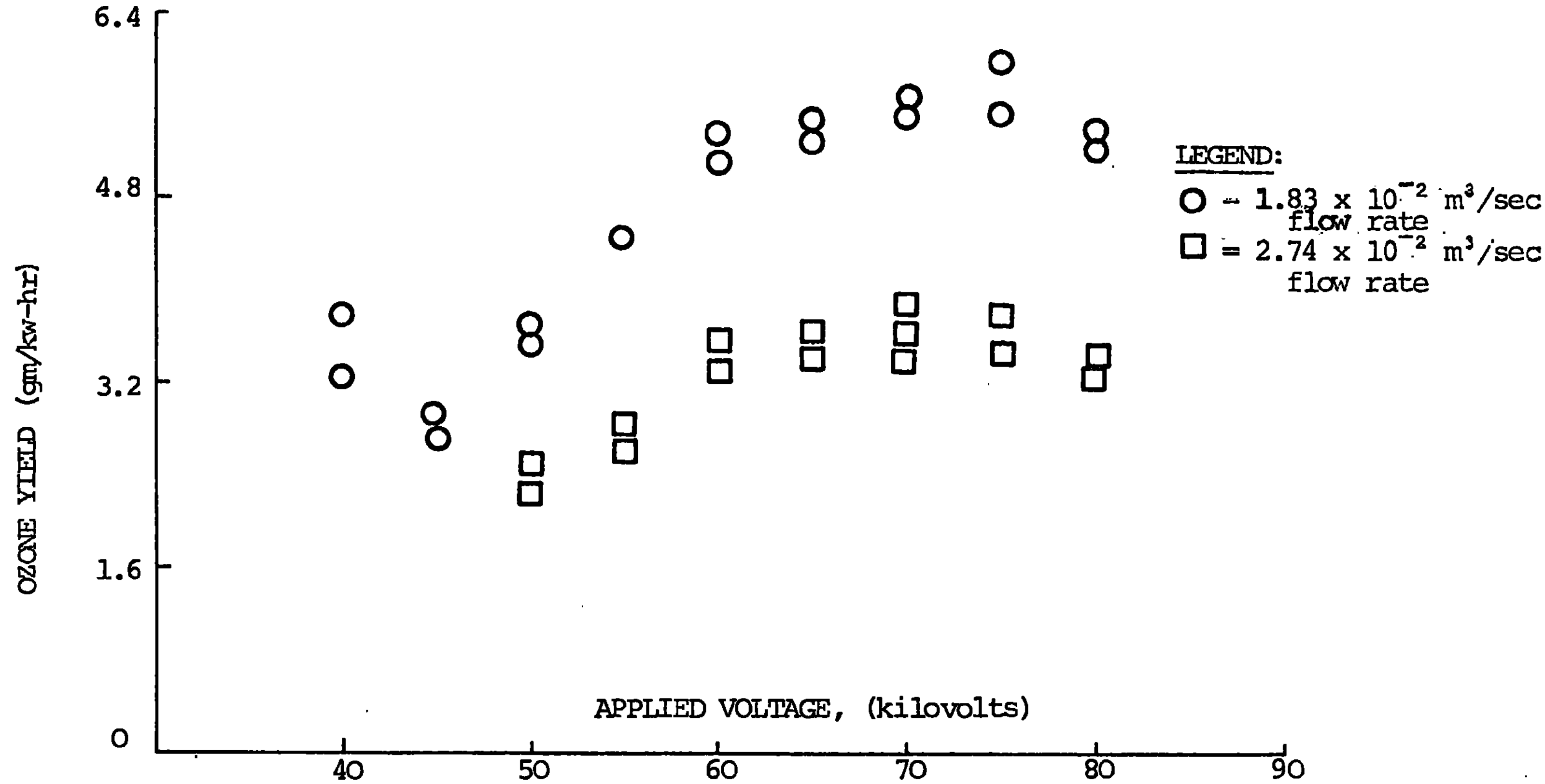

Figure 24. Plot of Ozone Yield Versus Applied Voltage for 0.635 cm Diameter Sample (Temp. = 299°K, Relative Humidity = 51%)

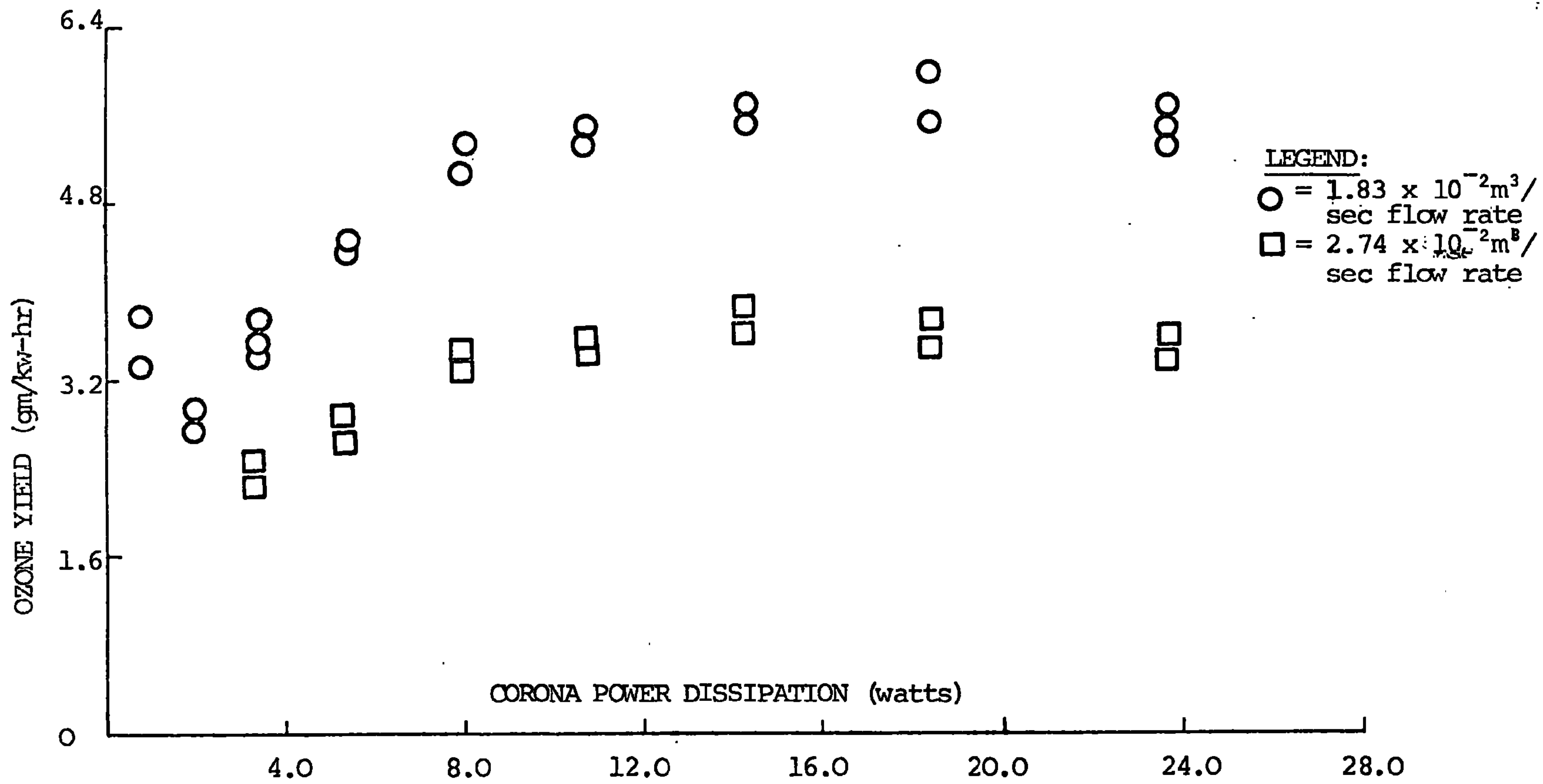

Figure 25. Plot of Ozone Yield versus Corona Power Dissipation for 0.635 cm Diameter Sample (Conditions on Figure 24)

Then:

$$\frac{dC}{dt} = \frac{BP}{V} - (\lambda + \frac{Q}{V})C \quad .$$

Integrating, $$C = \frac{BP}{V\lambda + Q}(1 - e^{-(\lambda+\frac{Q}{V})t} \qquad (13.)$$

At steady state $C = C_e, t \rightarrow \infty$

$$\frac{1}{C_e} = \frac{V\lambda}{BP} + \frac{Q}{BP}$$

$$\frac{1}{C_e} = a + bQ \qquad (14.)$$

Thus a plot of $\frac{1}{C_e}$ *vs* Q with V, T, relative humidity and geometry fixed should be a straight line as is shown in Figure 26.

Recalling that:

$$B \sim \frac{QC}{P}\text{, then } \frac{1}{B} \sim \frac{P}{QC}$$

or $$\frac{1}{B} \sim \frac{a}{Q} + b, \qquad (15.)$$

which is illustrated in Figure 27.

The most significant feature of the curves in Figure 27 lies in the drastic change in behavior noted at $Q^{-1} \sim 35$ or $Q \sim 2.85 \times 10^{-2}$ m^3/sec whereas the behavior of $\frac{1}{B}$ *vs* $\frac{1}{Q}$ is markedly altered. Taking the chamber dimension of 0.249 m^3, the Q/V ratio is then equal to 0.104 sec^{-1} corresponding to a "time constant" of the order of 8.8 seconds. Recalling the very rapid decay in ozone concentration under static conditions that occurs in the first few seconds of a lifetime measurement, (see Figures 18 through 20), it is likely that for very short dwell times (less than approximately 10 seconds) and thus,

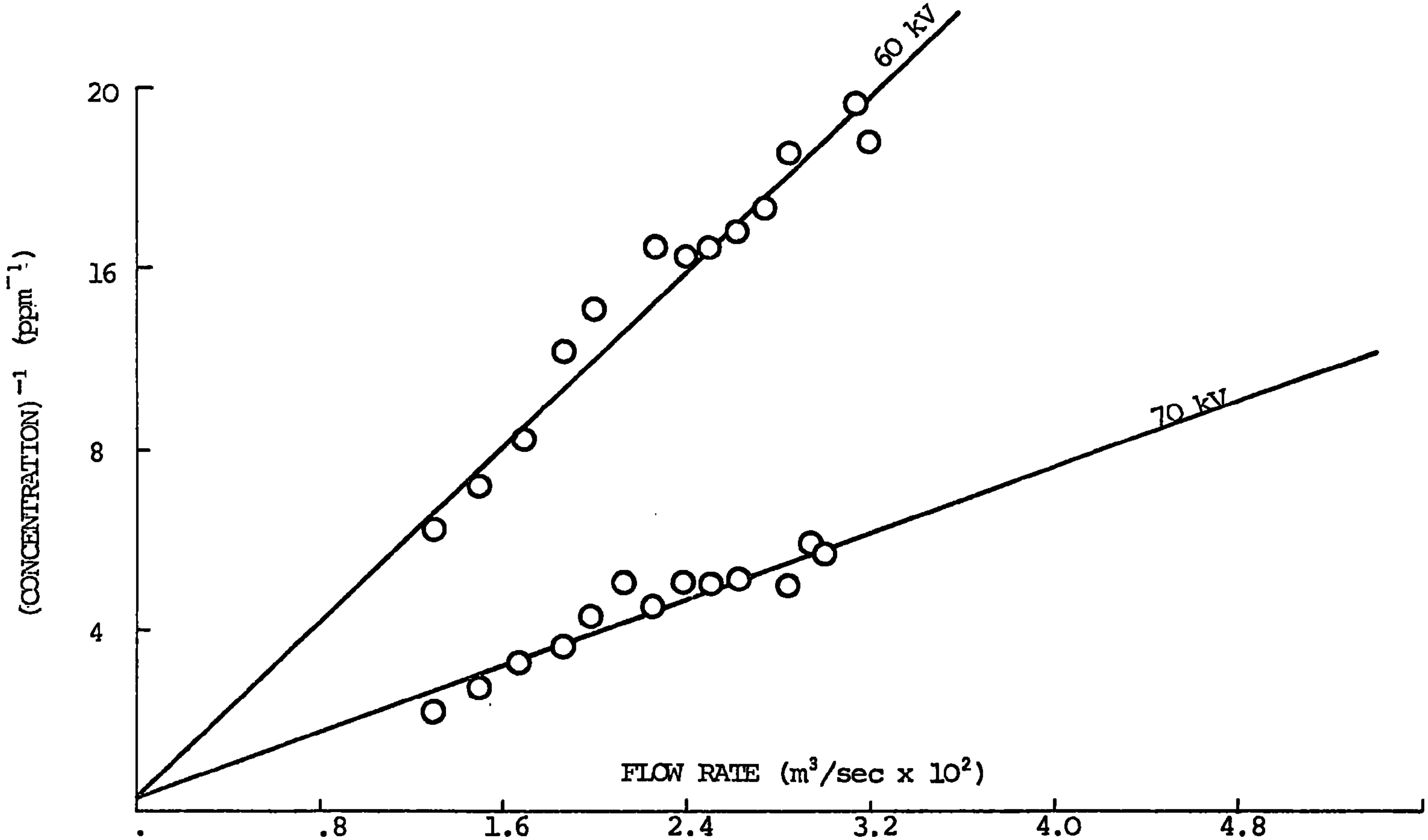

Figure 26. Plot Equilibrium Concentration of Ozone as a Function of Flow Rate (Eq. 14.) (Temp. = 300°K, Relative Humidity = 66%, 1.04 cm diameter sample)

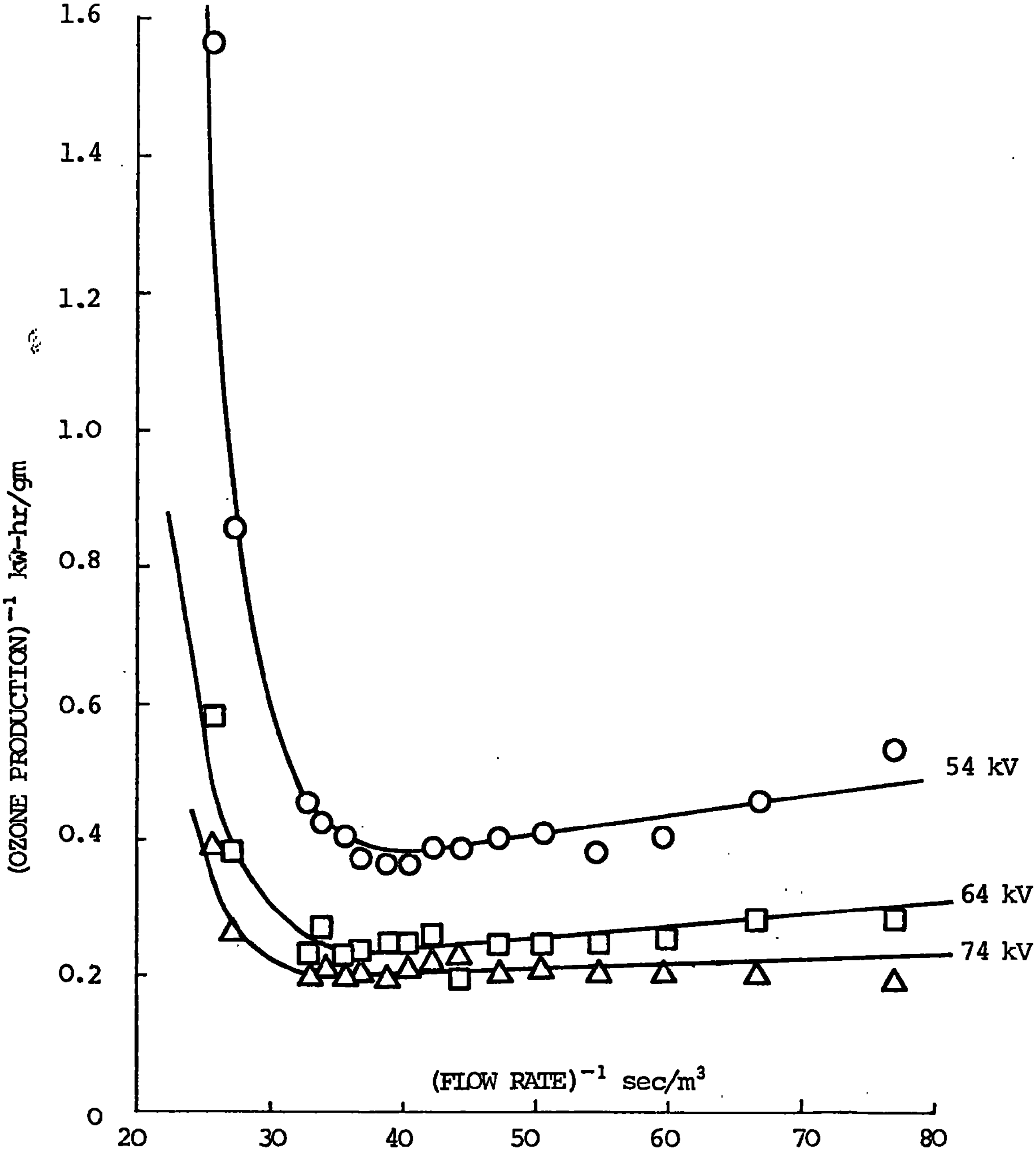

Figure 27. Plot of Effect of Flow Velocity on Ozone Production (Temp. = 297°K, Relative Humidity = 36%, 1.04 cm Diameter Wire)

for very high flow rates, this initial decay process is effective in establishing the ozone levels. This behavior is best shown in the example plotted in Figure 28 which shows B in gm/kw-hr *vs* Q^{-1} for the 1.04 cm diameter sample at relative humidity of 66%, and temperature of 297°K and applied voltage 54 kilovolts. The latter plot clearly indicates the altered behavior of B *vs* Q^{-1} at flow rates of the order of 2.50×10^{-2} m^3/sec or dwell times of the order of 10 seconds or less.

Careful consideration of these results yields the result that, for this geometry and relative humidity,

$$\lambda = -0.1 \text{ sec}^{-1}$$

so that the exponential in Eq. (13.) is positive for $\frac{Q}{V} \leq 0.1$ and that B increases as $\frac{Q}{V}$ increases from 0 to 0.1, or Q increases from 0 to 2.5×10^{-2} m^3/sec. For values of $Q > 2.5 \times 10^{-2}$ m^3/sec, the exponential is negative. The relevant equation then takes the form

$$B \sim \alpha \frac{(Q/V)}{(\frac{Q}{V} - 0.1)} \left\{ 1 - e^{-(\frac{Q}{V} - 0.1)t} \right\}$$

where t, the transit time, is given by $\frac{V}{Q}$, whereupon

$$B \sim \alpha \frac{(Q/V)}{(\frac{Q}{V} - 0.1)} \left\{ 1 - e^{-(1 - \frac{V}{10Q})} \right\} \qquad (16.)$$

which yields a maximum in B at $\frac{Q}{V} \to 0.1$. Expression does not vanish because the denominator approaches zero at approximately the same rate as does the numerator at $\frac{Q}{V} \to 0.1$, and the resulting indeterminate form has a finite limit $B_{\left(\frac{Q}{V} \to 0.1\right)} \sim \frac{\alpha}{V}$.

It should be noted that the particular value of $Q \sim 2.5 \times 10^{-2}$ m^3/sec at which B approaches its maximum value is dictated by the combination of the chamber short time constant $\lambda \sim 10$ sec and the volume of the chamber.

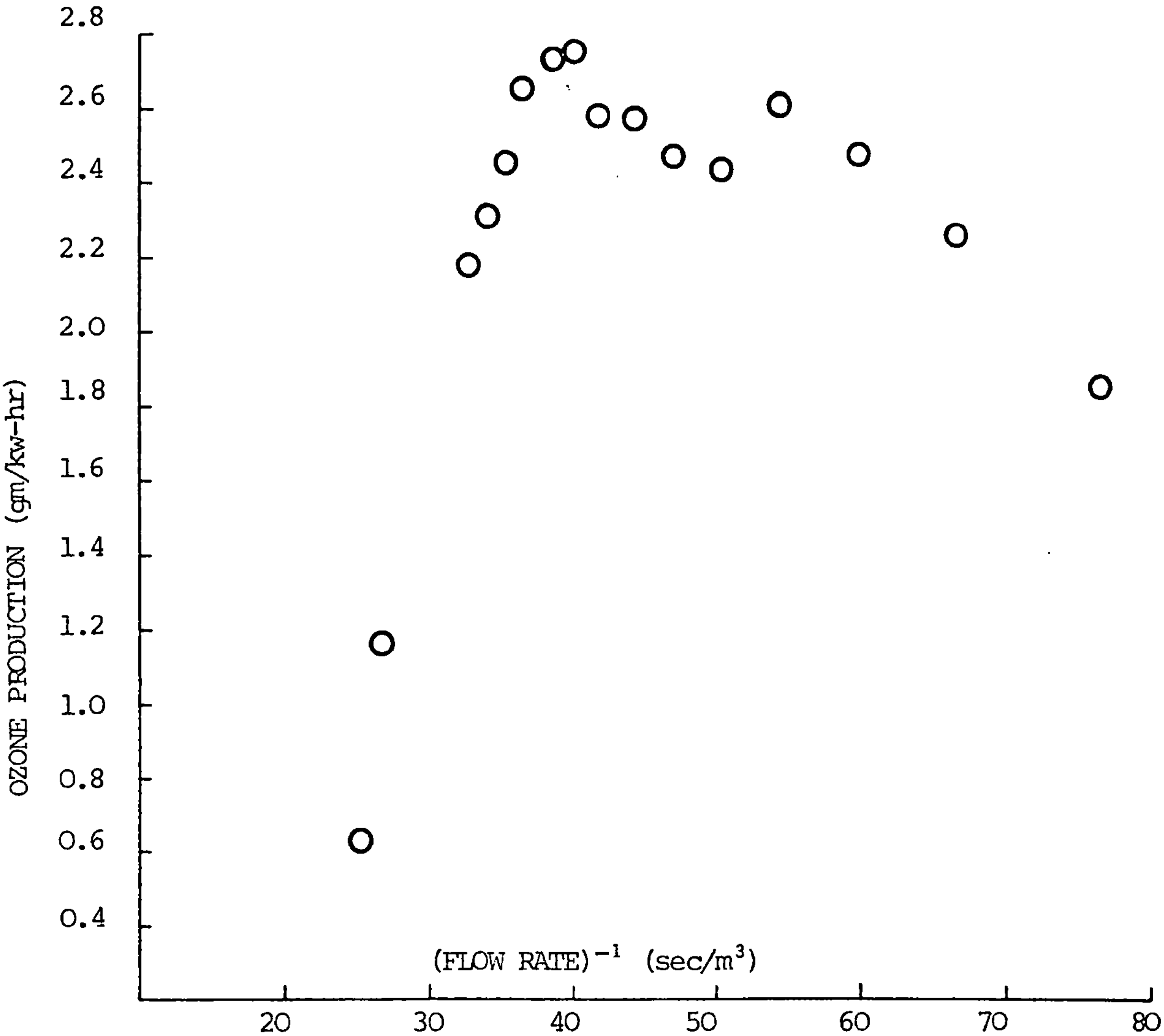

Figure 28. Plot of Ozone Production as a Function of (flow velocity)$^{-1}$ (Temp. 296-298°K, Relative Humidity 65-66%, 1.04 cm Diameter Specimen)

When the corresponding analysis is applied to the data from the 0.635 cm wire at 51% relative humidity the corresponding peak flow rate is about 3.25 x 10^{-2} m^3/sec, corresponding to a transit time of the value of 7.7 sec. The data for this analysis are shown in Tables 5 through 8 and in Figures 29 through 31 which follow.

4.4 Effects of Relative Humidity

From the data presented in the previous section it is apparent that the salient effect of relative humidity lies in its effect on those molecular processes that affect the life time of the electrically created ozone. Specifically, one can determine a rough estimate of the rate constant defined as λ above, from the plots of ozone production against Q^{-1} (sec/m^3) as shown in Figures 29 through 31.

Equation (16.) in general form is

$$B \sim \frac{\frac{Q}{V}}{\frac{Q}{V} + \lambda} \left\{ 1 - e^{-(\frac{Q}{V} + \lambda)t} \right\} \qquad (16.)$$

where the factor $\lambda = \lambda(RH)$ and where the appropriate numerical factors have been omitted. Hence, the relative humidity effects on ozone production clearly depend on the magnitude of the ratio of the flow velocity to the static volume of the test cell (Q/V) and the dwell time within the chamber (t = V/Q). The data shown in Figure 32 suggest that λ is essentially constant above about 40% relative humidity, but that there is a real decrease in λ at relative humidities well below 40%.

4.5 Effects of Air Temperature

The data presented in Appendix A represent ozone production measurements over the temperature range of 293°K to 307.4°K, a range of 14°C. To the precision of the data presented there is no significant effect on the ozone production due to variation in air temperature over this range. Because of this lack of

Table 5. Flow Velocity Effects on Ozone Production (1.04 cm Wire, Relative Humidity 65-66%, Air Temperature 296-298°K)

Q (m /sec x 10^2)	1/Q (sec/m)	B_{54kV} (gm/kw-hr)	B^{-1}_{54kV} (gm/kw-hr)$^{-1}$	B_{64kV} (gm/kw-hr)	B^{-1}_{64kV} (gm/kw-hr)$^{-1}$	B_{74kV} (gm/kw-hr)	B^{-1}_{74kV} (gm/kw-hr)$^{-1}$
1.30	77	1.86	.535	3.50	.286	5.07	.197
1.50	66.7	2.28	.459	3.50	.286	5.07	.197
1.67	39.8	2.49	.402	3.96	.252	4.87	.205
1.83	54.6	2.61	.383	4.02	.248	5.04	.199
1.98	50.5	2.44	.41	4.03	.248	4.78	.209
2.12	47.2	2.47	.405	4.07	.246	4.98	.201
2.24	44.6	2.57	.390	5.10	.196	4.54	.221
2.37	42.2	2.57	.390	3.84	.260	4.73	.211
2.48	40.4	2.76	.362	4.02	.248	4.69	.213
2.59	39	2.73	.366	4.12	.243	5.20	.193
2.71	36.9	2.66	.375	4.35	.230	4.85	.206
2.80	35.7	2.46	.406	4.43	.226	5.04	.199
2.90	34.5	2.31	.423	3.68	.272	4.95	.202
2.99	33.0	2.18	.457	4.45	.225	4.78	.209
3.67	27.2	1.17	.855	2.59	.386	3.82	.262
3.89	25.7	0.642	1.56	1.72	.58	2.53	.396

Table 6. Flow Velocity Effects on Ozone Production (0.635 cm wire, Relative Humidity 51%, Air Temperature 297°K)

Q (m^3/sec x 10^2)	1/Q (sec/m^3)	B_{50KV} (gm/kw-hr)	B_{60KV} (gm/kw-hr)	B_{70KV} (gm/kw-hr)	B_{80KV} (gm/kw-hr)
1.83	54.5	3.57	5.32	5.58	5.45
1.83	54.5	3.71	5.32	5.63	5.37
1.83	54.5	3.50	5.10	5.58	5.65
2.26	44.2	1.07	3.15	3.66	3.70
2.26	44.2	1.15	3.15	3.66	3.90
2.26	44.2	1.13	4.22	3.88	4.26
2.74	36.6	2.49	3.29	3.78	3.40
2.74	36.6	2.28	3.29	3.86	3.45
2.74	36.6	2.28	3.42	3.52	3.27
3.86	26.5	.768	2.26	4.35	5.30
3.67	27.3	4.55	5.12	6.10	6.57
3.53	28.4	6.80	7.50	7.50	-
3.26	30.7	6.60	8.56	8.04	-
3.14	31.8	8.00	12.2	9.30	-
2.79	35.8	8.40	9.2	9.02	-

Table 7. Flow Velocity Effects on Ozone Production (0.635 cm Diameter Specimen, Temperature 299°K, Relative Humidity 38%)

Q (m^3/sec)	Q^{-1} (sec/m^3)	B (gm/kw-hr) 50 kilovolts	B (gm/kw-hr) 80 kilovolts
2.11×10^{-2}	47.4	1.81	4.61
2.11×10^{-2}	47.4	1.91	4.61
2.11×10^{-2}	47.4	1.91	4.76
2.52×10^{-2}	39.7	2.59	4.61
2.52×10^{-2}	39.7	2.79	4.56
2.52×10^{-2}	39.7	2.74	4.61
2.83×10^{-2}	35.3	1.25	5.40
2.83×10^{-2}	35.3	1.11	5.40
2.83×10^{-2}	35.3	1.25	5.27
3.16×10^{-2}	31.8	.565	4.15
3.16×10^{-2}	31.8	.775	4.06
3.16×10^{-2}	31.8	-	4.18
3.47×10^{-2}	28.8	1.07	3.38
3.47×10^{-2}	28.8	1.24	3.56
3.47×10^{-2}	28.8	-	3.38
4.02×10^{-2}	24.8	-	3.73
4.02×10^{-2}	24.8	-	3.55
4.02×10^{-2}	24.8	-	3.55

Table 8. Flow Velocity Effects on Ozone Yield (0.635 cm diameter specimen, Temperature 299°K, Relative Humidity 33%)

Q (m^3/sec)	Q^{-1} (sec/m^3)	B (gm/kw-hr) 50 kilovolts	B (gm/kw-hr) 60 kilovolts	B (gm/kw-hr) 70 kilovolts
3.85×10^{-2}	25.6	0.875	2.11	3.27
3.78×10^{-2}	26.4	4.52	5.65	7.30
3.34×10^{-2}	30.0	6.64	8.24	10.30
3.17×10^{-2}	31.6	7.12	9.25	11.20
2.83×10^{-2}	35.3	9.05	10.90	-

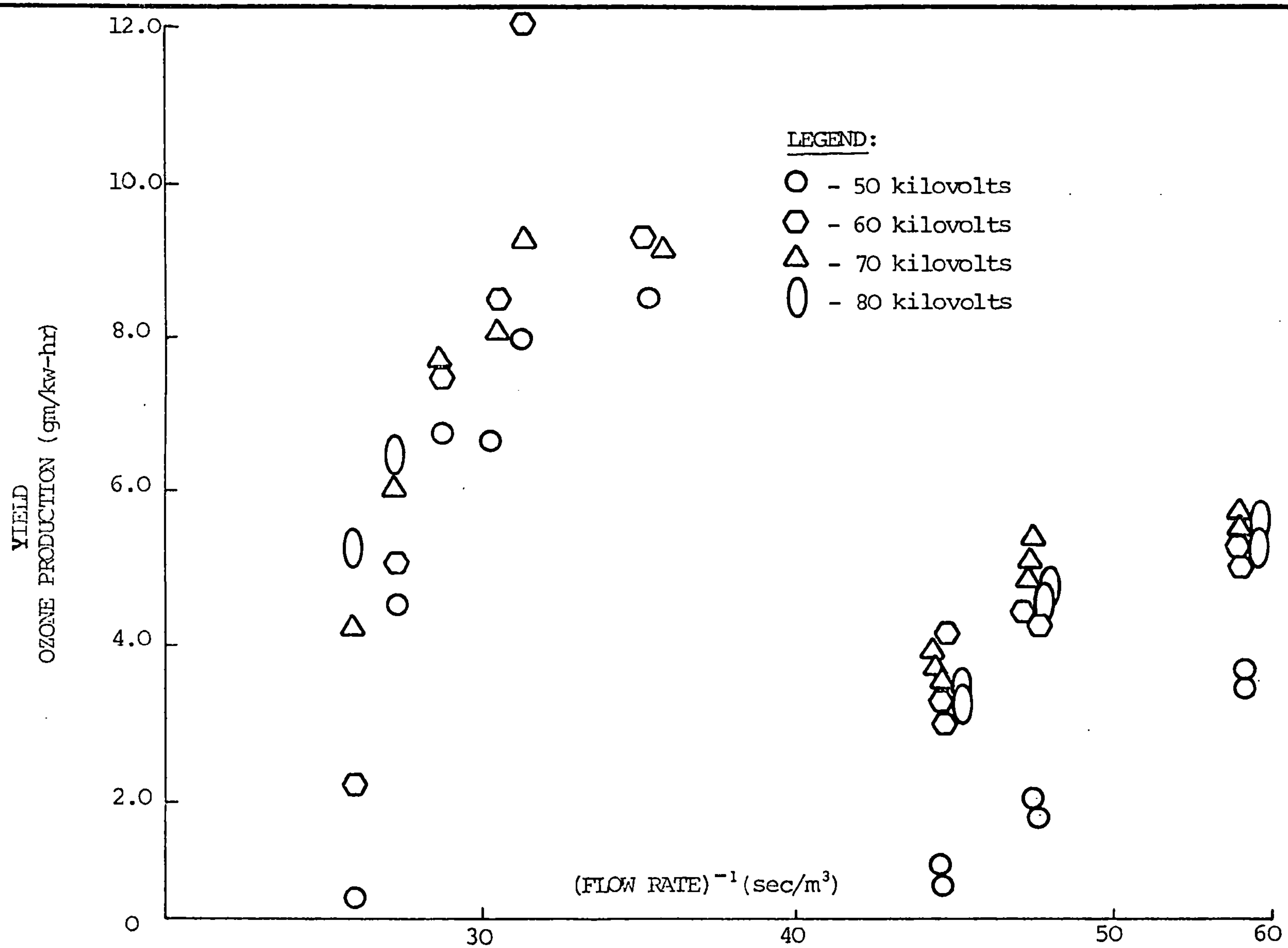

Figure 29. Plot of Ozone Production as a Function of (flow rate)$^{-1}$ (Temperature 298°K, Relative Humidity 51%, 0.635 cm Diameter Specimen).

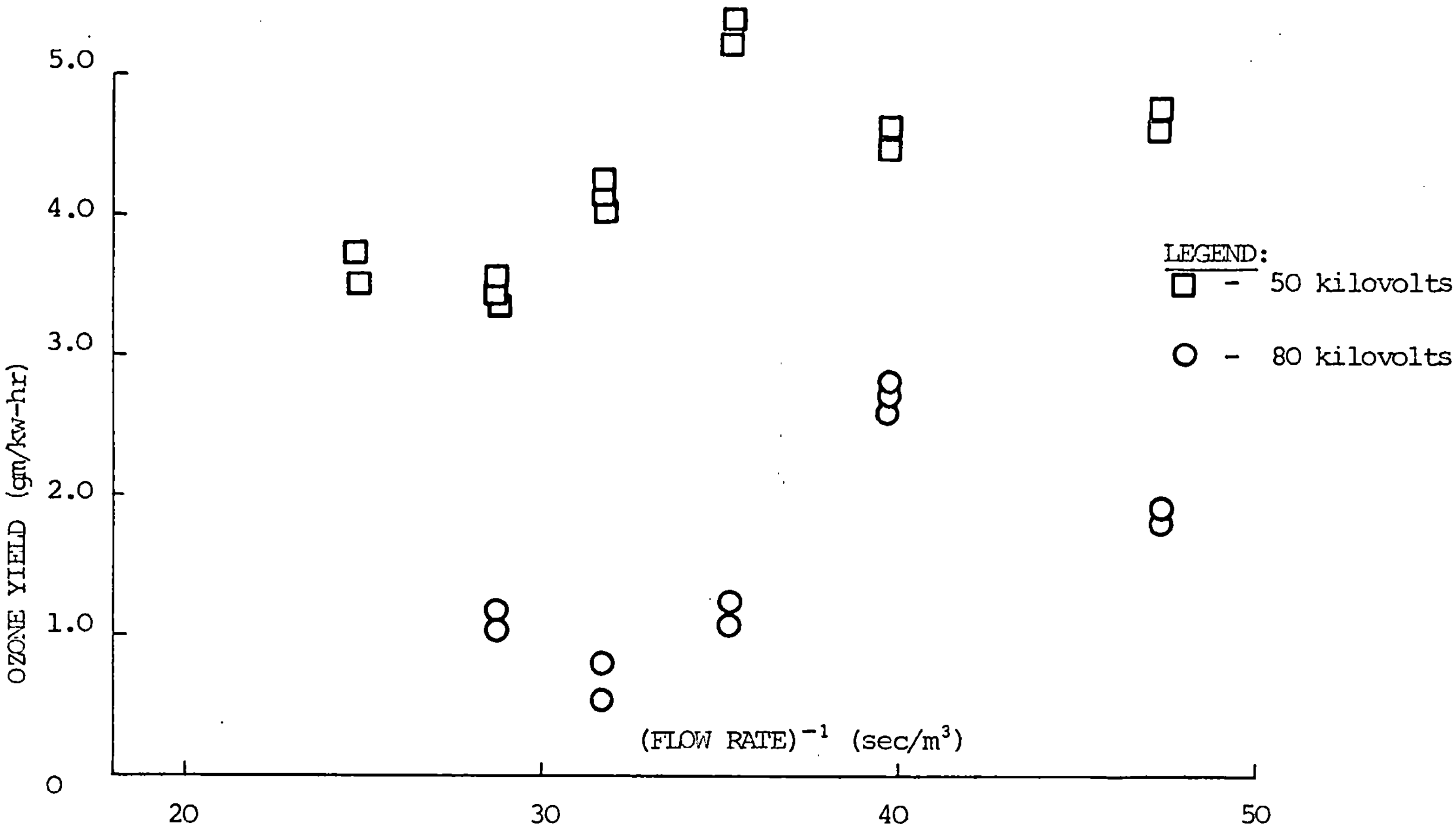

Figure 30. Plot of Ozone Yield as a Function of (flow rate)$^{-1}$
(Temp. 299°K, Relative Humidity 38%, 0.635 cm Diameter Specimen)

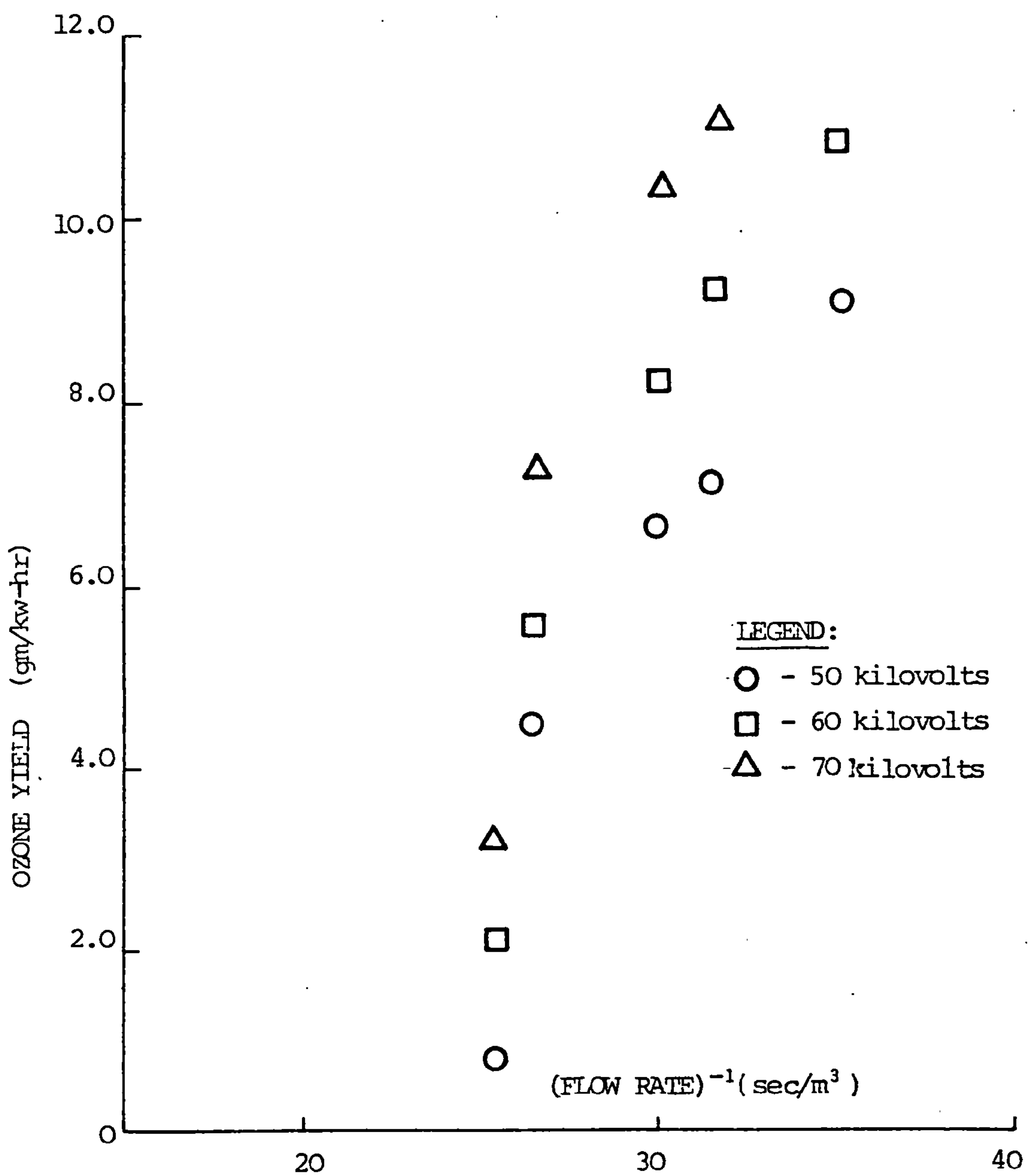

Figure 31. Plot of Ozone Yield as a Function of (flow rate)$^{-1}$ (Temp. 299°K, Relative Humidity 33%, cm Diameter Specimen)

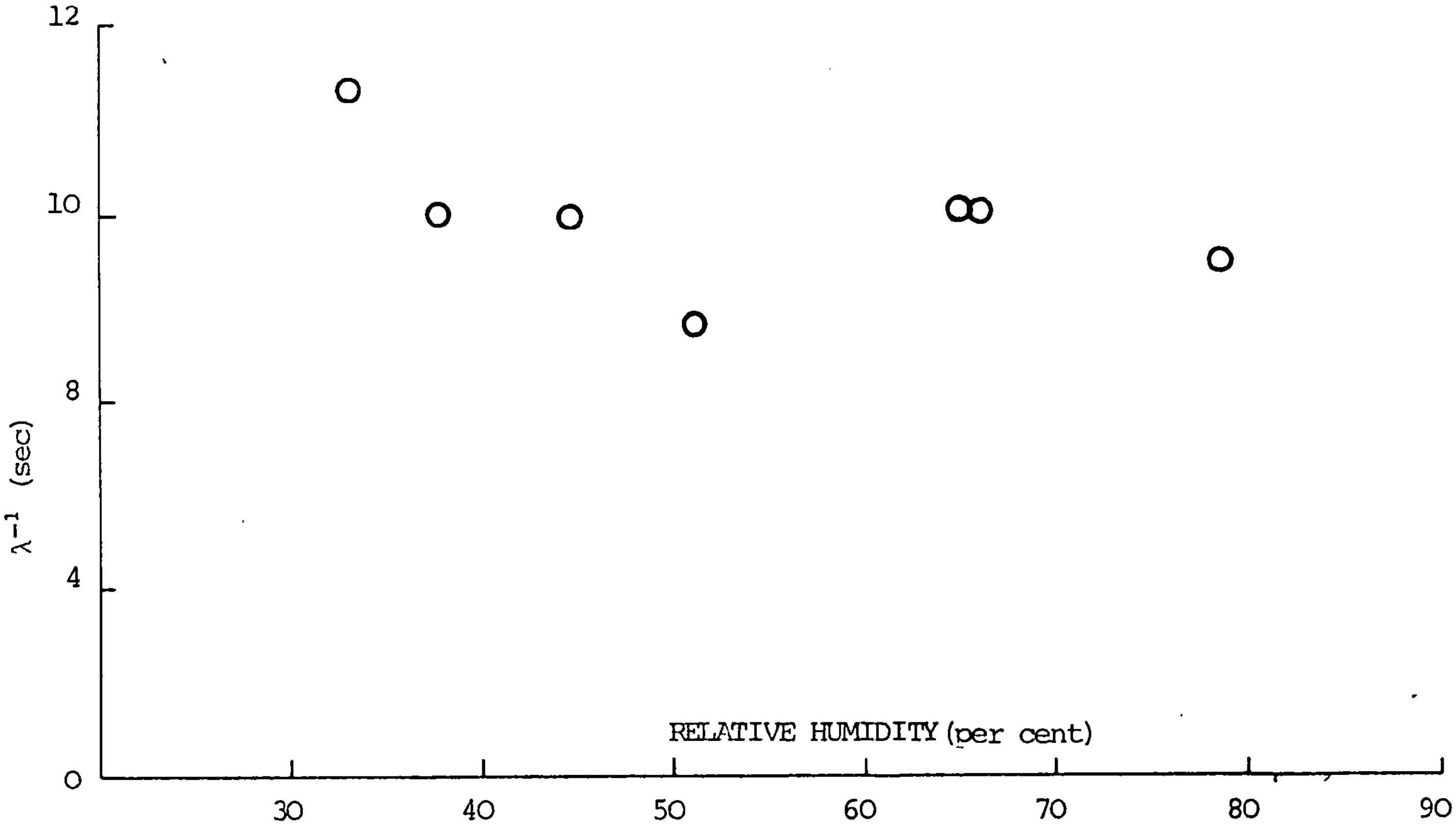

Figure 32. Plot of λ^{-1} Versus Relative Humidity

a temperature dependence, no further range of air temperature was investigated.

The lack of temperature dependence for ozone yield is discussed further and supported by averaged data in Section 5.2.

4.6 Effects of Surface Treatment of Conductor

In order to determine something of the nature of surface effects, the 1.04 cm diameter aluminum conductor was, after an extensive series of tests on the as-received conductor was completed, exposed to a 0.1N sodium hydroxide solution for 48 hours. The appearance of the sample was altered by the treatment from shing aluminum to a mottled gray color with gray-white patches. The patches were rough to the touch, but some of this roughness could be wiped off easily. Subsequent to this the appropriate electrical parameters of the conductor in the test cell were measured. The results of this test showed, at least to the extent of surface alteration produced by this treatment, there was no discernible alteration in electrical characteristics. In this connection, it should be pointed out that this particular conductor showed, in the as-received condition, significant surface roughness as shown in Figure 12 and as demonstrated by the relatively low corona onset and sparkover voltages as compared to the smaller sample.

A total of 21 data points (nos. 672-692 on Table A-4) were obtained with the surface-treated wire at 77 per cent relative humidity. The data obtained exhibited excellent correlation with the other data at high humidity. Points 621-671 at 68 per cent relative humidity for the untreated wire exhibited average ozone yields of 1.89 gm/kw-hr at 50 kv and 3.65 gm/kw-hr at 70 kv, as compared to 1.78 and 3.21 gm/kw-hr, respectively, for the treated wire. This result indicated little if any direct effect of surface treatment. The scale of the surface roughness resulting from surface treatment of this type (chemical etch) was obviously much less than the scale of the scratches, pits, and other malformations present on the surface of the as-received sample. Thus, no further tests of this type appeared necessary.

4.7 Efforts with Airborne Particles

When airborne dust or other particulate matter was introduced into the test chamber, the line filter upstream of the ozone meter was observed to plug readily. It was decided not to expose the ozone meter to dust-laden air without the filter in place for fear of damaging the instrument; this effectively eliminated the ozone meter as an analytical method for these particular tests. Similarly, the use of the colorimetric method was not judged sufficiently accurate for use with particle-laden streams because of light-scattering by the particles in the samples. Any filtration other than use of the same type of Teflon filter used upstream of the ozone meter would compromise the colorimetric analysis by decomposing some of the ozone in the sample. Thus, the efforts to study effects of airborne particles produced no information because of the lack of an appropriate analytical method.

VERSAR INC.

5.0 DISCUSSION OF RESULTS

5.1 Variation of Ozone Yield with Corona Power Dissipation

Figures 23 and 25 indicate that the ozone yield, or production efficiency, in gm/kw-hr generally increased with corona power at the lower voltages and then tended to become constant at the higher values of corona power (or voltage). If the sets of data obtained are grouped so that each set of environmental conditions (all variables except voltage) is constant for a given set, there are 57 such sets within the 810 total points. Within each set, then, the voltage was varied upwards, and ozone yields calculated for each voltage setting. Of the 57 sets, 39 or about two-thirds exhibited the general increase in ozone yield as voltage was increased. A total of 14 sets exhibited very little variation of yield with voltage, or varied higher or lower but returned to near the low voltage values as voltage was increased; and 4 sets exhibited a general decrease of yield as voltage was increased.

Because of the preponderance of such sets exhibiting general increases (or increases followed by attainment of a nearly constant value), we must conclude that our results indicate relatively lower ozone yields at voltage values near the corona threshold. Using the stylized plot below (where zero corona power dissipation occurs at the threshold voltage corresponding to the onset of ozone production):

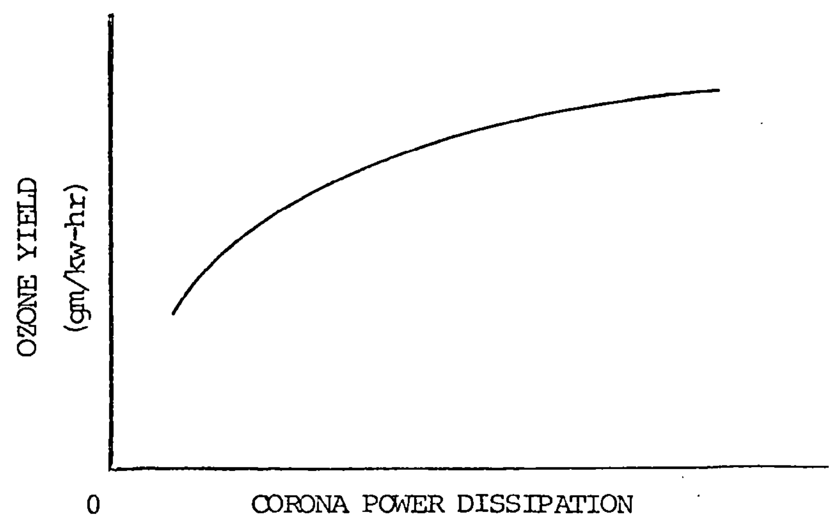

we must ask where on this curve an operating transmission line would be expected to lie. At high values of corona power dissipation, such as during periods of precipitation or unsettled weather (high earth potential gradients), the yield would appear to be higher than during fair weather (except for humidity effects), unless all operating conditions lie at corona power values corresponding either to zero (which is obviously not so) or to the relatively constant values for a given set of environmental conditions. It seems likely that the ozone yield of an operating line might shift up and down depending on the conditions, of which the most important appear to be corona power, humidity, and wind velocity.

In this sense, it is possible that an operating line could never be simulated electrically by an enclosed experiment, since the ozone yield could be continuously fluctuating as a result of fluctuating corona power dissipation on an operating line.

5.2 Analysis of Averaged Data

If the effects of corona power dissipation on ozone yield (as discussed above) are disregarded, then general or overall effects of relative humidity and air flow rate can be shown. To accomplish this, the yields for each data set (as described above) were averaged, with the results tabulated in Appendix A as Table A-5. Ranges of relative humidity were assigned, and the average yield values for each data set falling within each range were averaged. The resulting data, tabulated on Table 9 and plotted on Figure 33, show that the general effect of increasing relative humidity was to reduce ozone yield.

Selecting humidity ranges of 35-39 per cent and 65-69 per cent (in each of which a relatively large number of data sets lie) and plotting the average ozone yields versus the air flow rate for each set within these humidity ranges produced the plot on Figure 34. This plot indicates the general reduction in ozone yield as flow rate through the chamber was increased.

Examination of the averaged data on Table A-5, which is in approximately chronological order, indicates little or no effect of sample aging or sample diameter. These observations are subjective, of course, since the

TABLE 9

Variation of Averaged Ozone Yield Data with Relative Humidity

Relative Humidity Range (per cent)	No. of Data Sets Within RH Range	Averaged Value of Ozone Yield for All Sets in Range (gm/kw-hr)
25 - 29	5	6.81
30 - 34	5	6.76
35 - 39	8	3.64
40 - 44	3	3.82
45 - 49	4	1.85
50 - 54	9	5.70
55 - 59	2	4.46
65 - 69	18	3.87
75 - 79	3	2.85

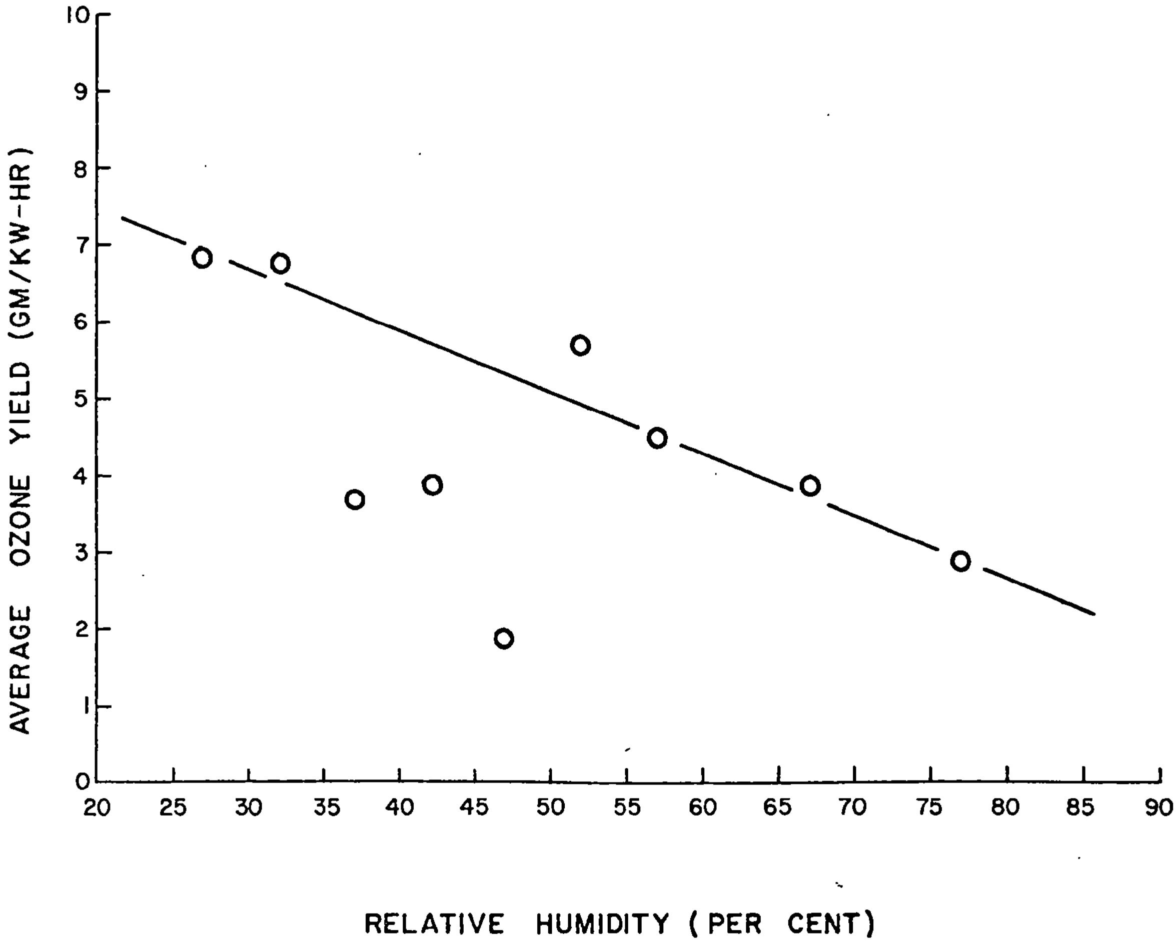

FIGURE 33. GENERAL EFFECT OF RELATIVE HUMIDITY ON OZONE YIELD FROM ENERGIZED HIGH-VOLTAGE CABLE

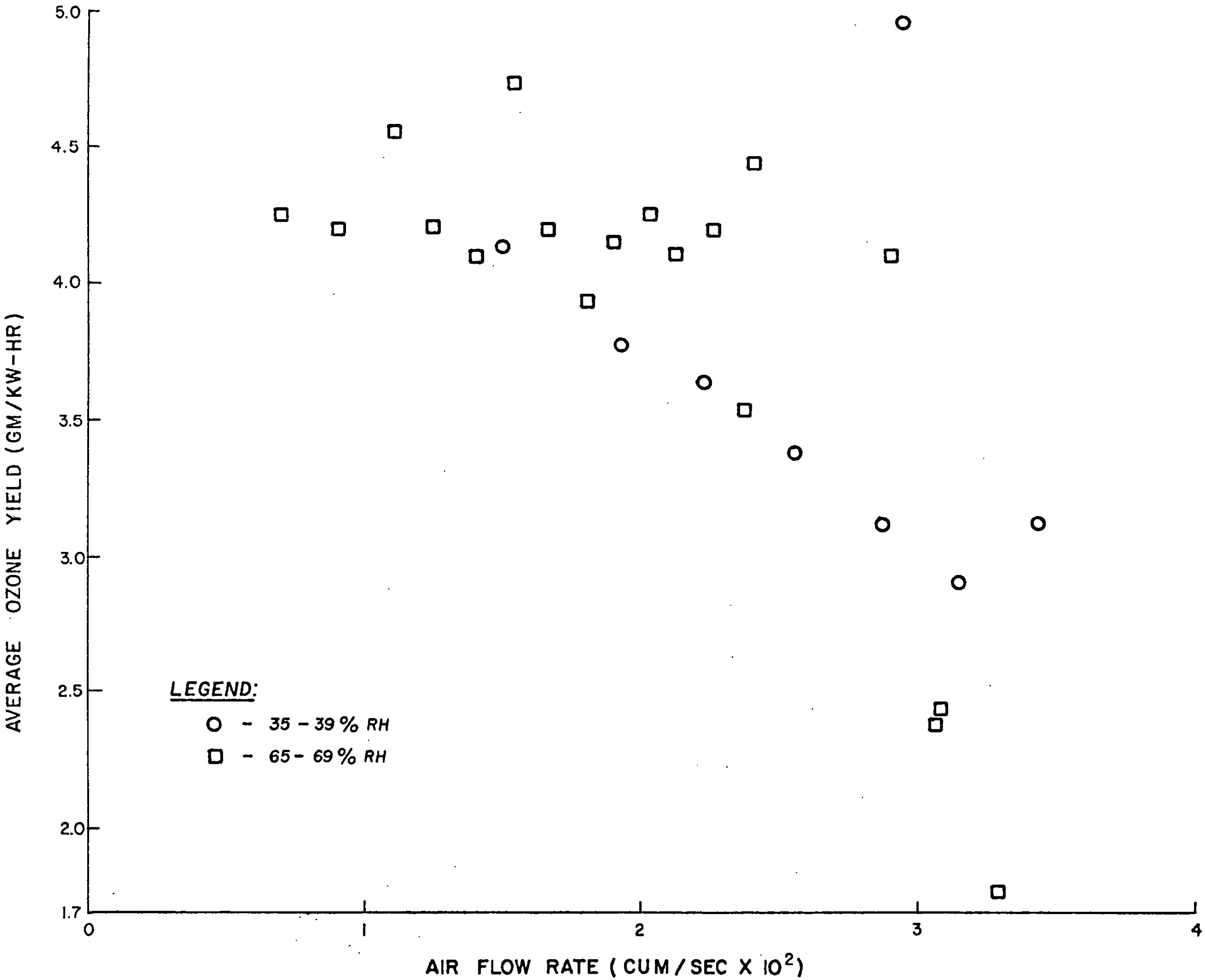

FIGURE 34. GENERAL EFFECT OF AIR FLOW RATE ON OZONE YIELD FROM ENERGIZED HIGH-VOLTAGE CABLE

corona process and chemical reactions therein are inherently variable. This type of variation appeared in our system both as point-to-point fluctuations and as day-to-day variations. The process and the test results were less variable at the higher humidities, which is typical of corona behavior.

The averaged data on Table A-5 also can be used to illustrate the effect, or the lack of significant effect, of air temperature on ozone yield. If one eliminates data corresponding to the highest and lowest relative humidities, the averaged ozone yield data over a temperature range of 293 °K to 300°K exhibit no effect of temperature. This result is presented in tabular form on Table 10. The data at the lowest humidities corresponds to the highest yield values and also the highest air temperatures. Thus, its inclusion in Table 10 would reflect essentially an effect of humidity rather than temperature. Likewise, use of the data at 77 per cent relative humidity, corresponding to a temperature of 298°K, might introduce an effect which would be primarily that of humidity and not temperature.

5.3 Summary of Ozone Yield Results

The experimental results reported herein indicate overall ozone production efficiencies of the order of 2 to 10 gm per kilowatt hour dissipated within the corona. It has been shown that, within the range of variables covered, this ozone production efficiency is independent of ambient air temperature and of conductor dimension and apparently independent of the nature of surface roughness; the effect of the latter variable is reflected in increased corona power losses and not in the efficiency of ozone production. In the experimental apparatus used in this experiment there has been found a marked dependence of ozone production efficiency on the longitudinal flow velocity which is apparently a result of a very short time constant for reduction of ozone concentration (~10 seconds) coupled with a fortuitous combination of geometrical factors characteristic of the experimental apparatus. This flow velocity dependence also strongly involves the effect of relative humidity which exhibits a marked increase in ozone production efficiency at the lower relative humidities. To the extent such an analysis is reliable, it appears that this relative humidity effect is associated with

Table 10. Effects of Air Temperature on Ozone Yields over Relative Humidity Range of 36-68 per cent

Temperature (°K)	Average Ozone Yield (gm/kw-hr)	No. of Data Sets at Temp.	Relative Humidities for Data Sets (per cent)
293	1.82	1	45
294	6.06	7	45,51
295	3.00	4	45,58
296	2.08	2	65
297	3.86	5	36,42
298	3.59	5	51,68
299	3.55	6	38
300	4.21	14	66

VERSAR INC.

an alteration of the abovementioned very short life time as is shown in Figure 32.

Ozone yields which can be applied to operating transmission lines in the field should be better represented by the averaged data presented and discussed previously in this section than by data within individual sets. However, the relatively strong dependence of yield on corona power observed in most data sets casts some doubt on the direct application of even the averaged data to operating lines, as discussed in Section 5.1. Nevertheless, our best estimates for average ozone yields for transmission lines (following Figure 33) are:

(1) 5 gm/kw-hr at typical average relative humidities of 50 per cent;

(2) 8 gm/kw-hr at low humidities (10-30 per cent) typical of arid areas; and

(3) 3 gm/kw-hr during periods of high humidity (65-85 per cent) but no precipitation.

5.4 Comparison with Published Results

In order to obtain some reasonable idea of the reliability of the reported data we may compare the losses as indicated in Figures 9 and 11 with those reported by Foley and Olsen [5] on a field set-up involving a 2-conductor system made up of approximately 1 kilometer of 0.412 cm diameter conductor spaced 3.66 meters apart parallel to and approximately 11 meters above ground. Foley and Olsen [5] report a 60-cycle power loss for this system at 60 kilovolts of the order of 1.3 watts per meter of a pair of conductors; this value contrasts to the approximately 7 watts per meter for the 0.635 cm conductor and approximately 4.7 watts per meter for the 1.04 cm conductor obtained in this program. The possible contribution to the present results that could arise from corona from the test conductor to the corners of the copper sheets which formed the outer (ground) conductor of the test arrangement has not been separately determined, but the data of Foley and Olsen show that the observed dissipation in corona reported herein is of the proper order of magnitude for the geometry used. Although efforts were made to suppress undesired corona by coating the edges of the copper sheets with acrylic resin layers (and, further, no visible evidence of streamer discharges to those edges were obtained), the low breakdown voltages for full corona could have arisen from this source. This situation of the unexpectedly low breakdown voltages (~95 kilovolts for the 0.635 cm specimen and ~90 kilovolts for the 1.04 cm specimen) is not clear since, for reasons of experimental necessity, it was always necessary to begin at the lowest voltage at which detectable levels of ozone were produced and to gradually approach the upper voltages; this procedure had the possibly undesirable effect of gradually causing an increase in conductivity of the air within the test chamber leading to relatively low breakdown potentials. Clearly, it would be desirable to make attempts in future work to even further suppress corona losses from any source other than that directly associated with the high field gradient in the vicinity of the test specimen.

As has been pointed out above, the reference capacitance for the Schering bridge was taken to be the capacitance of the high voltage assembly, including the 25 cm sphere which was the vertical termination of the high voltage assembly, to the suspended ground plane. To clarify this it should be pointed out that the return line for the "ground plane" was insulated and connected to the Schering bridge at the top end of Z_3 as is shown in Figure 4. The actual capacitance used as C_o in the bridge is the total of all capacitances lying between the high voltage network and the "ground plane." A reasonable approximation of an upper bound on this capacitance can be made by assuming the entire high voltage structure to be enclosed in a conducting sphere of 70 cm diameter located 1.20 meters from the plane. Referring to equation (3.), we find:

$$(C_o)_{upper} \sim 19.5 \times 10^{-12} \text{ farads.}$$

One should expect the measured C_o to lie between the limits of (3.5 to 19.5) $\times 10^{-12}$ farads, as is the case.

The measured capacitance of the test specimen has been found to be sharply voltage dependent as is shown in Figures 8 and 10. Referring again to the work of Foley and Olsen [5], we find equivalent changes in line capacitance with operating voltage. The rather dramatic effect of high relative humidity as seen in Figures 8 and 10 remains unexplained and will require additional work to determine the nature of this effect. The consistency of the experimental data used to construct Figures 8 and 10 (tabulated in Appendix A) suggests that the relative humidity effect seen is real but verificiation studies will be required before a detailed explanation can be attempted.

The ozone production measurements reported herein seem to be consistent with those reported by other workers in the field. Scherer, et al[6] report the following observations:

(1) The average production rate is approximately 489 kw-hr/kg (which is equivalent to approximately 2 gm/kw-hr), with a total range reported (Westinghouse work) of about 0.5 to 5.0 gm/kw-hr;

(2) The oxidant production rate is insensitive to temperature variation;

(3) The humidity has an adverse effect on the oxidant production, i.e., the yield decreases as the relative humidity increases; and

(4) The half life was about 10 minutes in a chamber comparable in size to that described herein, and varied about 45 minutes in clean dry air to about 27 minutes with water spray in a larger chamber.

Clearly, the results of Scherer, et al, agree very well with the data reported herein. It does not seem possible at this time to account for the quantitative differences in ozone production rate reported by Scherer[6] and those reported herein. Additional work will be required to resolve these quantitative differences.

Comparison of the results with those reported in reference (6) in terms of corona power dissipation is as follows. In the work by Westinghouse, the corona power dissipation on the four-conductor bundle ranged up to 160 watts/m, whereas in our tests the highest value of corona power dissipation was about 27 watts/m (data point No. 517). Considering a single conductor of the bundle, so that the maximum corona power dissipation would be about 40 watts/m in the Westinghouse work, the ranges of corona power dissipation covered appear to be very comparable.

Maximum conductor surface voltage gradients calculated by Westinghouse were between 16 and 29 kV (rms)/cm, as compared to a range of 20-40 for the present program. This factor also appears comparable between the two programs, even though voltages used in the Westinghouse work were much higher (up to 700 kV) in order to simulate operating conditions of a full-scale four-conductor line.

6.0 ESTIMATE OF ATMOSPHERIC OZONE CONTRIBUTION FROM CONCENTRATION OF TRANSMISSION LINES IN SELECTED AREAS

6.1 Site Selection

Study of the 1972 edition of "Principal Electric Facilities in the United States" (published by the Federal Power Commission) revealed that the highest concentrations of high voltage (69 kV and up) transmission occur around major urban areas and to a lesser extent in the vicinity of major power generating stations[7]. Reference (7) consists of a map with major transmission lines marked and is based on reports filed with the FPC to June, 1970. It is the most recent information available.

Three sites with apparently high transmission line concentrations were selected for study:

(1) A circular area of 81 km. radius, centered at the Amos, West Virginia generating plant, near the Kanawha and Ohio Rivers and including small portions of Ohio and Kentucky, plus seven generating plants besides Amos.

(2) A circular area of 81 km. radius, centered at the Four Corners generating plant in northwest New Mexico; and

(3) A circular area of 18 km. radius comprising much of south eastern Los Angeles and centered between the Los Angeles and the San Gabriel Rivers at the intersection of a major Southern California Edison line and (apparently) two major Los Angeles Municipal lines.

The EHV Transmission Line Reference Book[8] describes seven climatic areas in the United States, and the three sites described above lie in three separate such climatic areas:

Site (1) - Area 1; Northeastern
Site (2) - Area 4 (primarily); Western Mountain
Site (3) - Area 6; Coastal Pacific Southwest

Site (3), in the Los Angeles area, contains one of the highest local concentrations of high-voltage transmission lines anywhere in the world. Site (1) appears from Reference 7 to hold a relatively high concentration for a non-urban area, and Site (2) contains a lower concentration of lines from one large generating complex (Four Corners) and is essentially open country. The total length of three-phase transmission line within each site, as derived from measurements made on Reference 7 , are as follows:

Site (1) (Amos) - 1,345 mi. (2,420 km.)
Site (2) (Four Corners) - 472 mi. (850 km.)
Site (3) (Los Angeles) - 429 mi. (772 km.)

6.2 Corona Losses from Each Site

Selection of average corona loss factors for these sites is very difficult, since voltages range from 115 kV to 765 kV, corona losses vary widely between lines of the same voltage (due to geometric differences, local weather, etc.), and relatively little data are available concerning actual corona losses. Consultation and analysis of the information on operating and design factors in the EHV Handbook[8] produced the following information:

Site	Climatic Area	Base Line (Fair Weather) Corona Loss (Ave.) (kw/mi)	Average Adder for 500 kV Line (kw/mi)	Total Design Corona Loss (500kV) (kw/mi)
1	1	345 kV - 3.0		
		500 kV - 5.0	3.4	8.4
		735 kV - 10.0		
2	4	345 kV - 2.7		
		500 kV - 4.2	2.6	6.8
		735 kV - 8.0		
3	6	345 kV - 2.2		
		500 kV - 3.0	1.4	4.4
		735 kV - 5.7		

VerSar Inc.

Based on this and other similar information, the following values were assigned as the average corona loss per mile for all major lines in a given area:

Site (1) - 5.0 kw/mi
Site (2) - 4.0 kw/mi
Site (3) - 3.0 mw/mi.

These values do not take into account lines operating at voltages below 115 kV, lines operating at less than design voltage, new lines or loss of lines since 1970, or corona losses in substations and immediately around generating plants. These factors should, in general, tend to cancel each other.

The corona losses for the three sites calculated from the average losses per mile times miles of lines are as follows:

Site (1) (Amos) - 6,730 kw
Site (2) (Four Corners) - 1,888 kw
Site (3) (Los Angeles) - 1,287 kw

6.3 Ozone Contribution from Corona Losses

The following analysis was performed to determine, as an order of magnitude approximation, the potential contribution of transmission lines to the local ozone concentration levels at the three sites described above. Since many assumptions were necessary for the analysis, the reader should bear in mind that the results of the analysis are only rough approximations. Other assumptions can be made and applied to the analysis with equal impunity.

The change in ozone concentration with respect to time $(\frac{dC}{dt})$ arising from the corona losses can be expressed as:

$$\frac{dC}{dt} = \frac{(O_3 \text{ production rate}) - (O_3 \text{ destruction rate})}{\text{Volume}}$$

At steady state, $(\frac{dC}{dt}) = 0$, production equals destruction, and a limiting ozone concentration is maintained. For a given and closed volume, and assuming perfect mixing, this limiting concentration depends on the production rate (which, for our purposes, is assumed to be constant) and the nature of the decomposition process. Assuming a single decomposition process following:

$$C = C_o e^{-\lambda t} ,$$

the limiting concentration is given by:

$$C_\infty = \frac{BP}{V\lambda}$$

where:

C_∞ = limiting concentration, gm/m^3

B = ozone yield, gm/kw-hr

P = power dissipated, kw-hr

V = volume, m^3

λ = time constant, hr^{-1}

Values of λ over a range of ozone half-lives from one hour to 100 hours are:

Half-Life (hours)	λ (hr^{-1})
1	0.693
10	0.0693
100	0.00693

VERSAR INC.

It then remained to select an appropriate altitude, below which all of the ozone so produced would be contained. This height of our cylindrical container was chosen to be one kilometer, based on the typical height of an inversion layer being below this altitude and other considerations.

Thus, we assume that:

(1) The ozone produced is at a constant (average) rate based on the mean values from our work described herein (and assuming that the average relative humidity of Sites (2) and (3) is 25-30 per cent, that of Site (1) 50 per cent, and a linear relationship between ozone yield and relative humidity on either side of the selected mean);

(2) The ozone so produced is maintained in a constant cylindrical volume contained within the circular areas about the sites as described above and a height of one kilometer; and

(3) The ozone concentration throughout the volume is constant (alternatively, an average concentration may be considered).

The steady-state (or limiting) ozone concentrations calculated on the basis of these and the other assumption as described previously, are as follows (air density = 1.2×10^3 gm/cu m):

Site (1) - Amos, W. Va. (B = 5.5 gm/kw-hr; V = 2.06×10^{10} cu m)

O_3 Half-Life (hr)	C_∞ (ppb)
1	2.15
10	21.5
100	215

Site (2) - Four Corners, N.Mex. (B = 8 gm/kw-hr; V = 2.06×10^{10} cu m)

VERSAR INC.

O_3 Half-Life (hr)	C_∞ (ppb)
1	0.88
10	8.8
100	88

Site (3) - Los Angeles, Calif. (B = 8.0 gm/kw-hr; V = 1.02×10^9 cu m)

O_3 Half-Life (hr)	C_∞ (ppb)
1	12.2
10	122
100	1,220

The linear dependence of the steady-state concentration of ozone lifetime shows clearly that the lifetime is the single most important factor considered here in determining the relative contribution of transmission lines to local ozone levels. In reality, any wind condition other than calm will dramatically reduce the local contribution which can be attributed to transmission lines.

Lifetime measurements of ozone in smoggy air[9] in a glass container indicate a half-life under these conditions of about one hour. Other work with cleaner air in a metal enclosure[10] has resulted in reported half-lives of ozone of up to 8.2 hours. It is very difficult to relate these values to free air above the three selected sites, but it appears reasonable to assign a half-life of a few hours for Site (3), so that the corresponding C_∞ would be 15-30 ppb. Thus, coronal ozone production would be a sizeable contribution to the ambient ozone level in the area of Site (3), particularly to nighttime levels since photochemical production would be minimal and the half-life could increase.

The ozone half-life for Sites (1) and (2) may be of the order of five hours (possibly ten hours in the Four Corners area), and from the analysis the contribution from transmission lines could be as high as 20 ppb for Site (1) and 10 ppb for Site (2). Both would have to be considered significant contributions.

One could conclude from the above analysis that, under atmospheric conditions of relative calm, transmission lines might contribute to local ozone levels. Such conditions can ensue from the presence of trapped air (as under an inversion layer or because of terrain-wind interactions) in the vicinity of transmission lines. There are many areas of the United States, particularly near the larger cities, where this combination of conditions could be present.

In 1969 it was estimated that over 300,000 miles (540,000 km) of high-voltage (69 kV-765 kV) transmission lines were operating in the contiguous 48 states of the United States(11), and an estimate of 250,000 miles (450,000 km) in 1966 was made by Rose(12). A reasonable estimate at present appears to be 350,000 miles (630,000 km). A reasonable projection for 1990 appears to be 500,000 miles (900,000 km)(11), unless significant new construction of underground lines is begun soon.

At an overall average of 4 kw/mile (2.22 kw/km) of corona loss on all of these lines, and an average ozone yield of 5 gm/kw-hr, the total yearly productions over the country in 1973 and 1990 are estimated to be:

1973 - 6.1×10^7 kg/yr (6.0×10^4 tons/yr)
1990 - 8.8×10^7 kg/yr (8.7×10^4 tons/yr)

These amounts of ozone spread over the entire area of the country would not appear to be significant. However, in actual fact, transmission lines tend to be concentrated about urban areas as discussed previously and this would tend to magnify the effects of the ozone so produced.

VERSAR INC.

7.0 CONCLUSIONS AND RECOMMENDATIONS

The following conclusions and recommendations are based on the results obtained from the program, and from analysis and interpretation of the results.

7.1 Conclusions

(1) The experimental method used and the results observed and consistent with previous efforts in the field, and represent simulation of an operating transmission line in terms of environmental conditions in the region where ozone is produced (coronal sheath about the conductor);

(2) Ozone yield (in gm/kw-hr) was not found to be affected significantly by conductor geometry, surface condition, or air temperature;

(3) Ozone yield exhibited a complex dependence on longitudinal air flow rate (wind velocity);

(4) Ozone yield exhibited a relatively strong dependence on relative humidity, increasing as humidity was decreased. Yields were more constant at higher humidity and ranged from 5 to 8 gm/kw-hr at relative humidities above about 40 per cent;

(5) Ozone yields were low at values of corona power dissipation (which, in turn, was a complex function of applied voltage) near the ozone production threshold, and reached an apparently constant value at higher values of corona power dissipation;

(6) At least two ozone decomposition processes were observed in the experiment, one with a time constant (e-fold decrement) on the order of ten seconds and the other with a time constant on the order of ten minutes. Both processes appeared to be affected by relative humidity; and

(7) Ozone from transmission lines contribute to local ozone levels in areas where concentrations of transmission and distribution lines exist. Under these conditions the concentration of lines and local wind conditions would have much greater effects on the local ozone contribution from transmission lines than any of the variables studied in this program.

7.2 Recommendations

(1) Regions in which locally high concentrations of transmission lines exist should be studied more closely with respect to local ozone contributions from these lines during calm weather;

(2) The decomposition processes involved in ozone destruction should be defined, particularly those processes which could limit the accuracy of ozone production studies in enclosed volumes and those which could affect persistence in free air; and

(3) Since corona losses are greatly increased by precipitation, and since neither ozone yields nor decomposition processes occurring during precipitation appear to be well-defined at present, it is recommended that possible effects of precipitation on ozone production by transmission lines be studied in more detail.

8.0 BIBLIOGRAPHY

1. (a) W. P. Baker, J. Elec. Eng. Ed. 2, 103-113, 1964 - Pergamon Press, Great Britain.

   (b) E. Rawlinson, et al; IRE, Control & Science, 113, 705, 1966.

2. W. R. Smythe, "Static and Dynamic Electricity", McGraw-Hill, 1939, pp 119-120. (units in CGS).

3. EHV Transmission Line Reference Book, Edison Electric Institute, 1968, pp 124-127.

4. Federal Register, 36, 8195 ff (April 30, 1971).

5. A. H. Foley & F. Olsen; AIEE - Project EHV, pp 340-346, June 1960.

6. H. N. Scherer, et al, IEEE Transactions T72550-2, presented at the IEEE PES Summer Meeting, San Francisco, Calif; July 9-14, 1972.

7. "Principal Electric Facilities in the United States", published by the Federal Power Commission, 1972.

8. EHV Transmission Life Reference Book. Edison Electric Institute, 1968, pp 127-170.

9. (a) Haagen-Smit, A.J., and M. M. Fox, Ind. Eng. Chem, 48, pp 1484-7 (1956).

   (b) Haagen-Smit, A. J., and L. G. Wayne, "Atmospheric Reactions and Scavenging", in "Air Pollution" (A. C. Stern, ed.), Vol. 1,2 ed., pp. 168-71. Academic Press, New York, N.Y. (1968).

10. (a) R. Sabersky, et al; Environmental Sci & Tech; 7, 347 (1973).

    (b) F. Mueller, et al; Environmental Sci & Tech, 7, 342 (1973).

APPENDIX A

Tabulated Electrical Measurements and Ozone Production Data

VERSAR INC.

Table A-1. Tabulated Electrical Measurements for 0.635 cm Diameter Aluminum Cable Sample

V(kv)	R_3 (10^{-5})	C_3 (10^{8})	R_4 (10^{-5})	C_4 (10^{8})	X/S	X (10^{12})	r (10^{-7})	Ave P* (watts)	RH	Flow m /sec
30	1.14	5.3	1.13	5.26	1	5.61	-	-	48%	0
"	1.14	2.3	1.14	2.27	1	5.61	-	-	"	"
"	1.13	1.31	1.13	1.25	1	5.61	-	-	"	"
40	1.04	1.10	1.12	1.46	0.95	5.33	9.5	-	"	"
"	1.02	2.11	1.16	2.47	1.02	5.73	6.5	-	"	"
"	0.96	3.21	1.17	3.47	1.15	6.45	5.1	0.58	"	"
50	0.63	1.10	1.34	1.47	1.92	10.8	9.9	-	"	"
"	1.63	1.10	3.44	1.56	1.31	7.4	2.2	-	"	"
"	1.33	2.10	4.13	2.46	2.11	11.9	10.7	3.28	"	"
60	1.04	2.10	6.03	2.46	1.72	9.65	18.7	-	"	"
"	1.13	1.14	6.41	1.86	2.20	12.4	27.4	-	"	"
"	1.10	2.04	7.11	2.36	2.03	11.4	35.0	7.7	"	"
70	0.97	1.64	7.20	2.04	2.31	13.0	23.1	-	"	"
"	0.70	2.64	7.10	3.04	2.31	13.0	30.5	-	"	"
"	0.503	3.75	6.32	4.01	2.40	13.5	22.2	11.5	"	"
30	1.56	1.00	1.61	0.99	1.00	5.61	1.04	-	51%	2.3×10^{-2}
"	1.53	2.03	1.61	2.01	1.02	5.71	1.05	0.041	"	2.85×10^{-2}
40	1.50	2.06	2.11	2.30	2.34	13.3	4.2	0.684	"	2.85×10^{-2}
50	1.03	1.58	2.32	2.33	1.22	6.84	31.1	-	"	2.3×10^{-2}
"	0.95	2.96	3.53	2.43	1.79	10.0	13.3	3.63	"	2.85×10^{-2}

*Average value of corona loss calculated from mean of measurements at stated conditions.

Table A-1 (Continued)

V(kv)	R_3 (10^{-5})	C_4 (10^{8})	R_4 (10^{-5})	C_4 (10^{8})	X/S	X (10^{12})	r (10^{-7})	Ave P* (watts)	RH	Flow m/sec
60	0.75	2.26	3.52	2.96	1.90	10.7	20.4	-	51%	2.3×10^{-2}
"	0.65	3.32	4.53	3.86	1.82	10.2	24.5	-	"	2.85×10^{-2}
"	0.64	3.32	4.43	3.86	1.84	10.3	24.3	7.00	"	3.45×10^{-2}
70	0.63	2.23	4.74	2.85	2.61	14.6	22.6	-	"	3.45×10^{-2}
"	0.54	3.41	7.33	3.56	2.58	14.5	20.7	-	"	2.85×10^{-2}
"	0.54	3.32	7.33	3.56	2.60	14.5	22.0	13.0	"	2.3×10^{-2}
80	0.55	2.03	5.30	2.65	3.50	19.7	13.2	-	"	2.85×10^{-2}
"	0.45	2.83	6.22	3.35	3.58	20.0	20.7	-	"	2.85×10^{-2}
"	0.45	2.83	6.32	3.35	3.62	20.3	20.4	23.7	"	2.45×10^{-2}
45	0.60	2.20	0.90	3.61	1.17	6.58	20.5	-	34%	3.81×10^{-2}
"	0.70	1.20	1.00	2.41	1.21	6.80	18.0	2.00	"	"
50	0.58	1.00	1.00	2.71	1.47	8.25	21.1	-	"	"
"	0.55	2.30	1.10	3.81	1.40	7.86	21.0	3.60	"	"
55	0.44	2.10	1.10	4.11	1.76	9.90	22.8	-	"	"
"	0.38	3.10	1.00	5.11	1.71	9.60	22.0	5.47	"	"
60	0.35	3.00	1.11	5.21	2.03	11.4	24.4	-	"	"
"	0.35	1.72	0.90	4.51	2.00	11.2	22.9	7.08	"	"
65	0.30	3.02	1.12	5.41	2.34	13.1	21.9	-	"	"
"	0.35	2.10	1.22	4.42	2.40	13.5	22.0	11.2	"	"
70	0.33	2.20	1.40	4.42	2.76	15.5	20.8	-	"	"
"	0.35	3.30	2.30	4.42	2.94	16.6	22.3	14.4	"	"
75	0.34	3.50	3.20	4.32	3.39	19.1	19.8	-	"	"
"	0.32	2.60	2.00	4.22	3.43	19.2	20.0	19.1	"	"

*Average value of corona loss calculated from mean of measurements at stated conditions.

Table A-1 (Continued)

V(kv)	R_3 (10^{-5})	C_3 (10^{8})	R_4 (10^{-5})	C_4 (10^{8})	X/S	X (10^{12})	r (10^{-7})	Ave P* (watts)	RH	Flow m/sec
31	0.85	3.46	1.28	3.22	1.22	6.9	5.94	0.373	71%	3.47×10^{-2}
34	0.682	2.07	0.917	2.22	1.22	6.9	5.94	0.455	"	"
38	0.714	3.22	1.018	3.13	1.22	6.9	6.21	0.596	"	"
42	0.610	2.44	0.836	2.63	1.22	6.9	6.81	0.725	"	"
46	0.576	3.38	0.860	3.60	1.22	6.9	8.12	1.12	"	"
50	0.658	2.51	0.994	2.93	1.23	6.9	9.00	1.45	"	"
54	0.560	3.16	1.01	3.90	1.30	7.3	14.4	2.77	"	"
58	0.540	2.02	1.00	3.24	1.44	8.1	17.6	4.27	"	"
62	0.490	2.75	1.20	4.00	1.55	8.7	20.0	5.80	"	"
66	1.10	1.55	3.62	2.08	1.75	9.8	22.0	7.90	"	"
70	0.58	3.15	3.14	3.68	1.96	11.0	20.9	10.1	"	"
74	0.35	3.55	1.45	5.07	2.36	13.2	23.5	13.6	"	"
78	0.35	3.75	1.94	5.02	2.53	14.2	23.7	15.9	"	"
82	0.34	3.04	1.55	4.72	2.59	14.5	21.0	18.3	"	"
40	1.04	1.34	1.20	1.90	1.02	5.6	1.02	0.073	27%	3.95×10^{-2}
45	0.84	1.14	1.18	2.30	1.21	6.8	18.2	1.98	"	"
50	0.84	2.10	2.10	3.00	1.43	8.0	9.6	2.02	"	"
55	0.81	2.40	4.40	3.00	1.73	9.7	24.2	5.47	"	"
60	0.75	1.00	2.40	2.30	2.04	11.4	22.7	7.72	"	"
65	0.66	1.50	3.30	2.40	2.50	14.0	22.3	11.0	"	"

*Average value of corona loss calculated from mean of measurements at stated conditions.

Table A-1 (Continued)

V(kv)	R_3 (10^{-5})	C_3 (10^8)	R_4 (10^{-5})	C_4 (10^8)	X/S	X (10^{12})	r (10^{-7})	Ave P* (watts)	RH	Flow m/sec
30	1.015	2.71	0.971	2.64	1.00	5.01	-	-	38%	0
35	1.10	2.75	0.980	2.65	0.97	5.58	-	-	"	0
40	0.83	1.24	0.86	1.64	.995	5.61	5.35	-	"	2.07×10^{-2}
"	0.80	2.75	0.86	2.55	.98	5.59	2.50	0.281	"	3.83×10^{-2}
45	0.84	0.24	1.02	1.24	1.21	6.80	15.0	1.85	"	2.07×10^{-2}
"	0.78	1.02	1.02	2.24	1.15	6.35	18.7	-	"	3.17×10^{-2}
50	0.75	2.23	1.50	3.24	1.25	7.05	23.0	2.93	"	2.85×10^{-2}
"	0.84	1.24	1.40	2.30	1.29	7.25	20.2	-	"	3.45×10^{-2}
55	0.75	1.14	1.51	2.50	1.52	8.5	23.6	4.65	"	2.07×10^{-2}
"	0.65	2.34	1.70	3.50	1.52	8.5	24.7	-	"	3.17×10^{-2}
"	0.65	2.44	1.70	3.50	1.52	8.5	22.6	-	"	3.83×10^{-2}
60	0.67	2.34	2.50	3.20	1.80	10.1	21.9	6.7	"	3.17×10^{-2}
"	0.65	2.03	2.12	3.10	1.84	10.3	22.8	-	"	3.83×10^{-2}
65	0.55	2.04	2.00	3.30	2.09	11.7	22.9	9.4	"	2.45×10^{-2}
"	0.44	3.34	2.00	4.30	2.13	12.0	21.2	-	"	2.85×10^{-2}
"	0.45	3.34	2.10	4.30	2.11	11.8	21.5	-	"	3.17×10^{-2}
70	0.35	3.33	1.81	4.70	2.57	14.4	21.3	12.3	"	2.07×10^{-2}
"	0.34	4.33	2.31	5.20	2.53	14.2	21.1	-	"	3.17×10^{-2}
"	0.33	4.43	2.21	5.30	2.54	14.2	21.0	-	"	3.45×10^{-2}
75	0.35	4.24	4.21	4.70	3.26	18.3	-	-	"	2.07×10^{-2}
"	0.25	6.14	3.11	6.70	3.26	18.3	-	-	"	2.45×10^{-2}

*Average value of corona loss calculated from mean of measurements at stated conditions.

VERSAR INC.

VERSAR INC.

Table A-1 (Continued)

V(kv)	R_3 (10^{-5})	C_3 (10^{8})	R_4 (10^{-5})	C_4 (10^{8})	X/S	X (10^{12})	r (10^{-7})	Ave P* (watts)	RH	Flow m/sec
45	0.68	1.10	0.98	2.41	1.22	6.86	19.7	-	34%	3.95×10^{-2}
"	0.57	2.00	0.85	3.51	1.20	6.75	20.0	2.04	"	"
50	0.60	0.93	1.01	2.81	1.44	8.10	23.1	-	"	"
"	0.58	2.11	1.21	3.51	1.46	8.20	21.2	3.49	"	"
55	0.01	1.11	1.30	2.81	1.69	9.50	23.2	-	"	"
"	0.70	2.21	2.30	3.11	1.89	10.6	22.4	5.55	"	"
60	0.81	1.11	2.60	2.21	2.06	11.6	24.5	-	"	"
"	0.62	2.60	3.10	3.41	2.08	11.7	21.6	7.10	"	"
65	0.72	1.50	3.62	2.41	2.51	14.1	22.8	-	"	"
"	0.55	2.51	3.40	3.31	2.45	13.8	22.5	10.8	"	"
70	0.45	2.61	3.10	3.51	2.92	16.4	22.4	-	"	"
"	0.45	1.61	2.40	3.21	2.89	16.3	20.7	14.3	"	"
75	0.40	1.50	2.10	3.31	3.49	19.6	20.0	-	"	"
"	0.40	2.30	3.00	3.51	3.55	20.0	21.4	19.0	"	"

*Average value of corona loss calculated from mean of measurements at stated conditions.

Table A-2. Tabulated Electrical Measurements for 1.04 cm Diameter Aluminum Cable Sample

V(kv)	R_3 (10^{-5})	C_3 (10^8)	R_4 (10^{-5})	C_4 (10^8)	X/S	X (10^{12})	r (10^{-7})	Ave P* (watts)	RH	Flow m/sec
31	0.85	3.46	1.28	3.22	1.235	6.96	5.6×10^7	0.394	70%	-
"	0.67	2.08	0.90	2.21	1.228	6.87	6.3×10^7	-	"	-
34	0.687	2.07	0.917	2.22	1.22	6.85	6.6×10^7	0.49	"	-
"	0.723	3.22	1.027	3.12	1.21	6.79	5.5×10^7	-	"	-
38	0.714	3.22	1.018	3.13	1.22	6.85	6.1×10^7	0.60	"	-
"	0.610	2.46	0.825	2.62	1.22	6.85	6.4×10^7	-	"	-
42	0.610	2.44	0.836	2.63	1.23	6.90	7.0×10^7	0.73	"	-
"	0.572	3.48	0.806	3.53	1.22	6.85	6.7×10^7	-	"	-
46	0.576	3.38	0.860	3.60	1.23	6.90	8.6×10^7	1.10	"	-
"	0.616	2.46	0.850	2.79	1.21	6.79	8×10^7	-	"	-
50	0.658	2.51	0.994	2.93	1.24	6.95	1.1×10^7	1.60	"	-
"	0.638	3.57	1.00	3.80	1.23	6.90	9.7×10^7	-	"	-
54	0.560	3.16	1.01	3.90	1.31	7.35	1.5×10^7	2.70	"	-
"	0.530	2.03	0.80	3.04	1.28	7.7	1.4×10^7	-	"	-
58	0.540	2.02	1.00	3.24	1.44	8.07	1.8×10^8	4.15	"	-
"	0.540	2.77	1.12	3.80	1.44	8.07	1.8×10^8	-	"	-
62	0.490	2.75	1.20	4.00	1.61	9.04	2.0×10^5	5.95	"	-
"	1.08	1.46	2.60	2.02	1.50	8.41	2.0×10^8	-	"	-
66	1.10	1.55	3.62	2.08	1.73	9.70	2.3×10^8	7.90	"	-
"	0.58	4.15	3.62	4.38	1.77	9.93	2.1×10^8	-	"	-
"	0.67	3.15	3.15	3.58	1.75	8.90	2.2×10^8	-	"	-
70	0.58	3.15	3.14	3.68	1.99	11.2	2.1×10^8	9.92	"	-
"	0.39	3.45	1.34	4.87	1.93	10.8	2.0×10^8	-	"	-

*Average value of corona loss calculated from mean of measurements at stated conditions.

Table A-2 (Continued)

V(kv)	R_3 (10^{-5})	C_3 (10^{8})	R_4 (10^{-5})	C_4 (10^{8})	X/S	X (10^{12})	r (10^{-7})	Ave P* (watts)	RH	Flow m/sec
74	0.35	3.55	1.45	5.07	2.41	13.5	2.5×10^{8}	13.5	70%	-
"	0.34	2.65	1.23	4.77	2.31	13.0	2.2×10^{8}	-	"	-
78	0.35	3.75	1.94	5.02	2.47	13.9	2.2×10^{8}	17.7	"	-
"	0.35	3.75	2.04	5.01	2.52	14.2	2.3×10^{8}	-	"	-
"	0.34	2.75	1.64	4.72	2.61	14.7	2.3×10^{8}	-	"	-
82	0.34	3.04	1.55	4.72	2.54	14.3	2.1×10^{8}	18.0	"	-
"	0.28	4.04	1.45	5.72	2.64	14.8	2.0×10^{8}	-	"	-
40	1.11	2.53	1.15	2.46	1.04	5.7	-	-	38%	-
45	1.11	2.53	1.16	2.47	1.05	5.8	-	-	"	-
50	1.12	2.56	1.21	2.58	1.03	5.7	1.7×10^{7}	.197	"	-
55	0.92	2.17	1.21	2.67	1.08	6.1	1.0×10^{8}	1.65	"	-
60	0.95	2.18	1.72	2.85	1.19	6.7	1.7×10^{8}	3.38	"	2.95×10^{-2}
"	1.23	1.11	1.72	1.75	1.12	6.3	1.65×10^{8}	2.92	"	"
"	0.92	2.52	1.83	3.14	1.21	6.8	1.7×10^{8}	3.41	"	"
65	1.06	1.13	1.75	2.04	1.24	7.0	2.1×10^{8}	4.72	"	"
"	0.84	2.33	2.09	3.04	1.38	7.7	2.0×10^{8}	5.32	"	"
"	0.82	2.50	1.95	3.29	1.33	7.5	2.0×10^{8}	5.13	"	"
70	0.73	2.52	2.40	3.34	1.58	8.9	2.2×10^{8}	7.82	"	"

*Average value of corona loss calculated from mean of measurements at stated conditions.

VERSAR INC.

Table A-2 (Continued)

V(kv)	R_3 (10^{-5})	C_3 (10^{8})	R_4 (10^{-5})	C_4 (10^{8})	X/S	X (10^{12})	r (10^{-7})	Ave P (watts)	RH	Flow m/sec
40	1.20	2.40	1.45	2.32	1.11	6.2	3.4×10^{7}	0.30	65%	2.89×10^{-2}
45	1.24	2.37	1.58	2.34	1.11	6.2	4.5×10^{7}	0.86	"	2.89×10^{-2}
50	1.12	2.33	1.58	2.46	1.14	6.4	7.8×10^{7}	0.86	"	2.89×10^{-2}
53	1.00	2.25	1.70	2.65	1.20	6.7	1.35×10^{8}	2.16	"	3.09×10^{-2}
55	0.64	2.69	1.04	3.51	1.21	6.8	1.35×10^{8}	2.4	"	2.89×10^{-2}
"	1.07	2.36	1.98	2.74	1.23	"	"	"	"	3.09×10^{-2}
58	0.90	2.45	2.05	2.92	1.34	7.5	1.70×10^{8}	4.6	"	3.09×10^{-2}
"	0.62	1.48	0.98	2.74	1.32	"	"	"	"	2.89×10^{-2}
60	0.87	2.55	2.12	3.03	1.37	7.7	1.80×10^{8}	4.5	"	3.09×10^{-2}
"	0.62	1.47	1.01	2.78	1.33	"	"	"	"	2.89×10^{-2}
65	0.78	2.36	2.16	3.04	1.51	8.4	2.1×10^{8}	6.2	"	3.09×10^{-2}
"	0.62	1.45	1.20	2.88	1.50	"	"	"	"	2.89×10^{-2}
70	0.69	2.36	2.20	3.14	1.70	9.5	2.2×10^{8}	8.6	"	3.09×10^{-2}
"	0.53	1.36	1.12	3.18	1.66	"	"	"	"	2.89×10^{-2}
75	0.63	2.14	2.30	3.11	1.94	10.9	2.2×10^{8}	12.3	"	3.09×10^{-2}
40	1.02	3.14	1.22	3.01	0.95	5.3	1.25×10^{8}	0.76	65%	3.09×10^{-2}
50	0.91	2.50	1.24	2.73	1.13	6.3	8.4×10^{7}	1.14	"	3.09×10^{-2}
63	0.79	2.40	2.06	3.04	1.47	8.2	1.96×10^{8}	5.40	"	3.09×10^{-2}

Table A-2 (Continued)

V(kv)	R_3 (10^{-5})	C_3 (10^{8})	R_4 (10^{-5})	C_4 (10^{8})	X/S	X (10^{12})	r (10^{-7})	Ave P (watts)	RH	Flow m/sec
10	1.49	2.63	2.36	2.32	1.25	7.0	5.3×10^7	.036	77%	2.89×10^{-2}
15	1.50	2.63	2.36	2.34	1.24	6.9	4.0×10^7	.06	"	"
20	1.46	2.63	2.38	2.33	1.26	7.1	5.8×10^7	.16	"	"
25	1.50	2.60	2.37	2.36	1.23	6.9	5.8×10^7	.24	"	"
36	1.23	2.57	2.00	2.35	1.25	7.0	6.2×10^7	.64	"	"
"	1.45	1.48	2.00	1.37	1.48	8.3	-	-		
40	1.45	1.48	1.97	1.39	1.44	8.1	-	-	"	"
45	1.43	1.40	2.03	1.37	1.24	7.0	6.5×10^7	.86	"	"
50	1.29	1.45	2.14	1.60	1.31	7.3	1.1×10^8	1.92	"	"
55	1.13	1.44	2.27	1.79	1.42	7.9	1.58×10^8	3.45	"	"
60	1.22	1.43	3.27	1.78	1.68	9.4	1.9×10^8	5.78	"	"
65	1.06	1.50	3.17	1.98	1.68	9.4	1.9×10^8	6.95	"	"
70	0.94	1.60	3.57	2.17	1.88	10.5	2.2×10^8	10.6	"	"
75	0.82	1.70	3.77	2.27	2.04	14.8	3.0×10^8	13.8	"	"
80	0.71	1.50	3.37	2.27	2.56	14.3	2.2×10^8	17.2	"	"
85	0.67	1.40	3.47	2.27	2.79	15.6	2.3×10^8	20.3	"	"

Table A-3 - Ozone Production and Yield Data for 0.635 cm Diameter Aluminum Cable Sample

No.	Voltage (Kv)	O_3 Conc. (ppm)	Air Flow (m^3/sec)	O_3 Production (gm/min)	Corona Power (Watts)	O_3 Yield (gm/kw-hr)	RH %	Air Temp. (°K)	O_3 Density (gm/liter)
1	40	.028	2.5×10^{-2}	7.8×10^{-5}	0.7	6.69	42	297	1.95
2	"	.033	"	9.15×10^{-5}	"	7.85	"	"	"
3	45	.041	"	1.13×10^{-4}	1.95	3.47	"	"	"
4	"	.044	"	1.22×10^{-4}	"	3.75	"	"	"
5	50	.058	"	1.60×10^{-4}	3.4	2.82	"	"	"
6	"	.061	"	1.68×10^{-4}	"	2.96	"	"	"
7	"	.063	"	1.73×10^{-4}	"	3.05	"	"	"
8	55	.084	"	2.31×10^{-4}	5.5	2.52	"	"	"
9	60	.108	"	3.0×10^{-4}	7.8	2.28	"	"	"
10	"	.121	"	3.36×10^{-4}	"	2.6	"	"	"
11	"	.115	"	3.19×10^{-4}	"	2.5	"	"	"
12	65	.155	"	4.3×10^{-4}	10.8	2.39	"	"	"
13	"	.160	"	4.44×10^{-4}	"	2.47	"	"	"
14	"	.161	"	4.47×10^{-4}	"	2.49	"	"	"
15	70	.200	"	5.55×10^{-4}	14.3	2.34	"	"	"
16	"	.210	"	5.53×10^{-4}	"	2.45	"	"	"
17	"	.205	"	5.70×10^{-4}	"	2.40	"	"	"
18	75	.250	"	6.95×10^{-4}	18.5	2.3	"	"	"
19	"	.280	"	7.77×10^{-4}	"	2.5	"	"	"
20	80	.320	"	8.9×10^{-4}	24	2.24	"	"	"
21	"	.330	"	9.15×10^{-4}	"	2.31	"	"	"
22	85	.410	"	1.04×10^{-3}	30	2.1	"	"	"

VERSAR INC.

Table A-3 (Continued)

No.	Voltage (Kv)	O_3 Conc. (ppm)	Air Flow (m^3/sec)	O_3 Production (gm/min)	Corona Power (Watts)	O_3 Yield (gm/kw-hr)	RH %	Air Temp. (°K)	O_3 Density (gm/liter)
23	85	.405	2.5×10^{-2}	1.01×10^{-3}	30	2.0	42	297	1.95
24	90	.48	"	1.33×10^{-3}	3.75	2.13	"	"	"
25	"	.44	"	1.22×10^{-3}	"	1.95	"	"	"
26	"	.45	"	1.25×10^{-3}	"	2.00	"	"	"
27	40	.016	1.6×10^{-2}	2.91×10^{-5}	0.7	2.50	45	295	1.96
28	"	.019	"	3.46×10^{-5}	"	2.97	"	"	"
29	44	.028	"	5.10×10^{-5}	1.7	1.80	"	"	"
30	"	.035	"	6.37×10^{-5}	"	2.44	"	"	"
31	"	.033	"	6.00×10^{-5}	"	2.11	"	"	"
32	48	.042	"	7.65×10^{-5}	2.8	1.64	"	"	"
33	"	.048	"	8.74×10^{-5}	"	1.87	"	"	"
34	"	.051	"	9.30×10^{-5}	"	2.0	"	"	"
35	50	.052	"	9.45×10^{-5}	3.4	1.66	"	"	"
36	"	.055	"	1.00×10^{-4}	"	1.76	"	"	"
37	"	.056	"	1.02×10^{-4}	"	1.80	"	"	"
38	54	.080	"	1.46×10^{-4}	5.0	1.75	"	"	"
39	"	.082	"	1.49×10^{-4}	"	1.79	"	"	"
40	58	.120	"	2.18×10^{-4}	6.8	1.93	"	"	"
41	"	.115	"	2.09×10^{-4}	"	1.84	"	"	"
42	"	.115	"	2.09×10^{-4}	"	1.84	"	"	"

Table A-3 (Continued)

No.	Voltage (Kv)	O_3 Conc. (ppm)	Air Flow (m^3/sec)	O_3 Production (gm/min)	Corona Power (Watts)	O_3 Yield (gm/kw-hr)	RH %	Air Temp. (°K)	O_3 Density (gm/liter)
43	60	.130	1.6×10^{-2}	2.36×10^{-4}	7.9	1.80	45	295	1.96
44	"	.125	"	2.28×10^{-4}	"	1.73	"	"	"
45	"	.142	"	2.58×10^{-4}	"	1.96	"	"	"
46	65	.195	"	3.55×10^{-4}	10.8	1.97	"	"	"
47	"	.195	"	3.55×10^{-4}	"	1.97	"	"	"
48	"	.210	"	3.82×10^{-4}	"	2.13	"	"	"
49	70	.280	"	5.10×10^{-4}	14.3	2.14	"	"	"
50	"	.290	"	5.27×10^{-4}	"	2.21	"	"	"
51	75	.390	"	7.10×10^{-4}	18.5	2.30	"	"	"
52	"	.395	"	7.20×10^{-4}	"	2.33	"	"	"
53	80	.510	"	9.27×10^{-4}	23.8	2.34	"	"	"
54	"	.511	"	9.30×10^{-4}	"	2.35	"	"	"
55	84	.605	"	1.11×10^{-3}	28.5	2.34	"	"	"
56	"	.615	"	1.12×10^{-3}	"	2.36	"	"	"
57	86	.590	"	1.08×10^{-3}	31	2.09	"	"	"
58	"	.640	"	1.17×10^{-3}	"	2.27	"	"	"
59	90	.70	"	1.28×10^{-3}	37.5	2.06	"	"	"
60	"	.72	"	1.31×10^{-3}	"	2.10	"	"	"
61	92	.73	"	1.33×10^{-3}	41	1.95	"	"	"
62	"	.75	"	1.37×10^{-3}	"	2.01	"	"	"

Table A-3 (Continued)

No.	Voltage (Kv)	O_3 Conc. (ppm)	Air Flow (m^3/sec)	O_3 Production (gm/min)	Corona Power (Watts)	O_3 Yield (gm/kw-hr)	RH %	Air Temp. (°K)	O_3 Density (gm/liter)
63	45	.016	2.76×10^{-2}	5.1×10^{-5}	2	1.53	45	295	1.96
64	"	.014	"	4.46×10^{-5}	"	1.34	"	"	"
65	"	.017	"	5.41×10^{-5}	"	1.62	"	"	"
66	50	.024	"	7.65×10^{-5}	3.4	1.35	"	"	"
67	"	.022	"	7.02×10^{-5}	"	1.24	"	"	"
68	"	.022	"	7.02×10^{-5}	"	1.24	"	"	"
69	54	.029	"	9.25×10^{-5}	5.0	1.11	"	"	"
70	"	.033	"	1.05×10^{-4}	"	1.26	"	"	"
71	56	.035	"	1.11×10^{-4}	6.3	1.06	"	"	"
72	"	.035	"	1.11×10^{-4}	"	1.06	"	"	"
73	60	.039	"	1.24×10^{-4}	7.9	0.94	"	"	"
74	"	.044	"	1.40×10^{-4}	"	1.06	"	"	"
75	"	.042	"	1.34×10^{-4}	"	1.02	"	"	"
76	64	.055	"	1.75×10^{-4}	10	1.05	"	"	"
77	"	.056	"	1.79×10^{-4}	"	1.07	"	"	"
78	68	.068	"	2.17×10^{-4}	13	1.01	"	"	"
79	"	.067	"	2.13×10^{-4}	"	1.00	"	"	"
80	70	.072	"	2.29×10^{-4}	14.3	0.96	"	"	"
81	"	.074	"	2.36×10^{-4}	"	0.99	"	"	"
82	74	.085	"	2.71×10^{-4}	17.5	0.93	"	"	"
83	"	.086	"	2.74×10^{-4}	"	0.94	"	"	"

VERSAR INC.

Table A-3 (Continued)

No.	Volt-age (Kv)	O_3 Conc. (ppm)	Air Flow (m^3/sec)	O_3 Production (gm/min)	Corona Power (Watts)	O_3 Yield (gm/kw-hr)	RH %	Air Temp. (°K)	O_3 Density (gm/liter)
84	74	.081	2.76×10^{-2}	2.58×10^{-4}	17.5	0.89	45	295	1.96
85	78	.092	"	2.93×10^{-4}	21.5	0.82	"	"	"
86	"	.095	"	3.03×10^{-4}	"	0.85	"	"	"
87	80	.100	"	3.19×10^{-4}	23.8	0.80	"	"	"
88	"	.105	"	3.35×10^{-4}	"	0.84	"	"	"
89	84	.120	"	3.83×10^{-4}	28.5	0.81	"	"	"
90	"	.119	"	3.80×10^{-4}	"	0.80	"	"	"
91	90	.140	"	4.46×10^{-4}	37.5	0.72	"	"	"
92	"	.138	"	4.40×10^{-4}	"	0.70	"	"	"
93	40	.032	2.86×10^{-2}	8.55×10^{-5}	.67	7.65	42	297	1.97
94	"	.037	"	9.9×10^{-5}	"	8.85	"	"	"
95	"	.033	"	8.84×10^{-5}	"	7.90	"	"	"
96	45	.066	"	1.76×10^{-4}	2.0	5.3	"	"	"
97	"	.065	"	1.73×10^{-4}	"	5.2	"	"	"
98	"	.070	"	1.87×10^{-4}	"	5.6	"	"	"
99	50	.110	"	2.94×10^{-4}	3.4	5.2	"	"	"
100	"	.115	"	3.08×10^{-4}	"	5.44	"	"	"
101	"	.115	"	3.08×10^{-4}	"	5.44	"	"	"
102	55	.220	"	5.87×10^{-4}	5.4	6.52	"	"	"
103	"	.200	"	5.35×10^{-4}	"	5.95	"	"	"
104	"	.205	"	5.55×10^{-4}	"	6.16	"	"	"
105	60	.350	"	9.35×10^{-4}	7.9	7.10	"	"	"

Table A-3 (Continued)

No.	Voltage (Kv)	O_3 Conc. (ppm)	Air Flow (m^3/sec)	O_3 Production (gm/min)	Corona Power (Watts)	O_3 Yield (gm/kw-hr)	RH %	Air Temp. (°K)	O_3 Density (gm/liter)
106	60	.330	2.86×10^{-2}	8.82×10^{-4}	7.9	6.70	42	297	1.97
107	"	.335	"	8.96×10^{-4}	"	6.81	"	"	"
108	65	.44	"	1.18×10^{-3}	10.8	6.55	"	"	"
109	"	.49	"	1.32×10^{-3}	"	7.35	"	"	"
110	"	.48	"	1.29×10^{-3}	"	7.16	"	"	"
111	70	.64	"	1.72×10^{-3}	14.3	7.22	"	"	"
112	"	.65	"	1.74×10^{-3}	"	7.30	"	"	"
113	"	.60	"	1.61×10^{-3}	"	6.76	"	"	"
114	75	.78	"	2.09×10^{-3}	18.5	6.78	"	"	"
115	"	.80	"	2.14×10^{-3}	"	6.95	"	"	"
116	"	.81	"	2.17×10^{-3}	"	7.04	"	"	"
117	40	.015	1.83×10^{-2}	4.2×10^{-5}	.67	3.75	51	298	1.95
118	"	.013	"	3.64×10^{-5}	"	3.26	"	"	"
119	45	.033	"	9.25×10^{-5}	2.0	2.76	"	"	"
120	"	.035	"	9.80×10^{-5}	"	2.95	"	"	"
121	50	.072	"	2.02×10^{-4}	3.4	3.57	"	"	"
122	"	.075	"	2.10×10^{-4}	"	3.71	"	"	"
123	"	.071	"	1.98×10^{-4}	"	3.50	"	"	"
124	55	.140	"	3.92×10^{-4}	5.4	4.44	"	"	"
125	"	.140	"	3.92×10^{-4}	"	4.44	"	"	"
126	"	.144	"	4.03×10^{-4}	"	4.48	"	"	"
127	60	.250	"	7.00×10^{-4}	7.9	5.32	"	"	"

Table A-3 (Continued)

No.	Voltage (Kv)	O_3 Conc. (ppm)	Air Flow (m^3/sec)	O_3 Production (gm/min)	Corona Power (Watts)	O_3 Yield (gm/kw-hr)	RH %	Air Temp. (°K)	O_3 Density (gm/liter)
128	60	.250	1.83×10^{-2}	7.00×10^{-4}	7.9	5.32	51	298	1.95
129	"	.240	"	6.73×10^{-4}	"	5.10	"	"	"
130	65	.340	"	9.52×10^{-4}	10.8	5.30	"	"	"
131	"	.350	"	9.80×10^{-4}	"	5.44	"	"	"
132	"	.350	"	9.80×10^{-4}	"	5.44	"	"	"
133	70	.470	"	1.33×10^{-3}	14.3	5.58	"	"	"
134	"	.48	"	1.34×10^{-3}	"	5.63	"	"	"
135	"	.47	"	1.33×10^{-3}	"	5.58	"	"	"
136	75	.61	"	1.71×10^{-3}	18.5	5.55	"	"	"
137	"	.66	"	1.85×10^{-3}	"	6.00	"	"	"
138	"	.66	"	1.85×10^{-3}	"	6.00	"	"	"
139	80	.77	"	2.16×10^{-3}	23.8	5.45	"	"	"
140	"	.76	"	2.13×10^{-3}	"	5.37	"	"	"
141	"	.80	"	2.24×10^{-3}	"	5.65	"	"	"
142	45	.027	2.26×10^{-2}	2.97×10^{-5}	2.0	0.89	"	"	"
143	"	.033	"	3.64×10^{-5}	"	1.10	"	"	"
144	"	.031	"	3.42×10^{-5}	"	1.03	"	"	"
145	50	.055	"	6.05×10^{-5}	3.4	1.07	"	"	"
146	"	.059	"	6.49×10^{-5}	"	1.15	"	"	"
147	"	.058	"	6.37×10^{-5}	"	1.13	"	"	"
148	"	.155	"	4.15×10^{-4}	7.9	3.15	"	"	"
149	"	.155	"	4.15×10^{-4}	"	3.15	"	"	"

Table A-3 (Continued)

No.	Volt-age (Kv)	O_3 Conc. (ppm)	Air Flow (m^3/sec)	O_3 Production (gm/min)	Corona Power (Watts)	O_3 Yield (gm/kw-hr)	RH %	Air Temp. (°K)	O_3 Density (gm/liter)
150	60	.170	2.26×10^{-2}	5.55×10^{-4}	7.9	4.22	51	298	1.95
151	65	.255	"	6.83×10^{-4}	10.8	3.80	"	"	"
152	"	.250	"	6.70×10^{-4}	"	3.72	"	"	"
153	"	.255	"	6.83×10^{-4}	"	3.80	"	"	"
154	70	.330	"	8.85×10^{-4}	14.3	3.66	"	"	"
155	"	.330	"	8.85×10^{-4}	"	3.66	"	"	"
156	"	.350	"	9.38×10^{-4}	"	3.88	"	"	"
157	75	.445	"	11.9×10^{-4}	18.5	3.86	"	"	"
158	"	.450	"	12.1×10^{-4}	"	3.92	"	"	"
159	"	.455	"	12.2×10^{-4}	"	3.95	"	"	"
160	80	.550	"	14.7×10^{-4}	23.8	3.70	"	"	"
161	"	.58	"	15.5×10^{-4}	"	3.90	"	"	"
162	"	.63	"	16.9×10^{-4}	"	4.26	"	"	"
163	85	.66	"	17.7×10^{-4}	30	3.54	"	"	"
164	"	.70	"	18.7×10^{-4}	"	3.74	"	"	"
165	"	.71	"	19.0×10^{-4}	"	3.80	"	"	"
166	50	.044	2.74×10^{-2}	1.29×10^{-4}	3.4	2.49	"	"	"
167	"	.040	"	1.29×10^{-4}	"	2.28	"	"	"
168	"	.040	"	1.29×10^{-4}	"	2.28	"	"	"
169	55	.075	"	2.41×10^{-4}	5.4	2.68	"	"	"
170	"	.075	"	2.41×10^{-4}	"	2.68	"	"	"
171	"	.080	"	2.57×10^{-4}	"	2.86	"	"	"

Table A-3 (Continued)

No.	Voltage (Kv)	O_3 Conc. (ppm)	Air Flow (m^3/sec)	O_3 Production (gm/min)	Corona Power (Watts)	O_3 Yield (gm/kw-hr)	RH %	Air Temp. (°K)	O_3 Density (gm/liter)
172	60	.135	2.74×10^{-2}	4.34×10^{-4}	7.9	3.29	51	298	1.95
173	"	.135	"	4.34×10^{-4}	"	3.29	"	"	"
174	"	.140	"	4.50×10^{-4}	"	3.42	"	"	"
175	65	.190	"	6.10×10^{-4}	10.8	3.49	"	"	"
176	"	.198	"	6.37×10^{-4}	"	3.54	"	"	"
177	"	.190	"	6.10×10^{-4}	"	3.49	"	"	"
178	70	.280	"	9.00×10^{-4}	14.3	3.78	"	"	"
179	"	.285	"	9.17×10^{-4}	"	3.86	"	"	"
180	"	.260	"	8.35×10^{-4}	"	3.52	"	"	"
181	75	.330	"	10.7×10^{-4}	18.5	3.47	"	"	"
182	"	.335	"	10.8×10^{-4}	"	3.50	"	"	"
183	"	.360	"	11.6×10^{-4}	"	3.77	"	"	"
184	80	.420	"	13.5×10^{-4}	23.8	3.40	"	"	"
185	"	.425	"	13.7×10^{-4}	"	3.45	"	"	"
186	"	.400	"	12.9×10^{-4}	"	3.27	"	"	"
187	50	.054	2.11×10^{-2}	1.05×10^{-4}	3.4	1.81	38	299	1.94
188	"	.055	"	1.08×10^{-4}	"	1.91	"	"	"
189	"	.055	"	1.08×10^{-4}	"	1.91	"	"	"
190	55	.150	"	2.92×10^{-4}	5.4	3.24	"	"	"
191	"	.170	"	3.32×10^{-4}	"	3.69	"	"	"
192	"	.170	"	3.32×10^{-4}	"	3.69	"	"	"
193	60	.300	"	5.85×10^{-4}	7.9	4.45	"	"	"

VERSAR INC.

Table A-3 (Continued)

No.	Voltage (Kv)	O_3 Conc. (ppm)	Air Flow (m^3/sec)	O_3 Production (gm/min)	Corona Power (Watts)	O_3 Yield (gm/kw-hr)	RH %	Air Temp. (°K)	O_3 Density (gm/liter)
194	60	.315	2.11×10^{-2}	6.15×10^{-4}	7.9	4.66	38	299	1.94
195	"	.280	"	5.46×10^{-4}	"	4.15	"	"	"
196	65	.45	"	8.77×10^{-4}	10.8	4.87	"	"	"
197	"	.45	"	8.77×10^{-4}	"	4.87	"	"	"
198	"	.47	"	9.15×10^{-4}	"	5.07	"	"	"
199	70	.66	"	12.9×10^{-4}	14.3	5.42	"	"	"
200	"	.60	"	11.7×10^{-4}	"	4.92	"	"	"
201	"	.61	"	11.9×10^{-4}	"	5.00	"	"	"
202	75	.81	"	15.7×10^{-4}	18.5	5.09	"	"	"
203	"	.81	"	15.7×10^{-4}	"	5.09	"	"	"
204	"	.77	"	15.0×10^{-4}	"	4.87	"	"	"
205	80	.94	"	18.3×10^{-4}	23.8	4.61	"	"	"
206	"	.94	"	18.3×10^{-4}	"	4.61	"	"	"
207	"	.97	"	18.9×10^{-4}	"	4.76	"	"	"
208	45	.027	2.52×10^{-2}	$.722 \times 10^{-4}$	2.0	2.17	"	"	"
209	"	.033	"	$.884 \times 10^{-4}$	"	2.65	"	"	"
210	"	.031	"	$.830 \times 10^{-4}$	"	2.49	"	"	"
211	50	.055	"	1.47×10^{-4}	3.4	2.59	"	"	"
212	"	.059	"	1.58×10^{-4}	"	2.79	"	"	"
213	"	.058	"	1.55×10^{-4}	"	2.74	"	"	"
214	55	.099	"	2.65×10^{-4}	5.4	2.95	"	"	"
215	"	.110	"	2.95×10^{-4}	"	3.28	"	"	"

Table A-3 (Continued)

No.	Voltage (Kv)	O_3 Conc. (ppm)	Air Flow (m^3/sec)	O_3 Production (gm/min)	Corona Power (Watts)	O_3 Yield (gm/kw-hr)	RH %	Air Temp. (°K)	O_3 Density (gm/liter)
216	55	.109	2.52×10^{-2}	2.92×10^{-4}	5.4	3.24	38	299	1.94
217	60	.22	"	4.81×10^{-4}	7.9	3.66	"	"	"
218	"	.22	"	4.81×10^{-4}	"	3.66	"	"	"
219	"	.20	"	4.46×10^{-4}	"	3.49	"	"	"
220	65	.36	"	8.04×10^{-4}	10.8	4.45	"	"	"
221	"	.34	"	7.59×10^{-4}	"	4.21	"	"	"
222	"	.34	"	7.59×10^{-4}	"	4.21	"	"	"
223	70	.52	"	11.6×10^{-4}	14.3	4.88	"	"	"
224	"	.52	"	11.6×10^{-4}	"	4.88	"	"	"
225	"	.50	"	11.2×10^{-4}	"	4.71	"	"	"
226	"	.66	"	14.7×10^{-4}	18.5	4.76	"	"	"
227	"	.66	"	14.7×10^{-4}	"	4.76	"	"	"
228	"	.64	"	14.3×10^{-4}	"	4.63	"	"	"
229	80	.82	"	18.3×10^{-4}	24	4.61	"	"	"
230	"	.81	"	18.1×10^{-4}	"	4.56	"	"	"
231	"	.82	"	18.3×10^{-4}	"	4.61	"	"	"
232	50	.025	2.83×10^{-2}	0.652×10^{-4}	3.4	1.25	"	"	"
233	"	.024	"	0.626×10^{-4}	"	1.11	"	"	"
234	"	.025	"	0.652×10^{-4}	"	1.25	"	"	"
235	55	.077	"	2.01×10^{-4}	5.4	2.23	"	"	"
236	"	.077	"	2.01×10^{-4}	"	2.23	"	"	"
237	"	.075	"	1.96×10^{-4}	"	2.18	"	"	"
238	60	.160	"	4.17×10^{-4}	7.9	3.17	"	"	"

Table A-3 (Continued)

No.	Voltage (Kv)	O_3 Conc. (ppm)	Air Flow (m^3/sec)	O_3 Production (gm/min)	Corona Power (Watts)	O_3 Yield (gm/kw-hr)	RH %	Air Temp. (°K)	O_3 Density (gm/liter)
239	60	.160	2.83×10^{-2}	4.17×10^{-4}	7.9	3.17	38	299	1.94
240	"	.167	"	4.36×10^{-4}	"	3.31	"	"	"
241	65	.25	"	6.52×10^{-4}	10.8	3.62	"	"	"
242	"	.25	"	6.52×10^{-4}	"	3.62	"	"	"
243	"	.28	"	7.30×10^{-4}	"	4.05	"	"	"
244	70	.38	"	9.90×10^{-4}	14.3	4.15	"	"	"
245	"	.38	"	9.90×10^{-4}	"	3.15	"	"	"
246	"	.40	"	10.4×10^{-4}	"	4.36	"	"	"
247	75	.50	"	13.1×10^{-4}	18.5	4.25	"	"	"
248	"	.54	"	14.1×10^{-4}	"	4.57	"	"	"
249	"	.50	"	13.1×10^{-4}	"	4.25	"	"	"
250	"	.82	"	21.4×10^{-4}	24	5.40	"	"	"
251	"	.82	"	21.4×10^{-4}	"	5.40	"	"	"
252	"	.80	"	20.9×10^{-4}	"	5.27	"	"	"
253	85	.97	"	25.3×10^{-4}	30	5.06	"	"	"
254	"	.99	"	25.8×10^{-4}	"	5.16	"	"	"
255	"	.98	"	25.6×10^{-4}	"	5.12	"	"	"
256	50	.011	3.16×10^{-2}	$.32 \times 10^{-4}$	3.4	0.565	"	"	"
257	"	.015	"	$.44 \times 10^{-4}$	"	0.775	"	"	"
258	55	.066	"	1.92×10^{-4}	5.4	2.04	"	"	"
259	"	.070	"	2.04×10^{-4}	"	2.27	"	"	"
260	60	.150	"	4.38×10^{-4}	7.9	3.33	"	"	"

VERSAR INC.

Table A-3 (Continued)

No.	Voltage (Kv)	O_3 Conc. (ppm)	Air Flow (m^3/sec)	O_3 Production (gm/min)	Corona Power (Watts)	O_3 Yield (gm/kw-hr)	RH %	Air Temp. (°K)	O_3 Density (gm/liter)
261	60	.140	3.16×10^{-2}	4.08×10^{-4}	7.9	3.10	38	299	1.94
262	65	.230	"	6.71×10^{-4}	10.8	3.71	"	"	"
263	"	.21	"	6.13×10^{-4}	"	3.41	"	"	"
264	"	.205	"	6.00×10^{-4}	"	3.33	"	"	"
265	70	.31	"	9.05×10^{-4}	14.3	3.80	"	"	"
266	"	.33	"	9.63×10^{-4}	"	4.06	"	"	"
267	"	.33	"	9.63×10^{-4}	"	4.06	"	"	"
268	75	.40	"	11.7×10^{-4}	18.5	3.83	"	"	"
269	"	.40	"	11.7×10^{-4}	"	3.83	"	"	"
270	"	.44	"	12.8×10^{-4}	"	4.15	"	"	"
271	80	.55	"	16.1×10^{-4}	23.8	4.06	"	"	"
272	"	.50	"	14.6×10^{-4}	"	4.18	"	"	"
273	"	.51	"	14.9×10^{-4}	"	3.76	"	"	"
274	85	.72	"	21.0×10^{-4}	30	4.20	"	"	"
275	"	.74	"	21.6×10^{-4}	"	4.32	"	"	"
276	50	.019	3.47×10^{-2}	0.607×10^{-4}	3.4	1.07	"	"	"
277	"	.022	"	0.703×10^{-4}	"	1.24	"	"	"
278	55	.060	"	1.91×10^{-4}	5.4	2.12	"	"	"
279	"	.055	"	1.76×10^{-4}	"	1.96	"	"	"
280	60	.120	"	3.84×10^{-4}	7.9	2.92	"	"	"
281	"	.120	"	3.84×10^{-4}	"	2.92	"	"	"
282	65	.200	"	6.38×10^{-4}	10.8	3.55	"	"	"

Table A-3 (Continued)

No.	Volt-age (Kv)	O_3 Conc. (ppm)	Air Flow (m^3/sec)	O_3 Production (gm/min)	Corona Power (Watts)	O_3 Yield (gm/kw-hr)	RH %	Air Temp. (°K)	O_3 Density (gm/liter)
283	65	.180	3.47×10^{-2}	5.75×10^{-4}	10.8	3.70	38	299	1.94
284	70	.260	"	8.30×10^{-4}	14.3	3.49	"	"	"
285	"	.265	"	8.45×10^{-4}	"	3.55	"	"	"
286	"	.280	"	8.95×10^{-4}	"	3.76	"	"	"
287	75	.360	"	11.50×10^{-4}	18.5	3.74	"	"	"
288	"	.360	"	11.50×10^{-4}	"	3.74	"	"	"
289	"	.380	"	14.00×10^{-4}	"	4.54	"	"	"
290	80	.420	"	13.4×10^{-4}	23.8	3.38	"	"	"
291	"	.440	"	14.1×10^{-4}	"	3.56	"	"	"
292	"	.420	"	13.4×10^{-4}	"	3.38	"	"	"
293	85	.510	"	16.3×10^{-4}	30.0	3.26	"	"	"
294	"	.520	"	16.6×10^{-4}	"	3.32	"	"	"
295	"	.550	"	16.0×10^{-4}	"	3.20	"	"	"
296	55	.040	4.02×10^{-2}	1.49×10^{-4}	5.4	1.65	"	"	"
297	"	.044	"	1.63×10^{-4}	"	1.81	"	"	"
298	"	.040	"	1.49×10^{-4}	"	1.65	"	"	"
299	60	.100	"	3.71×10^{-4}	7.9	2.82	"	"	"
300	"	.102	"	3.78×10^{-4}	"	2.87	"	"	"
301	"	.095	"	3.52×10^{-4}	"	2.67	"	"	"
302	65	.150	"	5.55×10^{-4}	10.8	3.07	"	"	"
303	"	.150	"	5.55×10^{-4}	"	3.07	"	"	"
304	"	.170	"	6.30×10^{-4}	"	3.48	"	"	"

Table A-3 (Continued)

No.	Voltage (Kv)	O_3 Conc. (ppm)	Air Flow (m^3/sec)	O_3 Production (gm/min)	Corona Power (Watts)	O_3 Yield (gm/kw-hr)	RH %	Air Temp. (°K)	O_3 Density (gm/liter)
305	70	.240	4.02×10^{-2}	8.90×10^{-4}	14.3	3.74	38	299	1.94
306	"	.210	"	9.80×10^{-4}	"	3.28	"	"	"
307	"	.275	"	8.35×10^{-4}	"	3.51	"	"	"
308	75	.300	"	11.1×10^{-4}	18.5	3.60	"	"	"
309	"	.300	"	11.1×10^{-4}	"	3.60	"	"	"
310	"	.340	"	12.6×10^{-4}	"	4.09	"	"	"
311	80	.400	"	14.8×10^{-4}	23.8	3.73	"	"	"
312	"	.380	"	14.1×10^{-4}	"	3.55	"	"	"
313	"	.380	"	14.1×10^{-4}	"	3.55	"	"	"
314	85	.430	"	16.0×10^{-4}	30.0	3.20	"	"	"
315	"	.430	"	16.0×10^{-4}	"	3.20	"	"	"
316	"	.460	"	17.1×10^{-4}	"	3.42	"	"	"
317	40	.001	3.93×10^{-2}	$.036 \times 10^{-4}$	0.6	0.36	27	298	1.96
318	45	.007	"	$.254 \times 10^{-4}$	1.95	0.78	"	"	"
319	50	.018	"	$.652 \times 10^{-4}$	3.40	1.15	"	"	"
320	55	.048	"	1.94×10^{-4}	5.40	1.93	"	"	"
321	60	.10	"	3.62×10^{-4}	7.9	2.75	"	"	"
322	65	.20	"	7.24×10^{-4}	10.8	4.02	"	"	"
323	70	.36	"	13.5×10^{-4}	14.3	5.50	"	"	"
324	40	.006	3.78×10^{-2}	$.209 \times 10^{-4}$	0.6	2.09	28	"	1.955
325	45	.029	"	1.02×10^{-4}	1.95	3.14	"	"	"
326	50	.060	"	2.09×10^{-4}	3.4	3.50	"	"	"

Table A-3 (Continued)

No.	Voltage (Kv)	O_3 Conc. (ppm)	Air Flow (m^3/sec)	O_3 Production (gm/min)	Corona Power (Watts)	O_3 Yield (gm/kw-hr)	RH %	Air Temp. (°K)	O_3 Density (gm/liter)
327	55	.140	3.78×10^{-2}	4.90×10^{-4}	5.4	5.45	28	298	1.955
328	60	.203	"	7.10×10^{-4}	7.9	5.39	"	"	"
329	65	.37	"	12.9×10^{-4}	10.8	7.16	"	"	"
330	45	.004	3.85×10^{-2}	$.148 \times 10^{-4}$	1.95	0.46	33	304	1.915
331	50	.014	"	$.496 \times 10^{-4}$	3.4	.875	"	"	"
332	55	.031	"	1.09×10^{-4}	5.4	1.21	"	"	"
333	60	.077	"	2.72×10^{-4}	7.9	2.10	"	"	"
334	65	.140	"	4.96×10^{-4}	10.8	2.74	"	"	"
335	70	.22	"	7.80×10^{-4}	14.3	3.27	"	"	"
336	75	.45	"	15.9×10^{-4}	18.5	5.15	"	"	"
337	45	.039	3.78×10^{-2}	1.34×10^{-4}	1.95	4.12	"	"	"
338	50	.075	"	2.56×10^{-4}	3.4	4.52	"	"	"
339	55	.130	"	4.45×10^{-4}	5.4	4.95	"	"	"
340	62	.210	"	7.19×10^{-4}	7.9	5.65	"	"	"
341	65	.350	"	12.2×10^{-4}	10.8	6.77	"	"	"
342	70	.510	"	17.4×10^{-4}	14.3	7.30	"	"	"
343	75	.650	"	22.2×10^{-4}	18.5	7.20	"	"	"
344	45	.065	3.34×10^{-2}	2.06×10^{-4}	1.95	6.33	"	"	"
345	50	.120	"	3.76×10^{-4}	3.4	6.64	"	"	"
346	55	.210	"	6.68×10^{-4}	5.4	7.41	"	"	"
347	60	.340	"	10.6×10^{-4}	7.9	8.24	"	"	"
348	65	.530	"	16.7×10^{-4}	10.8	9.27	"	"	"
349	70	.790	"	24.6×10^{-4}	14.3	10.30	"	"	"

Table A-3 (Continued)

No.	Voltage (Kv)	O_3 Conc. (ppm)	Air Flow (m^3/sec)	O_3 Production (gm/min)	Corona Power (Watts)	O_3 Yield (gm/kw-hr)	RH %	Air Temp. (°K)	O_3 Density (gm/liter)
350	45	.095	3.17×10^{-2}	2.72×10^{-4}	1.95	8.35	33	304	1.915
351	50	.14	"	4.03×10^{-4}	3.4	7.12	"	"	"
352	55	.28	"	8.04×10^{-4}	5.4	0.92	"	"	"
353	60	.49	"	14.1×10^{-4}	7.9	9.25	"	"	"
354	65	.66	"	18.9×10^{-4}	10.8	10.5	"	"	"
355	70	.93	"	26.6×10^{-4}	14.3	11.2	"	"	"
356	45	.055	2.83×10^{-2}	1.41×10^{-4}	1.95	4.34	"	"	"
357	50	.20	"	5.12×10^{-4}	3.4	9.05	"	"	"
358	55	.34	"	8.71×10^{-4}	5.4	9.67	"	"	"
359	60	.55	"	14.1×10^{-4}	7.9	10.90	"	"	"
360	40	.020	4.05×10^{-2}	$.725 \times 10^{-4}$	0.6	7.25	27	307.4	1.895
361	42	.025	"	$.907 \times 10^{-4}$	1.2	4.54	"	"	"
362	44	.036	"	1.31×10^{-4}	1.7	4.62	"	"	"
363	46	.047	"	1.70×10^{-4}	2.2	4.64	"	"	"
364	48	.072	"	2.61×10^{-4}	2.8	5.60	"	"	"
365	50	.080	"	2.90×10^{-4}	3.4	6.88	"	"	"
366	52	.102	"	3.70×10^{-4}	4.1	5.41	"	"	"
367	54	.140	"	5.07×10^{-4}	5.0	6.09	"	"	"
368	56	.146	"	5.28×10^{-4}	5.8	5.45	"	"	"
369	58	.205	"	7.35×10^{-4}	6.7	6.58	"	"	"
370	60	.230	"	8.31×10^{-4}	7.9	5.55	"	"	"
371	62	.290	"	10.5×10^{-4}	9.0	7.00	"	"	"

Table A-3 (Continued)

No.	Voltage (Kv)	O_3 Conc. (ppm)	Air Flow (m^3/sec)	O_3 Production (gm/min)	Corona Power (Watts)	O_3 Yield (gm/kw-hr)	RH %	Air Temp. (°K)	O_3 Density (gm/liter)
372	64	.348	4.05×10^{-2}	12.6×10^{-4}	10.1	7.50	27	307.4	1.895
373	66	.400	"	14.5×10^{-4}	11.5	8.70	"	"	"
374	68	.460	"	16.7×10^{-4}	12.9	7.75	"	"	"
375	70	.560	"	20.2×10^{-4}	14.3	8.47	"	"	"
376	72	.580	"	21.0×10^{-4}	16	9.88	"	"	"
377	74	.630	"	22.8×10^{-4}	17.6	7.76	"	"	"
378	76	.700	"	25.4×10^{-4}	19.3	7.90	"	"	"
379	78	.755	"	27.4×10^{-4}	22.5	7.30	"	"	"
380	80	.820	"	29.5×10^{-4}	23.8	7.44	"	"	"
381	40	.03	3.82×10^{-2}	1.03×10^{-4}	0.6	10.1	27	"	"
382	42	.046	"	1.58×10^{-4}	1.2	7.9	"	"	"
383	44	.066	"	2.26×10^{-4}	1.7	7.95	"	"	"
384	46	.072	"	2.46×10^{-4}	2.2	6.70	"	"	"
385	48	.115	"	3.93×10^{-4}	2.8	8.45	"	"	"
386	50	.138	"	4.72×10^{-4}	3.4	8.31	"	"	"
387	52	.172	"	5.88×10^{-4}	4.1	8.60	"	"	"
388	54	.220	"	7.54×10^{-4}	5.0	9.04	"	"	"
389	56	.240	"	8.21×10^{-4}	5.8	8.50	"	"	"
390	58	.320	"	11.0×10^{-4}	6.7	9.75	"	"	"
391	60	.330	"	11.3×10^{-4}	7.9	7.55	"	"	"
392	62	.405	"	13.8×10^{-4}	9.0	9.20	"	"	"
393	64	.460	"	15.7×10^{-4}	10.1	9.32	"	"	"

Table A-3 (Continued)

No.	Voltage (Kv)	O_3 Conc. (ppm)	Air Flow (m^3/sec)	O_3 Production (gm/min)	Corona Power (Watts)	O_3 Yield (gm/kw-hr)	RH %	Air Temp. (°K)	O_3 Density (gm/liter)
394	66	.550	3.82×10^{-2}	18.8×10^{-4}	11.5	9.80	27	307.4	1.895
395	68	.620	"	21.2×10^{-4}	12.9	9.85	"	"	"
396	70	.730	"	25.0×10^{-4}	14.3	10.50	"	"	"
397	72	.740	"	25.3×10^{-4}	16	9.50	"	"	"
398	74	.800	"	27.4×10^{-4}	17.6	9.32	"	"	"
399	76	.850	"	29.1×10^{-4}	19.3	9.05	"	"	"
400	78	.910	"	31.2×10^{-4}	22.5	8.30	"	"	"
401	80	.970	"	33.2×10^{-4}	23.8	8.35	"	"	"
402	40	.04	3.56×10^{-2}	1.28×10^{-4}	0.6	13.6	"	"	"
403	42	.055	"	1.76×10^{-4}	1.2	8.8	"	"	"
404	44	.092	"	2.94×10^{-4}	1.7	10.4	"	"	"
405	46	.132	"	4.23×10^{-4}	2.2	11.5	"	"	"
406	48	.172	"	5.51×10^{-4}	2.8	11.7	"	"	"
407	50	.180	"	5.76×10^{-4}	3.4	13.5	"	"	"
408	52	.247	"	7.92×10^{-4}	4.1	11.5	"	"	"
409	54	.300	"	9.60×10^{-4}	5.0	11.5	"	"	"
410	56	.320	"	10.2×10^{-4}	5.8	10.6	"	"	"
411	58	.410	"	13.1×10^{-4}	6.7	11.7	"	"	"
412	60	.440	"	14.1×10^{-4}	7.9	9.4	"	"	"
413	62	.530	"	16.9×10^{-4}	9.0	11.3	"	"	"
414	64	.660	"	21.1×10^{-4}	10.1	12.6	"	"	"
415	66	.740	"	23.7×10^{-4}	11.5	12.4	"	"	"

Table A-3 (Continued)

No.	Voltage (Kv)	O_3 Conc. (ppm)	Air Flow (m^3/sec)	O_3 Production (gm/min)	Corona Power (Watts)	O_3 Yield (gm/kw-hr)	RH %	Air Temp. (°K)	O_3 Density (gm/liter)
416	68	.900	3.56×10^{-2}	28.8×10^{-4}	12.9	13.4	27	307.4	1.895
417	50	.012	$3.86 \times 10^{-}$	$.434 \times 10^{-4}$	3.4	.768	51	294	1.99
418	52	.018	"	$.651 \times 10^{-4}$	4.1	.955	"	"	"
419	54	.025	"	$.905 \times 10^{-4}$	5.0	1.09	"	"	"
420	56	.032	"	1.16×10^{-4}	5.8	1.21	"	"	"
421	60	.082	"	2.97×10^{-4}	7.9	2.26	"	"	"
422	64	.160	"	5.79×10^{-4}	10.1	3.44	"	"	"
423	68	.255	"	9.22×10^{-4}	12.9	4.29	"	"	"
424	72	.325	"	11.80×10^{-4}	16	4.43	"	"	"
425	76	.440	"	15.9×10^{-4}	19.3	4.95	"	"	"
426	80	.580	"	21.0×10^{-4}	23.8	5.30	"	"	"
427	82	.705	"	25.5×10^{-4}	25.8	5.94	"	"	"
428	40	.011	3.67×10^{-2}	$.381 \times 10^{-4}$	0.6	3.81	"	"	"
429	44	.031	"	1.07×10^{-4}	1.7	3.78	"	"	"
430	48	.058	"	2.02×10^{-4}	2.8	4.33	"	"	"
431	52	.094	"	3.26×10^{-4}	4.1	4.77	"	"	"
432	56	.130	"	4.50×10^{-4}	5.8	4.65	"	"	"
433	60	.195	"	6.75×10^{-4}	7.9	5.12	"	"	"
434	64	.255	"	8.82×10^{-4}	23.8	6.57	"	"	"
435	68	.360	"	12.45×10^{-4}	12.9	5.80	"	"	"
436	72	.495	"	17.1×10^{-4}	16.0	6.40	"	"	"
437	76	.600	"	20.8×10^{-4}	19.3	6.46	"	"	"

Table A-3 (Continued)

No.	Voltage (Kv)	O_3 Conc. (ppm)	Air Flow (m^3/sec)	O_3 Production (gm/min)	Corona Power (Watts)	O_3 Yield (gm/kw-hr)	RH %	Air Temp. (°K)	O_3 Density (gm/liter)
438	80	.725	3.67×10^{-2}	26.1×10^{-4}	23.8	6.57	51	294	1.99
439	40	.024	$3.53 \times 10^{-}$	$.801 \times 10^{-4}$	0.6	8.00	"	"	"
440	44	.057	"	1.90×10^{-4}	1.7	6.70	"	"	"
441	48	.095	"	3.16×10^{-4}	2.8	6.77	"	"	"
442	52	.140	"	4.67×10^{-4}	4.1	6.84	"	"	"
443	56	.210	"	7.01×10^{-4}	5.8	7.25	"	"	"
444	60	.295	"	9.85×10^{-4}	7.9	7.50	"	"	"
445	64	.380	"	12.70×10^{-4}	10.1	7.60	"	"	"
446	68	.480	"	16.0×10^{-4}	12.9	7.45	"	"	"
447	72	.605	"	20.4×10^{-4}	16	7.50	"	"	"
448	76	.760	"	25.4×10^{-4}	19.3	7.90	"	"	"
449	40	.0185	3.26×10^{-2}	$.567 \times 10^{-4}$	0.6	5.67	"	"	"
450	44	.056	"	1.72×10^{-4}	1.7	6.06	"	"	"
451	48	.100	"	3.07×10^{-4}	2.8	6.56	"	"	"
452	52	.150	"	4.60×10^{-4}	4.1	6.71	"	"	"
453	56	.240	"	7.37×10^{-4}	5.8	7.64	"	"	"
454	60	.315	"	9.67×10^{-4}	7.9	8.56	"	"	"
455	64	.430	"	13.2×10^{-4}	10.1	7.83	"	"	"
456	68	.560	"	17.2×10^{-4}	12.9	8.00	"	"	"
457	72	.700	"	21.5×10^{-4}	16	8.07	"	"	"
458	74	.770	"	23.6×10^{-4}	17.6	8.05	"	"	"
459	40	.027	3.14×10^{-2}	$.800 \times 10^{-4}$	0.6	8.00	"	"	"

Table A-3 (Continued)

No.	Voltage (Kv)	O_3 Conc. (ppm)	Air Flow (m^3/sec)	O_3 Production (gm/min)	Corona Power (Watts)	O_3 Yield (gm/kw-hr)	RH %	Air Temp. (°K)	O_3 Density (gm/liter)
460	44	.064	3.14×10^{-2}	1.89×10^{-4}	1.7	6.66	51	2.94	1.99
461	48	.120	"	3.55×10^{-4}	2.8	7.61	"	"	"
462	52	.200	"	5.92×10^{-4}	4.1	8.65	"	"	"
463	56	.270	"	8.00×10^{-4}	5.8	8.29	"	"	"
464	60	.400	"	13.8×10^{-4}	7.9	12.2	"	"	"
465	64	.520	"	15.4×10^{-4}	10.1	9.15	"	"	"
466	68	.670	"	19.8×10^{-4}	12.9	9.20	"	"	"
467	70	.750	"	22.2×10^{-4}	14.3	9.30	"	"	"
468	72	.840	"	24.8×10^{-4}	16.0	9.30	"	"	"
469	74	.940	"	27.8×10^{-4}	17.6	9.50	"	"	"
470	40	.030	2.79×10^{-2}	$.788 \times 10^{-4}$	0.6	7.88	"	"	"
471	44	.086	"	2.26×10^{-4}	1.7	7.95	"	"	"
472	48	.146	"	3.84×10^{-4}	2.8	8.25	"	"	"
473	52	.220	"	5.77×10^{-4}	4.1	8.47	"	"	"
474	56	.320	"	8.41×10^{-4}	5.8	8.70	"	"	"
475	60	.460	"	12.1×10^{-4}	7.9	9.20	"	"	"
476	65	.590	"	15.5×10^{-4}	10.8	8.61	"	"	"
477	68	.710	"	18.7×10^{-4}	12.9	8.70	"	"	"
478	70	.820	"	21.5×10^{-4}	14.3	9.02	"	"	"
479	72	.890	"	23.4×10^{-4}	16	8.80	"	"	"
480	40	.004	3.86×10^{-2}	$.151 \times 10^{-4}$	0.6	1.51	58	295	1.98

Table A-3 (Continued)

No.	Voltage (Kv)	O_3 Conc. (ppm)	Air Flow (m^3/sec)	O_3 Production (gm/min)	Corona Power (Watts)	O_3 Yield (gm/kw-hr)	RH %	Air Temp. (°K)	O_3 Density (gm/liter)
481	44	.007	3.86×10^{-2}	$.244 \times 10^{-4}$	1.7	1.51	58	295	1.98
482	48	.013	"	$.466 \times 10^{-4}$	2.8	1.00	"	"	"
483	52	.030	"	1.08×10^{-4}	4.1	1.58	"	"	"
484	56	.062	"	2.23×10^{-4}	5.8	2.30	"	"	"
485	60	.115	"	4.13×10^{-4}	7.9	3.14	"	"	"
486	64	.160	"	5.75×10^{-4}	10.1	3.20	"	"	"
487	68	.220	"	7.90×10^{-4}	12.9	3.68	"	"	"
488	72	.315	"	11.2×10^{-4}	16	4.21	"	"	"
489	76	.430	"	15.5×10^{-4}	19.3	4.72	"	"	"
490	80	.570	"	20.4×10^{-4}	23.8	5.14	"	"	"
491	84	.770	"	43.6×10^{-4}	28.5	9.17	"	"	"
492	40	.007	3.5×10^{-2}	$.232 \times 10^{-4}$	0.6	2.32	"	"	"
493	44	.044	"	1.44×10^{-4}	1.7	5.07	"	"	"
494	48	.073	"	2.39×10^{-4}	2.8	5.13	"	"	"
495	52	.128	"	4.17×10^{-4}	4.1	6.10	"	"	"
496	56	.190	"	6.20×10^{-4}	5.8	6.41	"	"	"
497	60	.230	"	9.51×10^{-4}	7.9	5.72	"	"	"
498	64	.300	"	8.80×10^{-4}	10.1	4.88	"	"	"
499	68	.400	"	13.1×10^{-4}	12.9	6.09	"	"	"
500	72	.500	"	16.4×10^{-4}	16	6.15	"	"	"

Table A-3 (Continued)

No.	Voltage (Kv)	O_3 Conc. (ppm)	Air Flow (m^3/sec)	O_3 Production (gm/min)	Corona Power (Watts)	O_3 Yield (gm/kw-hr)	RH %	Air Temp. (°K)	O_3 Density (gm/liter)
501	74	.530	3.5×10^{-2}	17.3×10^{-4}	17.6	5.90	58	295	1.98
502	80	.800	"	26.2×10^{-4}	23.8	6.60	"	"	"
503	84	.950	"	31.1×10^{-4}	28.5	5.55	"	"	"
504	60	.108	2.43×10^{-2}	3.02×10^{-4}	7.9	2.31	42	297	1.92
505	70	.22	"	6.15×10^{-4}	14.3	2.58	"	"	"
506	75	.25	"	6.98×10^{-4}	18.5	2.26	"	"	"
507	80	.32	"	8.95×10^{-4}	23.8	2.25	"	"	"
508	80	.33	"	9.22×10^{-4}	"	2.32	"	"	"
509	90	.48	"	13.4×10^{-4}	37.5	2.15	"	"	"
510	90	.44	"	12.3×10^{-4}	"	1.97	"	"	"
511	50	.014	1.6×10^{-2}	0.26×10^{-4}	3.4	0.46	45	293	1.96
512	60	.13	"	2.41×10^{-4}	7.9	1.83	"	"	"
513	66	.22	"	4.09×10^{-4}	11.5	2.14	"	"	"
514	72	.31	"	5.75×10^{-4}	16	2.06	"	"	"
515	80	.46	"	8.54×10^{-4}	23.8	2.15	"	"	"
516	86	.59	"	11.0×10^{-4}	31	2.12	"	"	"
517	92	.73	"	13.6×10^{-4}	41.5	1.97	"	"	"
518	50	.09	1.27×10^{-2}	1.34×10^{-4}	3.4	2.36	"	294	"
519	60	.25	"	3.72×10^{-4}	7.9	2.82	"	"	"
520	66	.36	"	5.35×10^{-4}	11.5	2.80	"	"	"
521	72	.48	"	7.15×10^{-4}	16	2.68	"	"	"
522	80	.52	"	7.74×10^{-4}	23.8	1.95	"	"	"
523	90	.96	"	14.3×10^{-4}	37.5	2.29	"	"	"

Table A-4 - Tabulated Ozone Production Data from 1.04 cm Diameter Aluminum Cable Sample

No.	Voltage (Kv)	O_3 Conc. (ppm)	Air Flow (m^3/sec)	O_3 Production (gm/min)	Corona Power (Watts)	O_3 Yield (gm/kw-hr)	RH %	Air Temp. (°K)	O_3 Density (gm/liter)
524	45	.002	3.74×10^{-2}	0.069×10^{-4}	1.00	.412	36	297	1.95
525	50	.005	"	0.172×10^{-4}	1.60	.646	"	"	"
526	55	.011	"	0.377×10^{-4}	2.27	.995	"	"	"
527	58	.018	"	0.617×10^{-4}	3.0	1.23	"	"	"
528	60	.020	"	0.686×10^{-4}	3.45	1.20	"	"	"
529	60	.024	"	0.823×10^{-4}	"	1.43	"	"	"
530	62	.032	"	1.10×10^{-4}	4.0	1.65	"	"	"
531	62	.035	"	1.70×10^{-4}	"	1.80	"	"	"
532	65	.055	"	1.89×10^{-4}	5.0	2.27	"	"	"
533	65	.070	"	2.40×10^{-4}	"	2.76	"	"	"
534	68	.090	"	3.09×10^{-4}	6.4	2.90	"	"	"
535	68	.090	"	3.09×10^{-4}	"	2.90	"	"	"
536	70	.102	"	3.50×10^{-4}	7.7	2.73	"	"	"
537	70	.130	"	4.45×10^{-4}	"	3.46	"	"	"
538	72	.160	"	5.48×10^{-4}	9.0	3.66	"	"	"
539	72	.175	"	6.00×10^{-4}	"	4.00	"	"	"
540	75	.277	"	9.50×10^{-4}	11.4	5.02	"	"	"
541	75	.290	"	10.0×10^{-4}	"	5.27	"	"	"
542	78	.450	"	15.5×10^{-4}	14.2	6.55	"	"	"
543	78	.490	"	16.8×10^{-4}	"	7.10	"	"	"
544	40	.006	3.54×10^{-2}	$.195 \times 10^{-4}$	0.695	1.69	"	"	"
545	45	.010	"	$.326 \times 10^{-4}$	1.00	1.96	"	"	"

Table A-4 (Continued)

No.	Voltage (Kv)	O_3 Conc. (ppm)	Air Flow (m^3/sec)	O_3 Production (gm/min)	Corona Power (Watts)	O_3 Yield (gm/kw-hr)	RH %	Air Temp. (°K)	O_3 Density (gm/liter)
546	50	.0150	3.54×10^{-2}	$.489 \times 10^{-4}$	1.55	1.90	36	297	1.95
547	50	.0180	"	$.586 \times 10^{-4}$	1.55	2.27	"	"	"
548	53	.031	"	1.01×10^{-4}	2.0	3.03	"	"	"
549	53	.030	"	1.00×10^{-4}	2.0	3.00	"	"	"
550	55	.040	"	1.31×10^{-4}	2.27	3.46	"	"	"
551	55	.041	"	1.32×10^{-4}	2.27	3.49	"	"	"
552	58	.059	"	1.93×10^{-4}	2.90	4.00	"	"	"
553	58	.064	"	2.08×10^{-4}	2.90	4.31	"	"	"
554	60	.100	"	3.26×10^{-4}	3.45	5.55	"	"	"
555	60	.080	"	2.61×10^{-4}	3.45	5.05	"	"	"
556	63	.120	"	3.91×10^{-4}	4.40	5.34	"	"	"
557	63	.150	"	4.89×10^{-4}	4.40	6.67	"	"	"
558	65	.150	"	4.89×10^{-4}	5.00	5.86	"	"	"
559	65	.170	"	5.54×10^{-4}	5.00	6.64	"	"	"
560	68	0.20	"	6.52×10^{-4}	6.4	6.13	"	"	"
561	68	0.23	"	7.50×10^{-4}	6.4	7.10	"	"	"
562	70	0.27	"	8.80×10^{-4}	7.7	6.85	"	"	"
563	70	0.27	"	8.80×10^{-4}	7.7	6.85	"	"	"
564	71	0.28	"	9.11×10^{-4}	8.4	6.52	"	"	"
565	71	0.29	"	9.45×10^{-4}	8.4	6.75	"	"	"
566	73	0.40	"	13.1×10^{-4}	9.8	8.0	"	"	"
569	73	0.38	"	12.1×10^{-4}	9.8	7.40	"	"	"

Table A-4 (Continued)

No.	Voltage (Kv)	O_3 Conc. (ppm)	Air Flow (m^3/sec)	O_3 Production (gm/min)	Corona Power (Watts)	O_3 Yield (gm/kw-hr)	RH %	Air Temp. (°K)	O_3 Density (gm/liter)
570	95	0.56	3.54×10^{-2}	18.2×10^{-4}	11.4	9.55	36	297	1.95
571	95	0.55	"	17.9×10^{-4}	11.4	9.39	"	"	"
572	50	.0013	$3.89 \times 10^{-}$	$.0448 \times 10^{-4}$	1.55	.181	65	296	1.96
573	53	.006	"	$.214 \times 10^{-4}$	2.00	.642	"	"	"
574	55	.007	"	$.250 \times 10^{-4}$	2.27	.662	"	"	"
575	60	.010	"	$.780 \times 10^{-4}$	3.45	1.36	"	"	"
576	60	.0180	"	$.632 \times 10^{-4}$	3.45	1.11	"	"	"
577	58	.0124	"	$.442 \times 10^{-4}$	2.90	.915	"	"	"
578	58	.0130	"	$.464 \times 10^{-4}$	"	.960	"	"	"
579	62	.0240	"	$.855 \times 10^{-4}$	4.00	1.28	"	"	"
580	62	.0265	"	$.945 \times 10^{-4}$	4.00	1.42	"	"	"
581	65	.04	"	1.43×10^{-4}	5.00	1.72	"	"	"
582	65	.055	"	1.97×10^{-4}	5.00	2.36	"	"	"
583	68	.070	"	2.50×10^{-4}	6.4	2.34	"	"	"
584	68	.070	"	2.50×10^{-4}	6.4	2.34	"	"	"
585	70	.085	"	3.04×10^{-4}	7.7	2.37	"	"	"
586	70	.092	"	3.28×10^{-4}	7.7	2.55	"	"	"
587	72	.120	"	4.28×10^{-4}	9.0	2.85	"	"	"
588	72	.125	"	4.46×10^{-4}	9.0	2.98	"	"	"
589	75	.135	"	4.81×10^{-4}	11.4	2.53	"	"	"
590	75	.150	"	5.35×10^{-4}	11.4	2.81	"	"	"
591	80	.200	"	7.14×10^{-4}	17.0	2.52	"	"	"

Table A-4 (Continued)

No.	Volt-age (Kv)	O_3 Conc. (ppm)	Air Flow (m^3/sec)	O_3 Production (gm/min)	Corona Power (Watts)	O_3 Yield (gm/kw-hr)	RH %	Air Temp. (°K)	O_3 Density (gm/liter)
592	80	.210	3.89×10^{-2}	5.70×10^{-4}	17.0	2.01	65	296	1.96
593	85	.300	"	10.70×10^{-4}	25.5	2.52	"	"	"
594	85	.280	"	10.00×10^{-4}	25.5	2.36	"	"	"
595	50	.004	3.67×10^{-2}	$.135 \times 10^{-4}$	1.55	.522	"	"	"
596	50	.005	"	$.168 \times 10^{-4}$	"	.650	"	"	"
597	55	.014	"	$.472 \times 10^{-4}$	2.27	1.250	"	"	"
598	55	.0175	"	$.590 \times 10^{-4}$	"	1.56	"	"	"
599	58	.024	"	0.81×10^{-4}	3.00	1.62	"	"	"
600	58	.020	"	0.675×10^{-4}	"	1.35	"	"	"
601	60	.029	"	0.968×10^{-4}	3.45	1.68	"	"	"
602	60	.033	"	1.11×10^{-4}	"	1.92	"	"	"
603	62	.041	"	1.38×10^{-4}	4.00	2.07	"	"	"
604	62	.044	"	1.48×10^{-4}	"	2.22	"	"	"
605	65	.064	"	2.16×10^{-4}	5.00	2.59	"	"	"
606	65	.068	"	2.49×10^{-4}	"	2.99	"	"	"
607	68	.090	"	3.04×10^{-4}	6.4	2.85	"	"	"
608	68	.080	"	2.70×10^{-4}	"	2.53	"	"	"
609	70	.110	"	3.67×10^{-4}	7.7	2.85	"	"	"
610	70	.113	"	3.76×10^{-4}	"	2.93	"	"	"
611	72	.140	"	4.66×10^{-4}	9.0	3.11	"	"	"
612	72	.138	"	4.61×10^{-4}	"	3.08	"	"	"
613	75	.180	"	6.00×10^{-4}	11.4	3.16	"	"	"

Table A-4 (Continued)

No.	Voltage (Kv)	O_3 Conc. (ppm)	Air Flow (m^3/sec)	O_3 Production (gm/min)	Corona Power (Watts)	O_3 Yield (gm/kw-hr)	RH %	Air Temp. (°K)	O_3 Density (gm/liter)
614	75	.185	3.67×10^{-2}	6.17×10^{-4}	11.4	3.25	65	296	1.96
615	78	.220	"	7.35×10^{-4}	14.2	3.10	"	"	"
616	78	.240	"	8.02×10^{-4}	"	3.49	"	"	"
617	80	.250	"	8.25×10^{-4}	17.0	2.91	"	"	"
618	80	.265	"	8.85×10^{-4}	17.0	3.12	"	"	"
619	83	.300	"	10.0×10^{-4}	21.5	2.79	"	"	"
620	83	.300	"	10.0×10^{-4}	"	2.79	"	"	"
621	50	.010	3.68×10^{-2}	$.326 \times 10^{-4}$	1.55	1.26	68	298	1.95
622	50	.011	"	$.371 \times 10^{-4}$	"	1.43	"	"	"
623	50	.009	"	$.302 \times 10^{-4}$	"	1.17	"	"	"
624	52	.015	"	$.505 \times 10^{-4}$	1.80	1.69	"	"	"
625	52	.015	"	$.505 \times 10^{-4}$	"	1.69	"	"	"
626	55	.023	"	$.775 \times 10^{-4}$	2.27	2.05	"	"	"
627	55	.022	"	$.740 \times 10^{-4}$	"	1.96	"	"	"
628	58	.033	"	1.11×10^{-4}	2.90	2.30	"	"	"
629	58	.033	"	1.11×10^{-4}	2.90	2.30	"	"	"
630	60	.041	"	1.38×10^{-4}	3.45	2.40	"	"	"
631	60	.044	"	1.48×10^{-4}	"	2.57	"	"	"
632	61	.046	"	1.55×10^{-4}	3.70	2.51	"	"	"
633	61	.047	"	1.58×10^{-4}	"	2.56	"	"	"
634	65	.076	"	2.56×10^{-4}	5.00	3.08	"	"	"

Table A-4 (Continued)

No.	Voltage (Kv)	O_3 Conc. (ppm)	Air Flow (m^3/sec)	O_3 Production (gm/min)	Corona Power (Watts)	O_3 Yield (gm/kw-hr)	RH %	Air Temp. (°K)	O_3 Density (gm/liter)
635	65	.080	3.68×10^{-2}	2.69×10^{-4}	5.00	3.23	68	298	1.95
636	68	.100	"	3.26×10^{-4}	6.4	3.06	"	"	"
637	68	.105	"	3.54×10^{-4}	6.4	3.32	"	"	"
638	70	.115	"	3.88×10^{-4}	7.7	3.02	"	"	"
639	70	.122	"	4.11×10^{-4}	"	3.21	"	"	"
640	75	.170	"	5.72×10^{-4}	11.4	3.01	"	"	"
641	75	.177	"	5.91×10^{-4}	11.4	3.12	"	"	"
642	80	.245	"	8.25×10^{-4}	17.0	2.92	"	"	"
643	80	.240	"	8.08×10^{-4}	"	2.96	"	"	"
644	45	.011	3.48×10^{-2}	$.342 \times 10^{-4}$	1.00	2.05	"	"	"
645	45	.014	"	$.434 \times 10^{-4}$	"	2.60	"	"	"
646	50	.775	"	$.775 \times 10^{-4}$	1.60	2.91	"	"	"
647	50	.023	"	$.714 \times 10^{-4}$	"	2.68	"	"	"
648	53	.035	"	1.09×10^{-4}	2.00	3.27	"	"	"
649	53	.035	"	1.08×10^{-4}	"	3.27	"	"	"
650	55	.046	"	1.43×10^{-4}	2.27	3.78	"	"	"
651	55	.053	"	1.64×10^{-4}	"	4.34	"	"	"
652	58	.065	"	2.04×10^{-4}	3.00	4.08	"	"	"
653	58	.065	"	2.04×10^{-4}	"	4.08	"	"	"
654	60	.085	"	2.64×10^{-4}	3.45	4.59	"	"	"
655	60	.089	"	2.76×10^{-4}	"	4.80	"	"	"
656	60	.092	"	2.86×10^{-4}	"	4.97	"	"	"

Table A-4 (Continued)

No.	Voltage (Kv)	O_3 Conc. (ppm)	Air Flow (m^3/sec)	O_3 Production (gm/min)	Corona Power (Watts)	O_3 Yield (gm/kw-hr)	RH %	Air Temp. (°K)	O_3 Density (gm/liter)
657	63	.110	3.48×10^{-2}	3.42×10^{-4}	4.40	4.66	68	298	1.95
658	63	.115	"	3.57×10^{-4}	"	4.86	"	"	"
659	65	.126	"	3.91×10^{-4}	5.00	4.70	"	"	"
660	65	.130	"	4.03×10^{-4}	"	4.85	"	"	"
661	65	.130	"	4.03×10^{-4}	"	4.85	"	"	"
662	68	.170	"	5.27×10^{-4}	6.4	4.94	"	"	"
663	68	.155	"	4.82×10^{-4}	"	4.52	"	"	"
664	70	.170	"	5.27×10^{-4}	7.7	4.10	"	"	"
665	70	.185	"	5.74×10^{-4}	7.7	4.46	"	"	"
666	72	.220	"	6.83×10^{-4}	9.0	4.55	"	"	"
667	72	.225	"	7.00×10^{-4}	"	4.66	"	"	"
668	75	.260	"	8.06×10^{-4}	11.4	4.25	"	"	"
669	75	.245	"	7.60×10^{-4}	"	4.00	"	"	"
670	78	.305	"	9.46×10^{-4}	14.2	4.00	"	"	"
671	78	.310	"	9.61×10^{-4}	"	4.07	"	"	"
672	50	.004	3.64×10^{-2}	$.134 \times 10^{-4}$	1.60	.503	77	"	"
673	55	.013	"	$.435 \times 10^{-4}$	2.27	1.15	"	"	"
674	60	.027	"	$.912 \times 10^{-4}$	3.45	1.59	"	"	"
675	65	.054	"	1.80×10^{-4}	5.0	2.16	"	"	"
676	70	.088	"	2.94×10^{-4}	7.7	2.49	"	"	"
677	75	.126	"	4.21×10^{-4}	11.4	2.21	"	"	"
678	80	.180	"	6.00×10^{-4}	17.0	2.12	"	"	"

Table A-4 (Continued)

No.	Voltage (Kv)	O_3 Conc. (ppm)	Air Flow (m^3/sec)	O_3 Production (gm/min)	Corona Power (Watts)	O_3 Yield (gm/kw-hr)	RH %	Air Temp. (°K)	O_3 Density (gm/liter)
679	50	.016	3.39×10^{-2}	$.496 \times 10^{-4}$	1.60	1.86	77	298	1.95
680	55	.029	"	$.902 \times 10^{-4}$	2.27	2.38	"	"	"
681	60	.060	"	1.86×10^{-4}	3.45	3.24	"	"	"
682	65	.090	"	2.79×10^{-4}	5.0	3.35	"	"	"
683	70	.126	"	3.92×10^{-4}	7.7	3.06	"	"	"
684	75	.185	"	5.75×10^{-4}	11.4	3.03	"	"	"
685	40	.012	3.14×10^{-2}	$.345 \times 10^{-4}$	.695	2.98	"	"	"
686	50	.034	"	$.976 \times 10^{-4}$	1.60	3.67	"	"	"
687	55	.063	"	1.81×10^{-4}	2.27	4.79	"	"	"
688	60	.078	"	2.24×10^{-4}	3.45	4.02	"	"	"
689	65	.130	"	3.74×10^{-4}	5.00	4.48	"	"	"
690	70	.182	"	5.23×10^{-4}	7.70	4.07	"	"	"
691	72	.198	"	5.70×10^{-4}	9.0	3.81	"	"	"
692	75	.270	"	7.75×10^{-4}	11.4	4.08	"	"	"
693	54	.047	1.30×10^{-2}	$.707 \times 10^{-4}$	2.07	2.05	66	300	1.94
694	60	.160	"	2.41×10^{-4}	3.45	4.20	"	"	"
695	64	.182	"	2.74×10^{-4}	4.70	3.47	"	"	"
696	68	.330	"	4.97×10^{-4}	6.4	4.66	"	"	"
697	70	.462	"	6.97×10^{-4}	7.7	5.45	"	"	"
698	72	.480	"	7.23×10^{-4}	9.0	4.83	"	"	"
699	74	.595	"	8.88×10^{-4}	10.4	5.11	"	"	"
700	54	.048	1.50×10^{-2}	$.835 \times 10^{-4}$	2.07	2.42	"	"	"

Table A-4 (Continued)

No.	Voltage (Kv)	O_3 Conc. (ppm)	Air Flow (m^3/sec)	O_3 Production (gm/min)	Corona Power (Watts)	O_3 Yield (gm/kw-hr)	RH %	Air Temp. (°K)	O_3 Density (gm/liter)
701	60	.140	1.50×10^{-2}	2.44×10^{-4}	3.45	4.24	66	300	1.94
702	64	.156	"	2.72×10^{-4}	4.70	3.48	"	"	"
703	68	.280	"	4.86×10^{-4}	6.40	4.57	"	"	"
704	70	.370	"	6.34×10^{-4}	7.70	4.94	"	"	"
705	72	.405	"	7.05×10^{-4}	9.00	4.70	"	"	"
706	74	.510	"	8.87×10^{-4}	10.4	5.11	"	"	"
707	54	.047	1.69×10^{-2}	$.911 \times 10^{-4}$	2.07	2.65	"	"	"
708	56	.100	"	1.94×10^{-4}	2.50	4.66	"	"	"
709	60	.122	"	2.37×10^{-4}	3.45	3.94	"	"	"
710	62	.155	"	3.02×10^{-4}	4.00	4.52	"	"	"
711	64	.158	"	3.08×10^{-4}	4.70	3.94	"	"	"
712	66	.210	"	4.07×10^{-4}	5.40	4.52	"	"	"
713	68	.265	"	5.15×10^{-4}	6.40	4.84	"	"	"
714	70	.310	"	6.02×10^{-4}	7.70	4.69	"	"	"
715	72	.325	"	6.30×10^{-4}	9.00	4.26	"	"	"
716	74	.440	"	8.52×10^{-4}	10.4	4.91	"	"	"
717	76	.570	"	11.1×10^{-4}	12.1	5.51	"	"	"
718	78	.660	"	12.8×10^{-4}	14.2	5.40	"	"	"
719	80	.810	"	15.7×10^{-4}	17.0	5.54	"	"	"
720	54	.045	1.86×10^{-2}	$.955 \times 10^{-4}$	2.07	2.77	"	"	"
721	60	.097	"	2.06×10^{-4}	3.45	3.58	"	"	"
722	64	.148	"	3.14×10^{-4}	4.70	4.01	"	"	"

Table A-4 (Continued)

No.	Voltage (Kv)	O_3 Conc. (ppm)	Air Flow (m^3/sec)	O_3 Production (gm/min)	Corona Power (Watts)	O_3 Yield (gm/kw-hr)	RH %	Air Temp. (°K)	O_3 Density (gm/liter)
723	68	.240	1.86×10^{-2}	4.88×10^{-4}	6.40	4.59	66	300	1.94
724	70	.285	"	6.05×10^{-4}	7.70	4.71	"	"	"
725	72	.325	"	6.90×10^{-4}	9.00	4.59	"	"	"
726	74	.415	"	8.80×10^{-4}	10.4	5.07	"	"	"
727	54	.039	2.00×10^{-2}	$.895 \times 10^{-4}$	2.07	2.59	"	"	"
728	60	.090	"	2.06×10^{-4}	3.45	3.58	"	"	"
729	64	.137	"	3.15×10^{-4}	4.70	4.03	"	"	"
730	68	.220	"	5.05×10^{-4}	6.40	4.74	"	"	"
731	70	.228	"	5.23×10^{-4}	7.70	4.08	"	"	"
732	72	.320	"	7.34×10^{-4}	9.00	4.90	"	"	"
733	74	.365	"	8.37×10^{-4}	10.4	4.81	"	"	"
735	54	.037	2.14×10^{-2}	$.905 \times 10^{-4}$	2.07	2.62	"	"	"
736	64	.083	"	3.18×10^{-4}	4.70	4.06	"	"	"
737	66	.126	"	4.17×10^{-4}	5.60	4.46	"	"	"
738	68	.170	"	5.05×10^{-4}	6.40	4.74	"	"	"
739	70	.200	"	5.84×10^{-4}	7.70	4.55	"	"	"
740	72	.231	"	7.70×10^{-4}	9.00	5.20	"	"	"
741	74	.305	"	8.71×10^{-4}	10.4	5.02	"	"	"
742	76	.345	"	11.5×10^{-4}	12.1	5.70	"	"	"
743	78	.468	"	12.5×10^{-4}	14.2	5.29	"	"	"
744	80	.510	"	15.5×10^{-4}	17.0	5.46	"	"	"

Table A-4 (Continued)

No.	Voltage (Kv)	O_3 Conc. (ppm)	Air Flow (m^3/sec)	O_3 Production (gm/min)	Corona Power (Watts)	O_3 Yield (gm/kw-hr)	RH %	Air Temp. (°K)	O_3 Density (gm/liter)
745	54	.036	2.26×10^{-2}	$.936 \times 10^{-4}$	2.07	2.71	66	300	1.94
746	60	.080	"	2.08×10^{-4}	3.45	3.62	"	"	"
747	64	.115	"	3.98×10^{-4}	4.70	5.08	"	"	"
748	68	.170	"	4.41×10^{-4}	6.40	4.15	"	"	"
749	70	.220	"	5.73×10^{-4}	7.70	4.47	"	"	"
750	72	.285	"	7.41×10^{-4}	9.00	4.95	"	"	"
751	74	.305	"	7.93×10^{-4}	10.4	4.46	"	"	"
752	54	.034	2.40×10^{-2}	$.936 \times 10^{-4}$	2.07	2.72	"	"	"
753	60	.082	"	2.26×10^{-4}	3.45	3.93	"	"	"
754	64	.109	"	3.00×10^{-4}	4.70	3.83	"	"	"
755	68	.140	"	3.76×10^{-4}	6.40	3.53	"	"	"
756	70	.200	"	5.52×10^{-4}	7.70	4.31	"	"	"
757	72	.250	"	6.89×10^{-4}	9.00	4.58	"	"	"
758	74	.300	"	8.26×10^{-4}	10.4	4.76	"	"	"
759	54	.035	2.50×10^{-2}	1.01×10^{-4}	2.07	2.92	"	"	"
760	60	.080	"	2.30×10^{-4}	3.45	4.00	"	"	"
761	64	.110	"	3.14×10^{-4}	4.70	4.02	"	"	"
762	68	.153	"	4.41×10^{-4}	6.40	4.14	"	"	"
763	70	.200	"	5.75×10^{-4}	7.70	4.48	"	"	"
764	72	.255	"	7.31×10^{-4}	9.00	4.87	"	"	"
765	74	.285	"	8.20×10^{-4}	10.4	4.72	"	"	"
766	54	.033	2.62×10^{-2}	1.00×10^{-4}	2.07	2.89	"	"	"

Table A-4 (Continued)

No.	Voltage (Kv)	O_3 Conc. (ppm)	Air Flow (m^3/sec)	O_3 Production (gm/min)	Corona Power (Watts)	O_3 Yield (gm/kw-hr)	RH %	Air Temp. (°K)	O_3 Density (gm/liter)
767	60	.079	2.62×10^{-2}	2.40×10^{-4}	3.45	4.17	66	300	1.94
768	64	.106	"	3.22×10^{-4}	4.70	4.11	"	"	"
769	68	.145	"	4.40×10^{-4}	6.40	4.13	"	"	"
770	70	.180	"	5.46×10^{-4}	7.70	4.26	"	"	"
771	72	.240	"	7.30×10^{-4}	9.80	4.86	"	"	"
772	74	.300	"	9.1×10^{-4}	10.4	5.25	"	"	"
773	54	.031	2.73×10^{-2}	$.975 \times 10^{-4}$	2.07	2.83	"	"	"
774	56	.044	"	1.38×10^{-4}	2.52	3.21	"	"	"
775	60	.075	"	2.35×10^{-4}	3.45	3.92	"	"	"
776	64	.108	"	3.40×10^{-4}	4.70	4.34	"	"	"
777	68	.144	"	4.52×10^{-4}	6.40	4.24	"	"	"
778	70	.190	"	5.95×10^{-4}	7.70	4.64	"	"	"
779	72	.225	"	7.07×10^{-4}	9.00	4.72	"	"	"
780	74	.270	"	8.48×10^{-4}	10.4	4.88	"	"	"
781	54	.027	2.86×10^{-2}	$.900 \times 10^{-4}$	2.07	2.61	"	"	"
782	56	.047	"	1.56×10^{-4}	2.52	3.34	"	"	"
783	60	.069	"	2.29×10^{-4}	3.45	3.98	"	"	"
784	64	.104	"	3.45×10^{-4}	4.70	4.41	"	"	"
785	68	.129	"	4.28×10^{-4}	6.40	4.02	"	"	"
786	70	.200	"	6.65×10^{-4}	7.70	5.19	"	"	"
787	72	.220	"	7.31×10^{-4}	9.00	4.88	"	"	"
788	74	.265	"	8.80×10^{-4}	10.4	5.06	"	"	"

Table A-4 (Continued)

No.	Voltage (Kv)	O_3 Conc. (ppm)	Air Flow (m^3/sec)	O_3 Production (gm/min)	Corona Power (Watts)	O_3 Yield (gm/kw-hr)	RH %	Air Temp. (°K)	O_3 Density (gm/liter)
789	50	.009	2.97×10^{-2}	$.304 \times 10^{-4}$	1.60	1.14	66	300	1.94
790	54	.025	"	$.813 \times 10^{-4}$	2.07	2.36	"	"	"
791	56	.044	"	1.48×10^{-4}	2.50	3.56	"	"	"
792	60	.064	"	2.06×10^{-4}	3.45	3.58	"	"	"
793	64	.085	"	2.87×10^{-4}	4.70	3.67	"	"	"
794	68	.109	"	3.67×10^{-4}	6.40	3.44	"	"	"
795	70	.168	"	5.65×10^{-4}	7.7	4.41	"	"	"
796	72	.215	"	7.25×10^{-4}	9.0	4.83	"	"	"
797	74	.255	"	8.60×10^{-4}	10.4	4.96	"	"	"
798	50	.009	3.00×10^{-2}	$.314 \times 10^{-4}$	1.60	1.18	"	"	"
799	54	.023	"	$.803 \times 10^{-4}$	2.07	3.10	"	"	"
800	56	.051	"	1.78×10^{-4}	2.50	4.27	"	"	"
801	60	.067	"	2.33×10^{-4}	3.45	3.88	"	"	"
802	64	.100	"	3.48×10^{-4}	4.70	4.44	"	"	"
803	66	.110	"	3.83×10^{-4}	5.60	4.10	"	"	"
804	68	.122	"	4.25×10^{-4}	6.40	3.98	"	"	"
805	70	.175	"	6.10×10^{-4}	7.7	4.75	"	"	"
806	72	.210	"	7.31×10^{-4}	9.0	4.88	"	"	"
807	74	.240	"	8.35×10^{-4}	10.4	4.81	"	"	"
808	76	.325	"	11.3×10^{-4}	12.1	5.60	"	"	"
809	78	.385	"	13.4×10^{-4}	11.4	7.05	"	"	"
810	80	.460	"	16.0×10^{-4}	17.0	5.65	"	"	"

VERSAR INC.

TABLE A-5

Average Ozone Yield Values for Data Sets

Set No.	Data Points in Set	Relative Humidity (per cent)	Air Flow Rate ($m^3/sec \times 10^2$)	Average Ozone Yield (gm/kw-hr)
1	1-26	42	2.5	2.87
2	27-62	45	1.6	2.06
3	63-92	45	2.76	1.03
4	93-116	42	2.86	6.33
5	117-141	51	1.83	4.78
6	142-165	51	2.26	3.22
7	166-186	51	2.74	3.39
8	187-207	38	2.11	4.22
9	208-231	38	2.52	3.79
10	232-255	38	2.83	3.64
11	256-275	38	3.16	3.39
12	276-295	38	3.47	3.12
13	296-316	38	4.02	3.12
14	317-323	27	3.93	2.36
15	324-329	28	3.78	4.46
16	330-336	33	3.85	2.26
17	337-343	33	3.78	5.79
18	344-349	33	3.34	8.03
19	350-355	33	3.17	9.22
20	356-359	33	2.83	8.49
21	360-380	27	4.05	6.78
22	381-401	27	3.82	8.86
23	402-416	27	3.56	11.59
24	417-427	51	3.86	3.05
25	428-438	51	3.67	4.76
26	439-448	51	3.53	7.35
27	449-458	51	3.26	7.32
28	459-469	51	3.14	8.90
29	470-479	51	2.79	8.56
30	480-491	58	3.86	3.43
31	492-503	58	3.50	5.49
32	504-510	42	2.43	2.26
33	511-517	45	1.60	1.82
34	518-523	45	1.27	2.48
35	524-543	36	3.74	2.90
36	544-571	36	3.54	4.96
37	572-594	65	3.89	1.76
38	595-620	65	3.67	2.40
39	621-643	68	3.68	2.47
40	644-671	68	3.48	4.10
41	672-678	77	3.64	1.75
42	679-684	77	3.39	2.82

VERSAR INC.

TABLE A-5 (Cont'd.)

Set No.	Data Points in Set	Relative Humidity (per cent)	Air Flow Rate (m^3/sec x 10^2)	Average Ozone Yield (gm/kw-hr)
43	685-692	77	3.14	3.99
44	693-699	66	1.30	4.25
45	700-706	66	1.50	4.21
46	707-719	66	1.69	4.57
47	720-726	66	1.86	4.19
48	727-733	66	2.00	4.10
49	735-744	66	2.14	4.71
50	745-751	66	2.26	4.21
51	752-758	66	2.40	3.95
52	759-765	66	2.50	4.16
53	766-772	66	2.62	4.24
54	773-780	66	2.73	4.10
55	781-788	66	2.86	4.19
56	789-797	66	2.97	3.55
57	798-810	66	3.00	4.44

BIBLIOGRAPHIC DATA SHEET	1. Report No. EPA-650/4-73-003	2.	3. Recipient's Accession No.
4. Title and Subtitle Determination of Coronal Ozone Production by High Voltage Power Transmission Lines			5. Report Date Issued November 1973 6.
7. Author(s) Frank C. Whitmore and Robert L. Durfee			8. Performing Organization Rept. No.
9. Performing Organization Name and Address Versar, Incorporated 6621 Electronic Drive Springfield, Virginia			10. Project/Task/Work Unit No. Program Element 1H1326 11. Contract/Grant No. 68-02-0553
12. Sponsoring Organization Name and Address Environmental Protection Agency National Environmental Research Center, RTP Quality Assurance and Environmental Monitoring Laboratory Research Triangle Park, North Carolina 27711			13. Type of Report & Period Covered Final Report 14.

15. Supplementary Notes

Formerly Program Element 110501

16. Abstracts

A sub-scale simulation of a high-voltage transmission line was constructed and operated in a chamber roughly 1.5 meters long by 0.5 meter in diameter to determine ozone production characteristics. Effects of voltage and corona power, conductor size and surface condition, air temperature, relative humidity, and air flow rate (wind velocity) on ozone yield were determined. Of these, corona power (voltage), relative humidity, and air flow rate exhibited significant effects on ozone yield. Averaged yield values ranged from about 3 gm/kw-hr at high humidity (75-80 per cent) to about 7 gm/kw-hr at low humidity (25-30 per cent). Application of these results to three areas of high concentration of transmission lines showed that, under minimal wind conditions, such transmission line concentrations can produce sizeable local ozone levels.

17. Key Words and Document Analysis. 17a. Descriptors

Air pollution
Ozone
Power transmission lines
Electric corona
Sources
Measurement

17b. Identifiers/Open-Ended Terms

Ozone concentrations
Transmission line simulation

17c. COSATI Field/Group 13B

18. Availability Statement	19. Security Class (This Report)	21. No. of Pages
Unlimited	UNCLASSIFIED	129
	20. Security Class (This Page) UNCLASSIFIED	22. Price